



Universitat Autònoma de Barcelona

ADVERTIMENT. L'accés als continguts d'aquesta tesi queda condicionat a l'acceptació de les condicions d'ús establertes per la següent llicència Creative Commons:  http://cat.creativecommons.org/?page_id=184

ADVERTENCIA. El acceso a los contenidos de esta tesis queda condicionado a la aceptación de las condiciones de uso establecidas por la siguiente licencia Creative Commons:  <http://es.creativecommons.org/blog/licencias/>

WARNING. The access to the contents of this doctoral thesis it is limited to the acceptance of the use conditions set by the following Creative Commons license:  <https://creativecommons.org/licenses/?lang=en>



**Universitat Autònoma
de Barcelona**

La formació d'esters i amides dels àcids grassos naturals
com un mecanisme per explicar els seus efectes en la salut
humana

Biosynthesis of esters and amides of natural fatty acids as
a mechanism to explain their effects on human health

Tesi Doctoral

Antoni Pastor Bosch

Director: Rafael de la Torre Fornell

Tutor: Magí Farré Albaladejo

Departament de Farmacologia, Terapèutica i Toxicologia

Programa de Doctorat en Farmacologia

Universitat Autònoma de Barcelona

Any 2015



**Universitat Autònoma
de Barcelona**

La formació d'esters i amides dels àcids grassos naturals
com un mecanisme per explicar els seus efectes en la salut
humana

Biosynthesis of esters and amides of natural fatty acids as
a mechanism to explain their effects on human health

Departament de Farmacologia, Terapèutica i Toxicologia

Universitat Autònoma de Barcelona

Any 2015

Antoni Pastor

Rafael de la Torre

Magí Farré

Firma:

Firma:

Firma

Rafael de la Torre Fornell, Professor Titular del Departament de Ciències Experimentals i de la Salut, Universitat Pompeu Fabra

CERTIFICA:

Que la memòria presentada per Antoni Pastor Bosch amb títol:

“La formació d’èsters i amides dels àcids grassos naturals com un mecanisme per explicar els seus efectes en la salut humana”

“Biosynthesis of esters and amides of natural fatty acids as a mechanism to explain their effects on human health”

ha estat realitzada sota la seva direcció. La memòria reuneix les condicions per ser presentada per optar al grau de Doctor.

I perquè consti als efectes oportuns signo el present certificat a Barcelona, a 3 de Desembre de 2015

Rafael de la Torre Fornell



MEMÒRIA PRESENTADA PER OPTAR AL GRAU DE
DOCTOR PER LA UNIVERSITAT AUTÒNOMA DE
BARCELONA.

La tesi doctoral ha estat dirigida pel Dr. Rafael de la Torre Fornell.

Barcelona, a 3 de desembre de 2015

Antoni Pastor Bosch

Agraïments

Aquesta tesi doctoral ha sigut un procés llarg i difícil amb una serie d'etapes o proves que s'han hagut d'anar superant i que et canvien degut a l'esforç que hi has hagut de dedicar i les noves coses que has après. És també com una mena d'aventura, perquè saps com comences però no saps com acabes i tampoc saps el que et trobaràs pel camí. Però és una aventura que no es fa sol i moltes persones m'han donat el seu suport i han col·laborat perquè aquest projecte fos possible.

En primer lloc agraeixo al Rafael de la Torre per donar-me la oportunitat de fer una tesi doctoral sota la seva direcció i de dedicar una part del seu temps a formar-me. L'excel·lent experiència d'en Rafael en àmbits tan diversos com són la farmacologia, la química analítica, i la neuropsicologia m'han ajudat a tenir una perspectiva des de diversos àmbits en el camp de la recerca. Tanmateix, crec que el paper més important que té un director de tesi no és el seu bagatge científic sinó la seva habilitat per ensenyar-te a pensar de manera científica i de donar-te les eines perquè hom pugui fer recerca de manera autònoma. En el seu estil de direcció en Rafael m'ha donat total llibertat per buscar solucions a problemes científics i també llibertat per equivocar-me i per poder créixer intel·lectualment. El seu tracte directe i franc, la seva preocupació sincera per les persones, i la seva dedicació entusiasta a la recerca són aspectes que m'han inspirat durant les discussions científiques que hem tingut al llarg de la tesi.

En segon lloc dedico aquesta tesi a la meva família i al Mario. A la meva mare, pel seu optimisme i pel seu suport i perquè sempre ha cregut amb mi. Al meu pare per ensenyarme el valor de l'estudi. Em sap greu que no hagi pogut veure el final papa. Al meu germà Marc i a la meva tieta Rosa Maria pels seus ànims. Vull dedicar molt especialment al Mario aquesta tesi, que ha sigut la meva roca i amb el qui he tingut la motivació més gran per seguir i superar aquest procés, i que ha viscut i ha sofert tant o més que jo amb aquesta tesi amb tots els seus alts i baixos. El seu recolzament i comprensió i les seves suggerències han sigut molt importants per mi.

En tercer lloc, agraeixo al Magí Farré per haver acceptat ser el meu tutor en aquesta tesi i per la col.laboració de la unitat d'assaigs clínics de l'IMIM que fa poc dirigia en els experiments que sense els quals aquesta tesi no hagués estat possible. Agraeixo també la col.laboració amb el Fernando Fernández de Aranda del programa CIBER, que ha permès aplicar la recerca a l'estudi de obesitat i olfacte, i que forma part dels resultats d'aquesta tesi i d'altres resultats en el camp de la neuropsicologia. Agraeixo les col.laboracions enriquidores amb els grups del Fernando Rodríguez de Fonseca i el Rafael Maldonado, les quals també han donat sentit a aquesta tesi i han permès aplicar la recerca a la medicina translacional. Agraeixo també a l'Ester Menoyo per la seva labor en els assaigs clínics, al Klaus Langohr per la seva ajuda en l'estadística, al Joan Rodríguez pel seu paper amb els voluntaris i els tests de l'olfacte del CIBER i a l'Ester Civit pel processament de les mostres de sang del CIBER.

En quart lloc, agraeixo la col.laboració dels meus companys de l'IMIM, que m'han acompanyat en aquesta aventura i que s'han convertit en amics meus. El Raul, que ha sigut el meu company de batalla del liquid-masses d'Agilent, que és l'instrument amb el que s'han fet els mètodes analítics i hem acabat d'entendre com "funciona". Al Josep Marcos, "el professor", que ha sigut com un mentor per mi i del qual n'he après molt.

En cinquè lloc, agraeixo als meus companys de laboratori de l'IMIM que m'han ajudat directa o indirectament, i que fan en aquest laboratori una excel.lent feina. Tots ells, fins i tot la sang nova del laboratori m'han donat una empenta final en aquest procés, la Neus Pizarro, el José Rodríguez, la Mitona Pujades, l'Anna Boronat, el Jordi Garcia i l'Eulàlia Olesti. Agraeixo també a la resta de companys de l'IMIM, que no puc nombrar a tots els que jo voldria perquè ja no puc escriure més per l'ambient agradable de feina i el seu companyerisme.

Finalment, agraeixo al programa CIBER, que ha jugat un paper fonamental per poder obtenir els resultats clínics d'aquesta tesi, i al IMIM per la seva ajuda econòmica en l'impressió d'aquesta tesi.

Barcelona, 3 de Desembre de 2015

Als meus pares,
al Mario

-L'essencial és invisible als ulls-

Antoine de Saint-Exupéry

1. INTRODUCTION

1.1. Lipidomics.....	1
1.2. Endocannabinoids	
1.2.1. History of endocannabinoids research.....	2
1.2.2. The endogenous cannabinoid system.....	3
1.2.2.1. Biosynthesis and inactivation of endocannabinoids.....	4
1.2.2.2. Endocannabinoid modulation of synaptic transmission.....	8
1.2.2.3. Peripheral endocannabinoid system.....	11
1.2.3. The endocannabinoidome.....	11
1.3. Obesity	
1.3.1. Definition of obesity. The obesity epidemic.....	16
1.3.2. Obesity, body fat and health consequences.....	17
1.3.3. Possible causes of obesity.....	18
1.3.4. Brain homeostatic and hedonic regulation of food intake	
1.3.4.1. Neural systems that modulate food intake and energy balance.....	19
1.3.4.2. Homeostatic modulation of food intake and energy balance.....	22
1.3.4.3. Integration of homeostatic and hedonic processes in the modulation of food intake.....	23
1.3.5. The endogenous cannabinoid system as a homeostatic and hedonic modulator of food intake.....	24
1.3.6. The endocannabinoid system and obesity. Possible influence of the diet on the endocannabinoid system.....	26
1.3.7. Olfaction and eating behaviour. Modulation by the endocannabinoid system.....	27

1.4. Evaluation of olfactory function. Relation to cognitive function.....	31
1.5. Methodological issues for the quantification of circulating plasma endocannabinoids.....	33
2. OBJECTIVES.....	35
3. HYPOTHESES.....	37
4. MATERIALS AND METHODS	
4.1. Quantification of endocannabinoids in human plasma	
4.1.1. Chemicals, standards and laboratory material.....	38
4.1.2. Human subjects.....	41
4.1.3. Sample preparation.....	41
4.1.4. Liquid chromatography/Mass spectrometry conditions.....	42
4.1.5. Method development and validation	
4.1.5.1. Linearity.....	44
4.1.5.2. Quantification calculations.....	45
4.1.5.3. Limits of detection and quantification.....	46
4.1.5.4. Accuracy and imprecision.....	47
4.1.5.5. Recovery and matrix effect.....	48
4.1.5.6. Stability of the analysis on re-injection.....	48
4.1.6. Chemical and biological stability of 2-monoacylglycerols	
4.1.6.1. Stability of the isomers 1 and 2 of monoacylglycerols in the biological matrix.....	49
4.1.6.2. Inhibition experiments of the ex-vivo generation of monoacylglycerols from plasma.....	49
4.1.6.3. Stabilization of monoacylglycerols (MG) measures in plasma with Orlistat.....	51
4.2. Quantification of endocannabinoids in animal models.....	51
4.3. The endocannabinoid system, weight categories, and olfaction	
4.3.1. Human subjects. Characteristics of the human sample.....	52

4.3.2. Endocannabinoid quantification, anthropometry and lipid profile.....	55
4.3.3. Olfactory capacity tests.....	55
4.3.3.1. Olfactory threshold (OT) test.....	57
4.3.3.2. Olfactory discrimination (OD) test.....	57
4.3.3.3. Olfactory identification (OI) test.....	57
4.3.3.4. Threshold-discrimination-identification (TDI) score.....	58
4.3.4. Statistical analysis.....	58
5. RESULTS AND DISCUSSION	
5.1. Method for the quantification of endocannabinoids in human plasma	
5.1.1. Method development.....	60
5.1.2. Method validation.....	64
5.1.3. Inhibition experiments of the ex-vivo generation of monoacylglycerols in plasma.....	71
5.1.4. Stability of the isomeric ratio of monoacylglycerols.....	80
5.2. Applicability of the endocannabinoid quantification method in clinical and translational studies.....	83
5.3. Endocannabinoids, weight categories and olfaction.....	87
6. CONCLUSIONS	
6.1. Method for the quantification of endocannabinoids in human plasma	102
6.2. Endocannabinoids, weight categories and olfaction.....	103
7. BIBLIOGRAPHY.....	104
ANNEX (PDF published article of the endocannabinoid quantification method in plasma)	

1. INTRODUCTION

1.1 Lipidomics

Membrane lipids have emerged as crucial regulators of many biological processes. In addition to their contribution to cellular architecture, and the regulation of membrane proteins by protein-lipid interactions, membrane lipids have a key function in cellular communication as precursors of hundreds of signalling molecules. A disruption in lipid signalling processes has been demonstrated in a number of human pathologies. Lipidomics is focused on identifying alterations in lipid metabolism and lipid-mediated signalling processes that regulate cellular homeostasis during health and disease. The approach of lipidomics, or study of the lipidome, is the large-scale identification of cellular lipids and quantification of alterations in lipid classes, subclasses, and individual molecular species present in a cell, tissue or bodily fluid [1] [2] [3,4].

The scope of this thesis is the study of the endocannabinoidome and its relation to human health. The endocannabinoidome is constituted by a family of endogenous bioactive long-chain fatty acid ester or amide derivatives historically related to the phytocannabinoid Δ^9 -tetrahydrocannabinol (Δ^9 -THC), a psychoactive lipid present in the marijuana plant [5].

1.2 Endocannabinoids

1.2.1 History of endocannabinoids research.

The resin of the flowering marijuana plant, *Cannabis sativa*, has been used since ancient times for recreation and religious purposes as well as medicine [6]. The earliest use of cannabis as a medicine is attributed to the legendary Chinese Emperor Shen Nung, the father of Chinese traditional medicine, who is thought to have lived around 2700 BC [7]. In the early 20th century advances in chemistry allowed to isolate and synthesize the active ingredients of medicinal plants, and the first plant cannabinoid -named cannabiol- was isolated. However, it was not until 1964 with the isolation and structure elucidation of Δ^9 -THC, responsible for its psychopharmacological effects, and later in the 1990s with the discovery of the cannabinoid receptors CB1 and CB2 and the characterization of endogenous lipid ligands of these receptors, the endocannabinoids (eCBs) anandamide (AEA) and 2-arachidonoylglycerol (2-AG) (**Figure 1**), that the existence of an endogenous cannabinoid system could be postulated [8]. Key later achievements in the understanding of the endocannabinoid (eCB) system have been the discovery of the first CB1 antagonist SR141716A (rimonabant), the discovery of retrograde signaling by eCBs, the cloning of eCB biosynthesizing and degrading enzymes, and the synthesis of potent inhibitors of these enzymes [6].

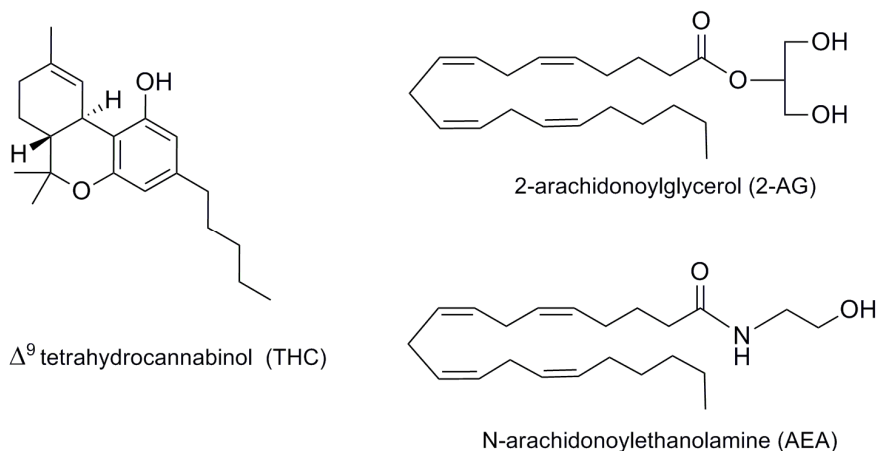


Figure 1. Structure of Δ^9 -THC and the endocannabinoids 2-arachidonoylglycerol (2-AG) and N-arachidonylethanolamine (AEA).

1.2.2 The endogenous cannabinoid system

The eCB system comprises (i) at least two G protein-coupled receptors (GPCR), known as the cannabinoid type 1 (CB1) and type 2 receptors (CB2); (ii) the endogenous ligands of these receptors, known as the eCBs 2-AG and AEA (or anandamide); and (iii) biosynthetic and degradative enzymes and carriers that regulate eCB levels and action at these receptors [9,10]. Both CB1 and CB2 receptors are coupled to G protein type G_i/o , and less frequently to the $G_q/11$ type. It is through this coupling that they mediate stimulation of mitogen-activated protein kinases (MAPKs) and inhibit adenyllyl cyclase, and cyclic AMP-protein kinase A (PKA) signaling. Only in case of CB1 receptors, the coupling to G_i/o inhibits voltage-gated calcium channels (VGCCs), and stimulates inwardly rectifying K^+ channels [11].

1.2.2.1 Biosynthesis and inactivation of endocannabinoids

The eCBs 2-AG and AEA are lipid-signaling molecules generated “on demand” from membrane phospholipids after cell stimulation by calcium-dependent lipases. ECBs are local mediators and their actions are terminated after uptake and subsequent intracellular enzymatic degradation. 2-AG and AEA are also called ester and amide eCBs, respectively, and they originate from very different biosynthetic pathways.

The biosynthesis of 2-AG is done by sequential hydrolysis of phosphatidylinositol 4,5-bisphosphate (PIP₂) that is cleaved from the membrane by phospholipase C β (PLC β) to yield the second messengers diacylglycerol (DAG), with arachidonic acid in the 2-position, and inositol triphosphate (IP₃). Next, diacylglycerol lipase alfa or beta (DAGL α , DAGL β) hydrolyses DAG to 2-AG and a free fatty acid. The hydrolysis of 2-AG to free arachidonic acid and glycerol is done by the monoacylglycerol lipase (MAGL) but other serine hydrolases as the α/β hydrolase domain 6 (ABHD6) and 12 (ABHD12) are also involved to a lesser extent on its degradation. [10,12]. Alternative 2-AG biosynthetic routes are also possible. DAG can be originated from phosphatidic acid instead of PIP₂ by the action of a phosphatase activity [13]. 2-AG can be originated by action of Ca²⁺ independent phospholipase A1 (PLA₁) that hydrolyzes PIP₂ to lysophosphatidylinositol (LysoPI), which is hydrolyzed by a LysoPI-PLC to yield 2-AG [14]. Whether these alternative routes are relevant for 2-AG biosynthesis is not known. 2-AG in the organism is also originated from an additional source. 2-AG and other 2-acylglycerols accumulate in the intestinal lumen from the hydrolysis by pancreatic lipase of dietary triacylglycerols [15](**Figure 2**) .

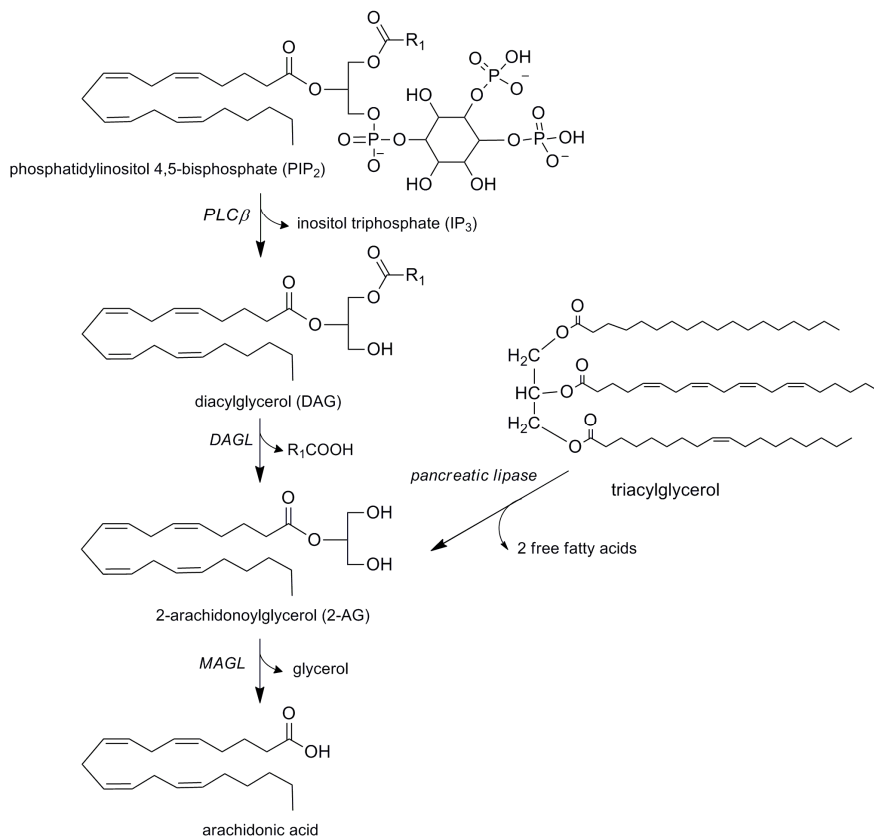


Figure 2. 2-arachidonoylglycerol (2-AG) biosynthetic and degradation pathways. Phospholipase C β (PLC β), diacylglycerol lipase (DAGL), monoacylglycerol lipase (MAGL)

The biosynthesis of AEA is less understood than the biosynthesis of 2-AG. The precursors of AEA are the N-arachidonoylphosphatidylethanolamines (NAPEs), which are formed from the transfer of arachidonic acid from the sn-1 position of phosphatidylcholine to the primary amine of phosphatidylethanolamine by calcium dependent or calcium independent N-acyltransferase activity (NAT). The most known biosynthetic route is the direct hydrolysis of NAPE by a phospholipase D-type activity (NAPE-PLD). AEA is then

degraded to free arachidonic acid and glycerol by the fatty acid amide hydrolase (FAAH) [10,16] (**Figure 3**). However, parallel biosynthetic routes have been described and they involve metabolism of NAPE to other intermediates before being metabolized to AEA. A second route is regulated by the alpha/beta-hydrolase 4 (ABHD4), that generates glycerophosphoanandamide, and the subsequent cleavage of glycerophosphate by glycerophosphodiesterase (GDE1) to produce AEA, a third route is by action of phospholipase C to generate phosphoanandamide, which is then dephosphorylated by the tyrosine phosphatase N22, and a fourth route is by action of phospholipase A₂ to generate lysoNAPE, which can then be hydrolyzed by a lysophospholipase D activity to produce AEA. These alternative routes may substitute for one another since mice lacking NAPE-PLD do not show reduced basal levels of AEA [10,16].

ECBs are derivatives of arachidonic acid (AA) and thus they are potential substrates of the enzymes of oxidative metabolism [17]. Cyclooxygenase 2 (COX-2), an enzyme that plays a key role in inflammatory processes and initiates the metabolism of AA to prostaglandins (PGs), is able to metabolize AEA and 2-AG to PGH₂ ethanolamide and PGH₂ glycerol ester, respectively. Following the action of PG synthases, the amides and esters of the corresponding PGs are formed. These compounds are bioactive and exert their biological effects through receptors that have not been fully identified [18]. The dual metabolism of AEA and 2-AG, which are subject to hydrolysis to AA by specific lipases and the oxidative metabolism initiated by COX-2, illustrates the crosstalk between eCB and eicosanoid signaling pathways. Notably, eCB hydrolysis yields free AA. It has been shown that the enzymes responsible for eCB biosynthesis and catabolism control also the production of AA and eicosanoids that lead to inflammation [19,20].

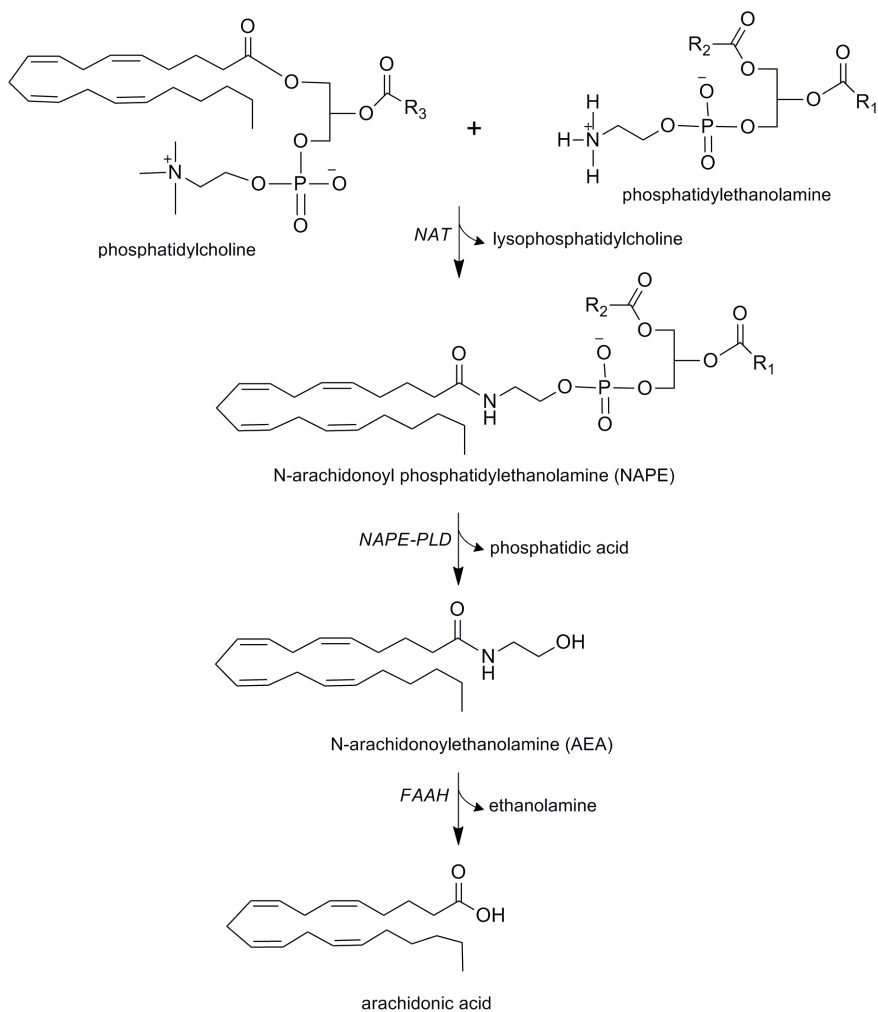


Figure 3. N-arachidonylethanolamine (AEA or anandamide) biosynthetic and degradation pathways. NAT (N-acyl transferase), NAPE-phospholipase D (NAPE-PLD), fatty acid amide hydrolase (FAAH)

1.2.2.2 Endocannabinoid modulation of synaptic transmission

ECBs are neuromodulators that maintain the homeostasis of the central nervous system. The neuromodulatory activities of the endocannabinoid system are involved in many human physiological and pathological functions [21-27]. ECB modulation of synaptic function is done by activation of the CB1 receptor, which is the most abundant GPCR in the mammalian central nervous system. CB1 expression is particularly high in cerebellar and cerebral cortex, basal ganglia, olfactory-associated structures, hippocampus, amygdala and the ventromedial hypothalamus. The psychoactive effects of Δ^9 -THC are also mediated by the activation of this receptor. CB1 brain distribution is consistent with known effects of eCBs and exogenous cannabinoids on learning, reward, memory, anxiety, pain, cognition, appetite, and motor functions [9,10,28].

ECBs modulate synaptic transmission by inhibiting the release of excitatory or inhibitory neurotransmitters. The principal mechanism by which eCBs modulate synaptic function is retrograde signaling. Neurotransmitter release to the post-synaptic terminal leads to the biosynthesis of eCBs in the post-synaptic terminal that move backward across the synapse by an unknown transport mechanism, and bind to pre-synaptic CB1-receptors that suppress neurotransmitter release. 2-AG is the eCB involved in retrograde signaling. The particular architecture throughout the central nervous system of the distribution of biosynthetic DAGL in postsynaptic terminals and degrading MAGL in pre-synaptic terminals system supports this theory (**Figure 4**). The role of AEA in the eCB modulation of synaptic transmission is less clear. FAAH, the enzyme that inactivates AEA is located in post-synaptic terminals, associated to intracellular membrane organelles. Thus AEA can act as an anterograde

signal or as an intracellular mediator. Further, AEA is a partial agonist of CB1 receptor, while 2-AG is a full agonist. The amount of 2-AG in the brain is approximately 200 times higher than AEA. AEA is also agonist of the transient receptor potential vanilloid type 1 channel (TPRV-1), which can modulate synaptic function in the brain [11,29].[26]. In addition, there seems to be crosstalk in AEA and 2-AG biosynthetic and signaling pathways so it is difficult to dissect AEA from 2-AG function [30].

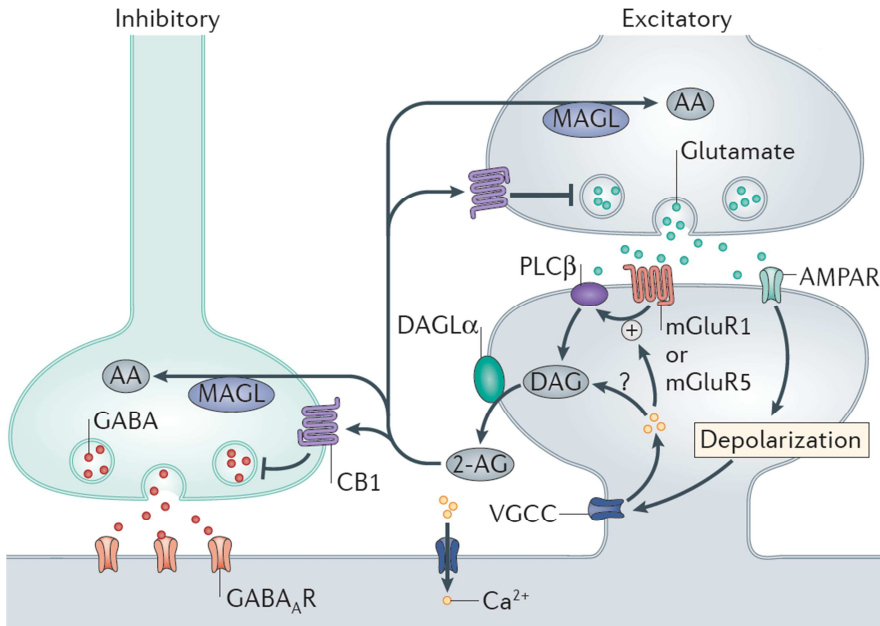


Figure 4. 2-arachidonoylglycerol (2-AG) modulation of synaptic transmission. Glutamate released from excitatory presynaptic terminals causes Ca²⁺ influx through both AMPA-type glutamate receptors (AMPA) and voltage-gated Ca²⁺-channels (VGCCs), and/or activation of metabotropic glutamate receptor 1 (mGluR1) or mGluR5, both of which induce 2-AG release. Activation of mGluR1 and mGluR5 stimulates phospholipase Cβ (PLCβ) to yield DAG. DAG is converted to 2-AG by DAG lipase α (DAGLα). The released 2-AG from postsynaptic terminals can act on CB1 receptors that are located either on the presynaptic terminals releasing glutamate (homosynaptic terminals) or on neighboring terminals (heterosynaptic terminals; although these neighboring terminals can be either inhibitory or excitatory, only the former type is shown). The activation of CB1 in homosynaptic or in heterosynaptic terminals suppresses neurotransmitter release. The former process is called retrograde signaling. 2-AG is degraded to arachidonic acid (AA) by monoacylglycerol lipase (MAGL). Notably, receptor-driven PLCβ stimulation is dependent on Ca²⁺ and is enhanced when combined with an increase in intracellular Ca²⁺ levels. Ca²⁺ influx through

VGCCs stimulates an unidentified enzymatic pathway (denoted by a question mark) to produce diacylglycerol (DAG); *Nat Rev Neurosci* 2015;16:264-277.

1.2.2.3 Peripheral endocannabinoid system

The eCB system is not only present in the central nervous system but it is also found in the periphery. The CB1 receptor is expressed in peripheral nervous tissue, and in somatic tissues like adipose tissue, liver, pancreas, skeletal muscle, and gut where eCBs are produced and where they control lipid and glucose metabolism [31]. The CB2 receptor is also called the peripheral cannabinoid receptor and it is expressed primarily in cells of the immune system, in all cell subtypes. CB2 is a potent regulator of immune responses [32]. CB2 is also found in the central nervous system in microglia cells, where it is over-expressed in neuroinflammation [26].

1.2.3 The endocannabinoidome

AEA and 2-AG belong, respectively, to two families of compounds N-acylethanolamines (NAEs) and 2-monoacylglycerols (2-MGs) (**Figure 5**). The NAEs and 2-MGs of all natural long-chain fatty acids other than arachidonic acid, such as oleic, palmitic, stearic, linoleic, or docosahexaenoic acids are biosynthesized and inactivated by the same pathways than AEA and 2-AG respectively [33] [34]. However, many of these compounds cannot be considered true eCBs since they do not bind to CB1 or CB2 receptors, and they are called eCB-like or cannabimimetic compounds. Polyunsaturated NAEs from the n-6 fatty acid series C20:3 n-6 (N-di-homo- γ -linoleoylethanolamine, DGLEA), and C22:4 n-6 (N-docosatetraenoylethanolamine, DEA) are putative eCBs since they have a similar binding affinity for the CB1 receptor than C20:4 n-6 (AEA) [35]

[36]. However, the biological relevance of DGLEA and DEA is not known. Polyunsaturated NAEs from the n-3 fatty acid series C20:5 n-3 (N-eicosapentaenylethanolamine, EPEA), and C22:6 n-3 (N-docosahexaenylethanolamine, DHEA) can bind to the CB1 and the CB2 receptors but with a lower affinity than AEA [36]. Their biological significance is also unknown. NAEs derived from less unsaturated fatty acids C18:2 n-6 (N-linoleoylethanolamide, LEA), C18:1 n-9 (N-oleoylethanolamine, OEA), C16:0 (N-palmitoylethanolamine, PEA) and C18:0 (N-stearoylethanolamine, SEA) do not bind to CB1 or CB2 receptors but they are bioactive at other receptors. Cannabimimetic compounds may also enhance the activity of AEA and 2-AG by competition with inactivating enzymes or carriers (entourage effect) [37,38]. The most studied of the cannabimimetic compounds are OEA, that has anorectic effects, and PEA that has anti-inflammatory effects. OEA and PEA display their biological activities by activation of peripheral peroxisome proliferator-activated receptor-alpha (PPAR α) [39,40] [41]. AEA is also agonist of PPAR α [42]. PPAR α belongs to the superfamily of nuclear hormone receptors. PPAR α is a transcription factor that binds to DNA and leads to the transcription of target genes upon ligand activation. PPAR α is highly expressed in metabolically active tissues, such as liver, heart, skeletal muscle, intestinal mucosa and brown adipose tissue. This receptor is involved in the regulation of fatty acid catabolism and inflammatory processes [43,44]. AEA and 2-AG are agonists of peripheral peroxisome proliferator-activated receptor-gamma PPAR γ , which is another isoform of the peroxisome proliferator-activated receptor [42]. PPAR γ is highly expressed in adipocytes and it plays a key role in the regulation of adipogenesis and lipid biosynthesis [43]. OEA, PEA, LEA, 2-oleoylglycerol (2-OG) and other 2-MGs are agonists of GPR119. The activation of this receptor stimulates the release of glucagon-like peptide 1 (GLP-1) in the intestine [45,46]. GLP-1 is an

incretin involved in glucose homeostasis and satiation [47]. OEA has the highest affinity for GPR119, but the endogenous agonists of this receptor remain to be elucidated. It is becoming clear that the eCB system seems to interact with several other endogenous systems [48]. AEA, in addition to be an agonist of CB1, CB2, PPAR α , and PPAR γ is an agonist of the vanilloid receptor 1 (TPRV-1). AEA may be considered a dual endocannabinoid/endovanilloid [48,49]. TPRV-1, or capsaicin receptor 1, is a non-selective cation channel that acts primarily as pain sensor in the periphery but also modulates neurotransmitter release and synaptic plasticity in the brain [29]. Capsaicin, an active component of chilly peppers is agonist of TPRV-1, and its ingestion produces a burning sensation [50]. In the gut TPRV-1 has a key role in pain and inflammation by modulating the release of anti-inflammatory neuropeptides and other signaling molecules [51]. The orphan receptor GPR55, discovered by an “in silico” approach, has been considered a possible “third” eCB receptor. AEA, PEA, and with a lower affinity OEA, can bind to GPR55 [52]. A lysophosphatidylinositol (LysoPI) lipid, 2-arachidonoyl-sn-glycero-3-phosphoinositol, which is a possible precursor of 2-AG, may be the endogenous agonist of this receptor [53]. It is questionable, however, that GPR55 can be a real eCB receptor due to the low degree of similarity with the aminoacid sequence of CB1 and CB2 receptors and the data regarding the signaling cascades of CB1, CB2 and GPR55 [48] [54].

The endocannabinoidome has been expanded in the last twenty years with the isolation in tissues of other bioactive fatty acid derivatives related to eCBs: i) acyl amides of aminoacids (lipoaminoacids) such as N-arachidonoylglycine; ii) acyl amides of catecholamines (liponeurotransmitters) such as N-arachidonoyldopamine (NADA), N-oleoyldopamine (OLDA) or N-oleoylserotonin; iii) derivatives with different functional groups such as an ether (noladin ether), a primary

amide (oleamide) or an ester linkage to an ethanolamine (virodhamine) (**Figure 5**). However, the biosynthetic mechanisms, the endogenous molecular targets and the biological significance of most of these compounds are unresolved. Noladin ether was initially identified as an endogenous agonist of the CB1 receptor [55], and virodhamine was identified as an antagonist of CB1 receptor [56]. However, their endogenous existence has been questioned since later studies have not detected noladin ether or virodhamine in tissues [57,58]. There has been more luck with the acyl amides of dopamine NADA and OLDA. NADA and OLDA were identified, like AEA, as agonists of the capsaicin or vanilloid receptor 1 (TPRV-1) [59,60], and their existence in brain tissues, although elusive due to their low levels and chemical instability, has been confirmed in later studies [61]. NADA also seems to modulate synaptic function by activating both CB1 and TPRV-1 receptors [62]. NADA is also agonist of PPAR γ [42]. Acyl serotonins, which are a subclass of acyl amides of catecholamine, were identified in the intestinal tract. Acyl serotonins can inhibit FAAH and the release of GLP-1 in vitro but their biological relevance is unknown [63]. Endogenous acyl amino acids were identified in brain tissues and highlight the potential large number of lipid molecules generated by the combination by the amide bond of a fatty acid and an amino acid [64]. The biological relevance of acyl amino acids is largely unknown. The most known acyl amino acid is N-arachidonoylglycine, that is an agonist of orphan GPR18 receptor [65]. Finally, oleamide a endogenous lipid that accumulates in the cerebrospinal fluid under conditions of sleep deprivation and that can be degraded by FAAH, seems to modulate serotonergic transmission [66].

In summary, the number of compounds that may be part of the endocannabinoidome is quite large, which adds further complexity to the eCB system, already complex for the existence of several possible

molecular targets for the each compound. The scope of this thesis is restricted to the compounds biosynthetically more related to the true eCBs AEA and 2-AG, which are NAEs and 2-MGs.

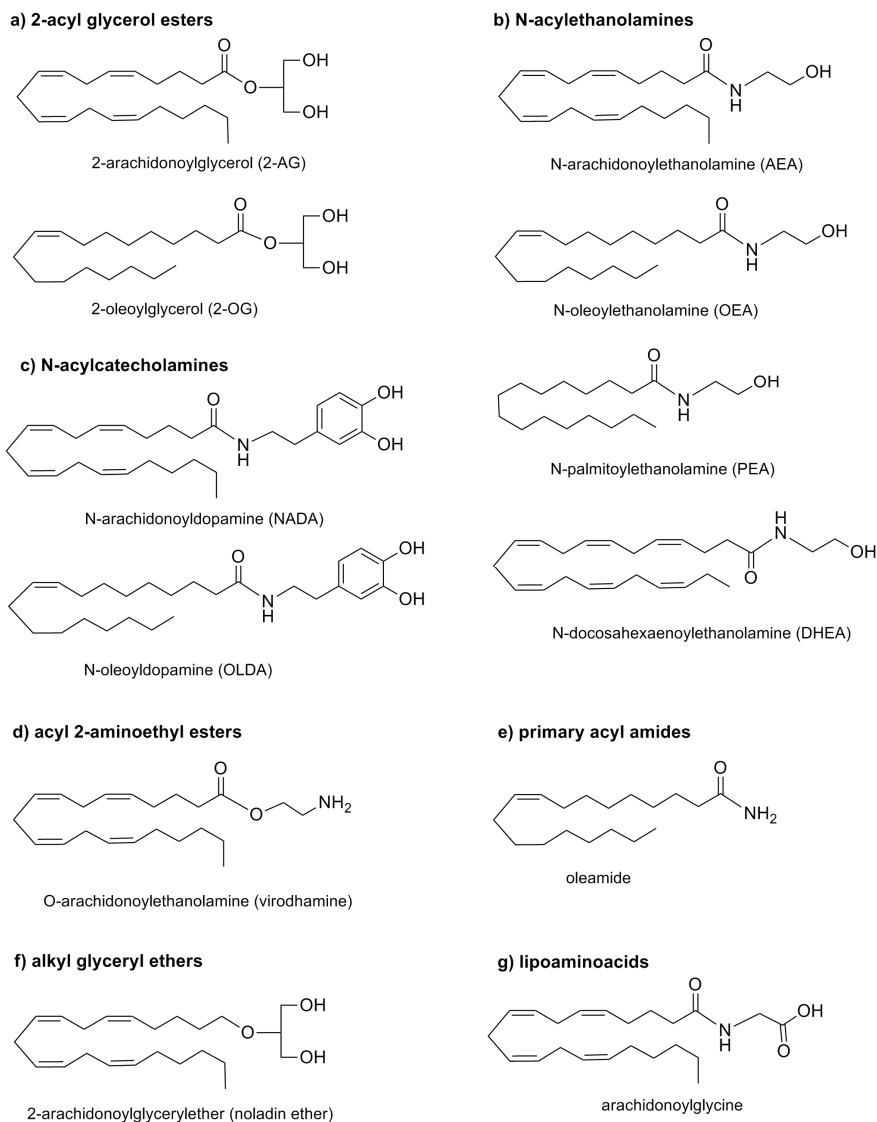


Figure 5. The endocannabinoidome

1.3 Obesity

1.3.1 Definition of obesity. The obesity epidemic

Obesity is a condition in which the excess of fat has accumulated in the body, in such a way that it can have an adverse effect on health. An increased consumption of highly caloric foods, without an equal increase in physical activity, leads to an unhealthy increase in weight. Decreased levels of physical activity result in an energy imbalance and lead to weight gain. Body mass index (BMI) is the most frequently used diagnostic score to classify overweight and obesity in adults, and it is a measure widely used in epidemiological studies. BMI is defined as a person's weight in kilograms divided by the square of his/her height in meters (Kg/m^2). The World Health Organization (WHO) defines obesity for a BMI greater than or equal to $30 \text{ Kg}/\text{m}^2$, and over-weight for a BMI greater than or equal to $25 \text{ Kg}/\text{m}^2$ [67,68]. Overweight and obesity represent a rapidly growing threat to the health of populations in an increasing number of countries. In 2005, 33% of the world adult population was over-weight or obese, and it is estimated that if the current trends continue, by 2030 up to 57.8% of the world adult population could be either over-weight or obese [69]. Overweight and obesity are the cause of a decreased life expectancy due to associated comorbidities such as cardiovascular disease, non-insulin-dependent diabetes mellitus, and cancer. Obesity is also associated to mood disorders, and in westernized countries it carries a social stigma. [67,68].

1.3.2 Obesity, body fat and health consequences

In obesity there is an excess of body fat in the organism. Body fat is accumulated in the form of triglycerides in adipose tissue. Adipocytes, which are the cells of adipose tissue, store triglycerides and release free fatty acids in response to energy demands. Adipose tissue is divided into specific regional depots with differences in structural organization, adipocyte size, and biological function. Adipose tissue is also an active endocrine tissue that regulates itself and other tissues [70]. Obesity is not a homogeneous condition. The relative distribution of excess fat between these adipose tissue depots seems to be more important than the total adipose tissue mass for the risk of developing obesity-associated diseases. Excess fat in the upper part of the body (central or abdominal obesity) vs. lower body or peripheral obesity (gluteofemoral) is associated with higher plasma glucose and insulin, hypertension, hyperlipidemia, and decreased HDL cholesterol concentrations, components of the insulin resistance syndrome, most known as metabolic syndrome, and constituting a cluster of risk factors for atherosclerotic cardiovascular disease [68,70]. Abdominal fat is composed of subcutaneous abdominal fat and visceral fat (or deep abdominal fat). Several studies have shown that the detrimental influence of abdominal obesity on metabolic processes is mediated by the visceral fat depot. Lipolysis, lipid synthesis, glucose uptake and gene expression are strongly influenced by adipocyte size. Omental adipocytes have smaller size and differential receptor expression than subcutaneous adipocytes. Fat deposited intracellularly, that enlarges the adipocyte, and the secretory products of the expanded adipocyte mass, which include free fatty acids, adipokines, and cytokines will overflow the liver and peripheral tissues. This will affect glucose, insulin, lipid and lipoprotein metabolism, which will lead to dyslipidemia, insulin resistance, type 2 diabetes and an inflammatory profile [68,70].

1.3.3 Possible causes of obesity

Obesity is the result of an imbalance between food intake and energy expenditure. An increase in food intake combined with lower lipid oxidation, lower thermogenesis or lower physical activity may account for this energy imbalance [71]. The underlying causes of obesity are not well understood since the control of body weight, essential for the survival of the organism, is a highly regulated process. The hypothesis of the thrifty genotype states, however, that evolution shaped us for an environment of food scarcity or to short intervals of food abundance mixed with large periods of food scarcity. Those individuals better shaped for this environment and that efficiently metabolized and stored nutrients were selected by evolution. Another hypothesis is the predator hypothesis. Archaic humans were subject to the evolutionary effects of predation that selected individuals with a lean mass. In either case, the environment that shaped our evolution for most part of human history is no longer present [71]. The effects of urbanization and industrialization have led to lifestyle changes such as less physically demanding work, mechanized transport, sedentarism, changes in daily food intake patterns, and changes in diet such as the consumption of highly caloric and processed foods, rich in saturated fat, sugar, and salt that have created an obesogenic environment. However, not everybody is becoming obese. There are individuals protected against obesity [71]. Certain human populations are more prone to obesity than others, and a number of genotypes associated to obesity are currently under investigation. Genes regulating human adipocyte formation and function may predispose to obesity [72,73]. Obesity is a multifactorial condition. Genetic variability and the environmental influence of an obesogenic environment promote that a substantial part of the world population is becoming over-weight or obese [68,69,71].

1.3.4 Brain homeostatic and hedonic regulation of food intake

1.3.4.1 Neural systems that modulate food intake and energy balance

In response to reduced body fat stores, adaptive changes occur in neuronal systems governing both food-seeking behavior (important for meal initiation) and satiety perception (important for meal termination). The net effect is that in response to weight loss, both the motivation to find food and the size of individual meals tend to increase until energy stores are replenished. This regulation is so fine-tuned that every day differences in the amount of food intake or energy expenditure do not translate to a change in body weight, which remains largely constant for long periods of time. The defense of body weight happens equally for normal-weight or obese individuals and explains the difficulty for any individual to lose weight once a set weight is achieved [74].

Food intake relies on our brain to obtain sensory information about a food, to evaluate for desirability and to choose the appropriate behavior. The brain regulates appetite and drives eating behavior by a complex interaction of homeostatic and hedonic processes involving hypothalamic and cortico-limbic circuits that integrate internal metabolic signals and internal and external stimuli [75]. With the aid of cognitive, visual, taste, and olfactory cues, foods are hedonically evaluated. This is integrated with short-term satiety signals and long-term adiposity signals regarding nutritional state, and an eating behavior is followed. During ingestion, the palatability of food is assessed using taste, smell, texture, and somatosensory information [76]. This information is combined with

satiety and adiposity signals and a reward value is assigned to food. Highly palatable foods have a higher reward value than bland foods. In other words, the motivation to eat is higher for palatable foods than for bland foods. However, the motivation to eat is also dependent on satiety and the current energy stores. The consequence of this neuronal systems integration is that the reward value of food is decreased with satiety and increased with hunger and lower energy stores. Following periods of positive energy balance, food intake is reduced through both a decrease in the rewarding properties of food and an increased response to input from satiety signals [77] (**Figure 6**).

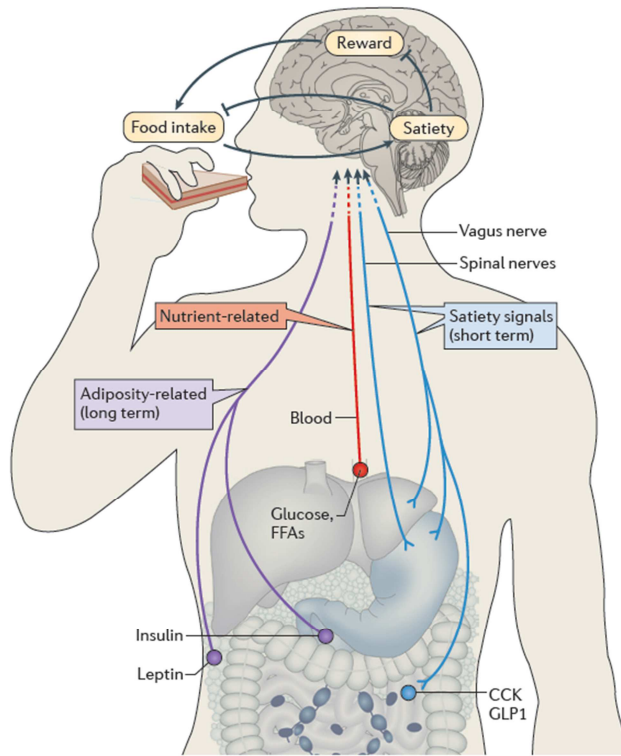


Figure 6. The central nervous system integrates input from long-term energy stores (for example, leptin) and short-term meal-related signals (nutrients and gut-derived satiety signals) to regulate food intake and energy expenditure in a manner that maintains stable body fat stores over time. Positive energy balance induced by overfeeding inhibits the rewarding properties of food while enhancing meal-induced satiety, thereby reducing food intake. In response to energy deprivation, central nervous system adaptive responses are engaged that both increase the rewarding properties of food and reduce the response to satiety signals, collectively resulting in increased food consumption until deficient fat stores are replenished. Cholecystokinin (CCK); free fatty acids (FFAs); glucagon-like peptide 1 (GLP-1); *Nat Rev Neurosci.* 2014;15:367-378.

1.3.4.2 Homeostatic modulation of food intake and energy balance

The main brain regions responsible for the regulation of energy homeostasis are the hypothalamus and the brainstem. The hypothalamus and brainstem receive neural and hormonal signals from the periphery that encode information about adiposity (long term signals) and acute nutritional state (short term signals). Nutrients themselves, like glucose and free fatty acids are also indicators of the nutritional state. Leptin, secreted by adipose tissue, and insulin, secreted by pancreas, are anorectic hormones that circulate in blood in proportion to body fat stores. The elevation of circulating leptin levels reduces food intake. Ghrelin is an orexigenic hormone secreted by the stomach. Circulating ghrelin levels increase by fasting, and fall after a meal. Receptors for these signals include two neurochemical distinct populations of neurons in the hypothalamic arcuate nucleus (ARC) which release neuropeptides that have opposing effects on food intake, such as neuropeptide Y (NPY), that stimulates food intake or α -melanocyte stimulating hormone (α MSH), that inhibits food intake. Neural and endocrine signals from the gastrointestinal tract have a role in short-term regulation of appetite. Glucagon-like peptide 1 (GLP-1) and cholecystokinin (CKK) are peptide hormones released from the gut in response to nutrient ingestion. GLP-1 and CKK are satiety signals that reduce food intake by supplying satiety information to the nucleus of the solitary tract (NTS) in the brainstem. Satiety information is also conveyed to the brainstem by neural signals generated on the vagus nerve by gastric distension. Homeostatic and satiety signals are integrated by direct and indirect connections between hypothalamic and brainstem areas. Neurons in ARC project to second order neurons in adjacent hypothalamic nuclei, including the paraventricular nucleus (PVN) and lateral hypothalamic area (LHA),

which in turn project to the nucleus of the solitary tract (NTS). In addition, leptin acts on receptors both in the hypothalamus and the NTS. In this regard, leptin reduces food intake in part by enhancing the response of the brain to satiety signals [74,77] [78].

1.3.4.3 Integration of homeostatic and hedonic processes in the modulation of food intake

The integration of homeostatic and hedonic signals is another key aspect in the brain regulation of food intake. Brain reward circuits that process the perception of food reward are modulated by homeostatic signals. These reward circuits include mesolimbic dopaminergic neurons in the ventral tegmental area (VTA) that project to the nucleus accumbens (NAc), the hedonic hotspot, and other forebrain areas to intensify the reward value of palatable food [77]. The consumption of palatable food promotes the release of dopamine in NAc. The release of dopamine in the NAc has been associated to the motivation behavior to other pleasant natural rewards like sex or to artificial rewards like drugs of abuse [79]. In the hypothalamus dopamine release inhibits food intake, and this is associated with the duration of meal consumption [80]. Neurons in the LHA integrate reward-related input from the NAc with information related to energy homeostasis from ARC neurons. In turn, LHA neurons project to and influence the mesolimbic dopaminergic system while also influencing satiety perception through projections to the hindbrain. Weight loss lowers plasma, insulin and leptin levels while increases plasma ghrelin levels. Working in concert, these responses increase the rewarding properties of food and hence the motivation to eat through either direct effects in the ventral striatum or indirect effects in the hypothalamus through the LHA. Conversely, following periods of positive

energy balance, body weight is returned to its biologically defended level through both a decrease in the rewarding properties of food and an increased response to input from satiety signals. [77]. Palatable foods are, however, often consumed even after energy requirements have been met. Thus, hedonic processes can override homeostatic and satiety signals. It has been postulated that the neural substrate of obesity is a higher sensitivity of vulnerable individuals to food reward. Our susceptibility to the sight, taste, or thought of foods, an environment full of food cues that impels over-consumption, and an easy and effortless access to energy-rich palatable foods are factors that lead to overweight and obesity when they are matched with reduced energy expenditure [81] [82] [83]. Another hypothesis is that obese subjects may have a diminished reward response or anhedonia due to low dopamine activity. Obese subjects would overeat to compensate for this deficiency. This condition may also be progressive. Thus, the overconsumption of palatable food could lead to obesity due to neuroadaptive changes in brain reward systems, such as down-regulation of dopamine receptors [79 , 80, 82, 83,84]

1.3.5 The endogenous cannabinoid system as a homeostatic and hedonic modulator of food intake

The appetite stimulating properties of *Cannabis sativa* preparations have been known since ancient times. Modern cannabis users are also very familiar with the drug's capacity to stimulate eating, which is referred colloquially as "the munchies" [8,85]. Following cannabis smoking, users report strong cravings for, and an intensification of the sensory and hedonic properties of food, which drives them to the over-consumption of palatable food [86]. These effects are mediated by $\Delta 9$ -

THC, the psychoactive compound present in cannabis, which activates brain CB1 receptors. The endocannabinoids (eCBs) anandamide (AEA) and 2-arachidonoylglycerol (2-AG), which are the endogenous agonists of this receptor (section 1.2.1), are lipid mediators of the endogenous cannabinoid system (section 1.2.2). Following the discovery of eCBs, eCB receptors and eCB biosynthetic and degrading enzymes, it was suspected that the endogenous cannabinoid system would be related to the modulation of food intake. It is now well established that the eCB system is both a homeostatic and hedonic modulator of food intake. The eCB system is thus intimately linked to our natural motivation to eat and enjoyment of food when hungry [87]. The orexigenic effects of eCBs are exerted in the brain by CB1-mediated stimulatory and inhibitory effects on hypothalamic orexigenic and anorectic neuropeptides, respectively; by facilitating dopamine release in the nucleus accumbens (NAc) shell; and by regulating the activity of sensory and vagal fibers in brainstem-duodenum neural connections. In turn, the levels of AEA and 2-AG and/or CB1 receptors in the brain are under the control of leptin, ghrelin and glucocorticoids in the hypothalamus, under that of dopamine in the limbic forebrain and under that of cholecystinin (CKK) and ghrelin in the brainstem. These bi-directional communications between the eCB system and other key players in energy balance ensure that eCBs act in a coordinated manner to enhance food intake, particularly after food deprivation. [87] [88].

The gut-brain axis has emerged as an important modulator of food intake. The eCB system is present in the intestine. It has been suggested that the orosensory properties of fat elevate eCB levels in the intestine, which reinforce fat intake via CB1 receptor activation. This effect would be mediated by vagal afferent and efferent terminals [89]. ECB-related compounds may also have a role in the peripheral regulation of food

intake, but which is opposite to the role of true eCBs. The most studied of such compounds is the anorectic lipid N-oleoylethanolamine (OEA) [90]. OEA does not bind to CB1 or CB2 receptors and its anorectic actions are mediated by activation peroxisome-proliferator-activated-receptor- α (PPAR α) in the gut [39]. OEA satiety effects need the participation of afferent fibers of the vagus nerve. It has been proposed that the ingestion of dietary fat increases the formation of OEA in the intestine and this is a mechanism to regulate satiety and prolong the interval between successive meals [91] [92].

1.3.6 The endocannabinoid system and obesity. Influence of the diet on the eCB system

A sustained hyperactivity of the eCB system may contribute to obesity. In obesity and type 2 diabetes the peripheral eCB system is dysregulated [93] [94]. Circulating eCB levels are higher in obese than lean individuals [95] and circulating 2-AG levels correlate with adiposity and metabolic parameters such as body mass index (BMI), waist circumference, intra-abdominal adiposity and insulin levels [93] [96,97]. The eCB system is also found in peripheral organs involved in energy balance such as liver, pancreas, skeletal muscle and adipose tissue where it plays an active role in glucose homeostasis, lipid metabolism and adipogenesis. The hyperactivity of the eCB system in those organs promotes lipogenesis, adipogenesis and the accumulation of body fat [85,88,98-100]. A hyperactive eCB system in obesity is related to dyslipidemia, leptin and insulin resistance [101] [102]. Leptin and insulin in turn modulate the release of eCBs [103]. The strong effect of the eCB on lipid metabolism led to the development of an anti-obesity drug, rimonabant, which is an inverse agonist of the CB1 receptor. Rimonabant

was effective in the reduction of body weight and dyslipidemia but it had to be withdrawn due to psychiatric effects (anxiety and depression). Currently, there is no equivalent drug to fight against obesity and peripheral antagonists of CB1 receptor are promising drug targets [10,103]. In obesity, the biosynthesis of N-acylethanolamines PEA and OEA may also be dysregulated in peripheral tissues such as adipose tissue and pancreas [104]. PEA is also the cannabimimetic compound more abundant in adipocytes [105]. A recent report has shown changes in plasma levels of AEA and PEA of morbid obese females following bariatric surgery [106].

The eCBs AEA and 2-AG are derived from arachidonic acid, which is an essential polyunsaturated fatty acid (PUFA) from the n-6 series. PUFA, from n-6 and n-3 series, can only be obtained through the diet. It has been suggested that the amount and PUFA content of the food consumed can directly influence eCBs, possibly by influencing the brain amounts of their phospholipid precursors. The dietary intake of linoleic acid, an n-6 PUFA precursor of arachidonic acid, has increased dramatically during the last decades and this has been associated with a greater prevalence of obesity. An imbalance in the diet between n-6 PUFA vs n-3 PUFA could thus lead to an increase in eCB biosynthesis and lead to obesity [107,108].

1.3.7 Olfaction and eating behavior. Modulation by the endocannabinoid system

Olfaction contributes to our food choices and eating behavior by participating in the hedonic evaluation of foods. The sense of smell is essential for human flavor perception [109]. The olfaction of foods can be

divided physiologically into orthonasal and retronasal olfaction. Orthonasal olfaction is olfaction through the external nares, and is important for the hedonic evaluation of foods by means of food aromas. Retronasal olfaction is olfaction of food volatiles that are released during food consumption and enter from the back of the mouth through the nasopharynx. Retronasal olfaction is necessary for flavor perception. Compared to taste, that has five basic tastes (salty, sour, sweet, bitter, and umami) humans can recognize more than 10,000 different food volatiles. The complexity of food flavors that we can experience is thanks to olfaction. And thus, when we refer to a food taste we also mean retronasal olfaction [76,109,110]. The loss of olfaction makes the food less flavorful and enjoyable and this may alter eating behavior [111]. Taste and olfaction are altered in eating disorders. Anorexic patients and bulimic patients have olfactory and taste deficits [112,113] [114,115]. At the other end of the BMI spectrum, olfactory deficits have been linked to obesity. Morbid obese individuals have a lower olfactory capacity than moderately obese individuals [116].

Flavor perception is one of the most complex of human behaviors. Flavor involves almost all of the senses, particularly the sense of smell, and taste. The color, texture and somatosensorial modalities of foods also contribute to flavor. The representation of flavor, which tells us about the pleasantness and palatability of foods is done in the orbitofrontal cortex (OFC), a region in the prefrontal cortex [109]. The OFC functions as part of various networks that include regions of the medial prefrontal cortex, hypothalamus, amygdala, hippocampus, insula/operculum and dopaminergic midbrain, and areas in the basal ganglia including the ventral and dorsal striatum.[117] (**Figure 7**).

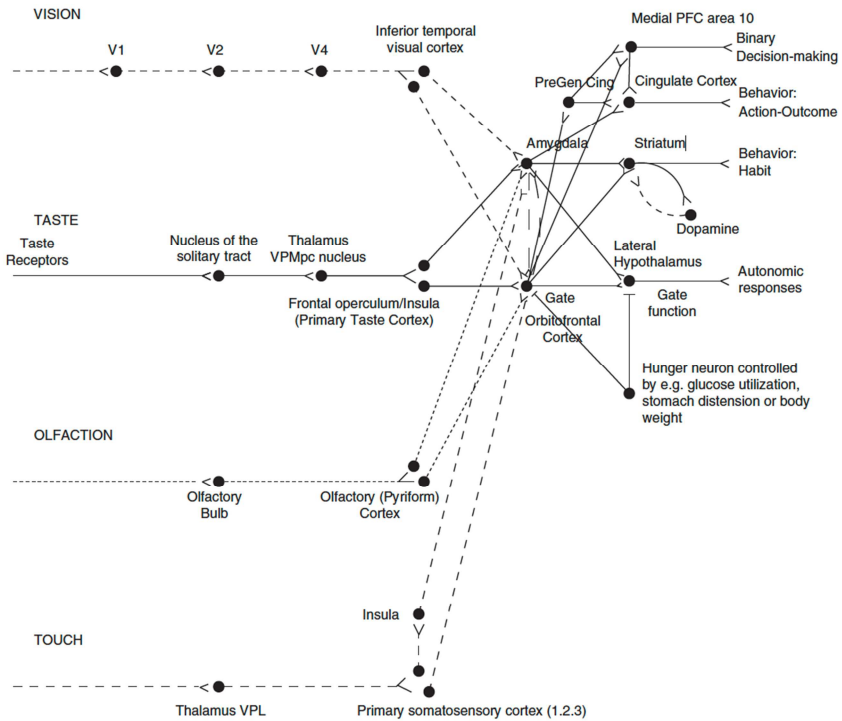


Figure 7. Schematic diagram showing some of the gustatory, olfactory, visual and somatosensory pathways to the orbitofrontal cortex (OFC), and some of the outputs of the OFC in primates. The secondary taste cortex and the secondary olfactory cortex are within the OFC. ‘Gate’ refers to the finding that inputs such as the taste, smell and sight of food in some brain regions only produce effects when hunger is present. The column of brain regions including and below the inferior temporal visual cortex represents brain regions in which what stimulus is present is made explicit in the neuronal representation, but not its reward or affective value, which are represented in the next tier of brain regions, the OFC and amygdala, and in areas beyond these. Medial prefrontal cortex area 10 (Medial PFC area 10); ventralposteromedial thalamic nucleus (VPMpc); V1, primary visual cortex (V1); visual cortical area V4 (V4); pregenual cingulate cortex (PreGen Cing); *Int J Obes (Lond)*. 2011;35:550-561

The OFC receives sensorial inputs of the five classic sensory modalities: gustatory, olfactory, somatosensory, auditory and visual. It also receives visceral sensory information. This information is then available for multi-modal integration and encoding of the reward value of the stimulus. The combination of these stimuli and the learned associations between them, for instance taste-smell interactions, color and texture of consumed foods and its postingestive consequences contribute to flavor. This integration also allows that food eaten to satiety will have reduced flavor pleasantness representations in the OFC. The neuroanatomical connectivity of the OFC makes it a unique nexus for sensorial integration, the modulation of autonomic reactions, and participation in learning, prediction and decision making for emotional and reward-related behaviors. The representations of the reward value of foods in the OFC can also be modulated by cognitive factors and attention to the affective properties of food. All these neural systems are the neural substrates for our desirability of foods, the motivation to eat and the inhibitory control of food intake [76,109,117].

Olfaction influences both appetite and satiety in humans [118]. A high reactivity to olfactory food cues has been observed in over-weight children [119]. Food-related odors activate brain reward circuits during hunger, and the more active areas are different in obese and normal-weight subjects [120]. Converging evidence suggests that the olfactory system is intimately linked to neural systems that regulate food intake by acting as a sensor of the metabolic state [121]. This is supported by the presence in the olfactory bulb of receptors of several hormones and neuromodulators that regulate food intake, among them: insulin, leptin, ghrelin, orexin or endocannabinoids [121].

The endocannabinoid (eCB) system promotes eating in fasted mice by enhancing the sense of smell. The decrease in odor threshold is mediated by eCB modulation of synaptic transmission in the main olfactory bulb [122]. This important finding raises issues regarding the role of odor perception in eating behavior and obesity. As reviewed by Kirkham [86], exogenous and endogenous cannabinoids stimulate food intake by increasing the motivation to eat and by amplifying the palatability, or orosensory reward of food. Administration of the cannabinoid Δ^9 -THC improves taste and smell and the enjoyment of food in cancer patients [123]. In obesity, the central and peripheral eCB system becomes over-active [95] [88]. Peripheral signals that regulate food intake like insulin, leptin or ghrelin that interact with the eCB system and which are also altered in obesity [103] seem to modulate olfactory sensitivity [121,124-126]. It is noteworthy that obese Zucker rats deficient in leptin signaling exhibit heightened sensitivity to olfactory food cues [125].

1.4 Evaluation of olfactory function. Relation to cognitive function

Olfaction has two components, detection and perception. Odor perception, which includes odor discrimination and odor identification, is much more complex than odor detection and it needs the processing of higher-order cognitive brain areas. First, the odorants are detected on the nasal epithelium by olfactory receptor neurons (ORN). Each ORN expresses just one receptor subtype out of approximately 350 receptors in humans. A single odorant can bind to multiple receptor subtypes and a single receptor can bind to multiple, different odorants. This allows the formation of and odor pattern. Second, the information is sent and

processed in the brain. Axonal projections of ORNs converge in the olfactory bulb glomeruli and form synapses with the dendrites of mitral and tufted cells. Axonal projections from these cells are conveyed via the lateral olfactory tract and terminate on several areas of the primary olfactory cortex, which include the anterior olfactory nucleus, olfactory tubercle, piriform cortex, amygdala, and entorhinal cortex. From the primary olfactory cortex odor information is relayed to other brain areas. Differently to other senses that need the thalamus relay, the olfactory sense is unique since it is the only sense that has a direct connection to the higher cognitive centers of the brain. The olfactory bulb has direct connections to the piriform cortex. The piriform cortex and the amygdala both project to the orbitofrontal cortex (OFC) which with the amygdala is involved in emotion and associative learning (Figure 7), and to the entorhinal/hippocampal system which is involved in long-term memory including episodic memory [127-129] [130]. In all humans olfactory function decreases gradually with age [131,132]. Olfactory dysfunction is involved in several neurodegenerative diseases, such as Parkinson disease and Alzheimer's disease [133]. It has been observed that cognitive performance in executive functioning, semantic memory, and episodic memory contribute significantly to odor discrimination and odor identification performance, while cognitive factors are less related to odor threshold capacity [134]. Patients with early stages of Alzheimer's disease, a neurodegenerative disorder characterized by a progressive memory loss and cognitive debilitation, exhibit perceptual deficits in odor identification due to disruption of odor quality coding in the piriform cortex [135]. The evaluation of olfaction capacity, particularly with regard to the domains of olfactory discrimination and olfactory identification can be used for early diagnosis of mild cognitive impairment and Alzheimer's disease [136]. The Sniffin' Sticks test, which is a commercial test validated for the evaluation of odor threshold, odor

identification, odor discrimination [137], is currently the most widely used test for the evaluation of olfactory function in medical practice.

1.5 Methodological issues for the quantification of circulating plasma endocannabinoids

Circulating plasma eCBs are considered biomarkers of the state of the eCB system. A number of publications have been devoted to the analysis of eCBs in plasma, and an effort has recently been made to establish reference intervals for five eCBs in human plasma [138]. As the chemistry and biology of eCBs are better understood, there is the need to improve measurements in human plasma through greater control of factors that introduce variability. At present, such factors still limit the inter-changeability of EC plasma concentrations from clinical studies. It has already been established that the chemical properties of eCBs, with respect to their stability during analytical procedures (extraction solvents, pH conditions, and evaporation of organic solvents) and their absorption by glassware and plastic materials, are very relevant factors to take into consideration. A comprehensive review has provided a full discussion on these issues [139] and several analytical methods have already taken into account these factors [138,140]. Discrepancies amongst laboratories probably originate from pre-analytical sample procurement protocols and compound-specific factors.

Concerning biological matrices, eCBs are unstable in those where enzymes are involved in their synthesis and clearance. Nevertheless, accumulated experience suggests that the incorporation of unspecific enzyme inhibitors of amidases, esterases and proteases, such as phenylmethylsulfonyl fluoride (PMSF), to sample collection tubes is not

justified. However, blood containing tubes not centrifuged immediately in cold conditions after withdrawal may cause artifactual, exaggerated N-acylethanolamine concentrations due to ex-vivo release of from erythrocytes or leukocytes [138]. Additionally, it has been reported ex-vivo synthesis of 2-AG for plasma preserved at room temperature and abundant 2-AG/1-AG isomerization or acyl-migration (**Figure 8**) due to sample analysis conditions. In aqueous solution 2-MG isomerize to 1-MG [138,140].

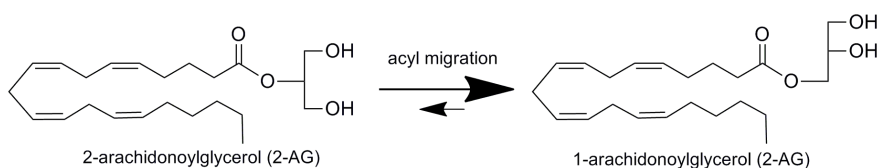


Figure 8. Acyl-migration (isomerization) of 2-arachidonoyl glycerol (2-AG) to 1-arachidonoyl glycerol (1-AG)

Both the issue of acyl migration (or isomerization) and the ex-vivo generation of eCBs from blood or plasma are important factors to take into consideration to be able to use plasma endocannabinoids as biomarkers for clinical and translation studies. In regards to acyl migration, only the isomer 2 is bioactive. ECBs generated ex-vivo from blood or plasma also do not have biological significance. These issues comprise one of the objectives of this thesis.

2. OBJECTIVES

2. OBJECTIVES

The foundation of this thesis started with the creation in 2006 of the Spanish Biomedical Research Centre in Physiopathology of Obesity and Nutrition (Centro de Investigación Biomédica en Red de Fisiopatología de la Obesidad y Nutrición: CIBERObn, www.ciberobn.com), a public research consortium. CIBERObn gathers 25 research groups from different Spanish Hospitals, Universities and Research Centers. The CIBERObn mission is to promote a better knowledge about the mechanisms contributing to obesity development in order to reduce its incidence and prevalence, as well as its medical comorbidities. In addition, CIBERObn is interested at eating disorders (anorexia, bulimia...). CIBERObn is structured into 8 scientific programs. The program that concerns this thesis is the P4. Neurocognition and environmental-biological factors. The basis of this program are the studies of genetic and psychiatric comorbidity that suggest that an underlying neurocognitive pathology is present in extreme weight situations, either in eating disorders such as anorexia nervosa that give rise to malnutrition or to extreme weight situations associated to obesity. This neurocognitive pathology is probably related to emotional and reward processes of eating behavior. The approach of this project is the multidimensional study of the environmental, neuropsychological and biological factors associated to extreme weight situations.

The endocannabinoid (eCB) system is a crucial regulator of many pathophysiological processes, which include pain, anxiety and obesity. The eCB system is a key modulator in the homeostatic and hedonic aspects of food intake, and thus a biological factor of interest for the study of obesity. The scope of this thesis is the study of eCBs and eCB-like

compounds, which are endogenous esters and amides of natural fatty acids, and its effects on health. The main objectives of this thesis are:

- I. To develop and validate analytical methodology for the quantification of eCBs and eCB-like compounds to be used as biomarkers in clinical and translational studies.

- II. To evaluate the interaction between the eCB system, olfactory capacity and obesity.

3. HYPOTHESES

3. HYPOTHESES

In this thesis we considered the following hypotheses:

- a) Endocannabinoids are under evaluation as biomarkers of number physiopathological conditions. The lack of interchangeability of endocannabinoid concentrations in biological matrices, limit their usefulness in clinics and translational research. To overcome these problems researchers should take into account a number of issues concerning sample procurement, preservation, processing and analysis. The artefactual monoacylglycerols (MGs) generation, the chemical isomerization of MGs in plasma and the artefactual generation of N-acylethanolamines (NAEs) in blood are some of the challenges to be confronted.
- b) Increasing subject's BMI has been associated to deficits in olfactory capacity. Olfaction is modulated by the endocannabinoid system, as this system enhances the sense of smell in animal models. It is expected that in extreme weight categories there is an association between BMI, olfactory capacity and endocannabinoids.

4. MATERIALS AND METHODS

4.1 Quantification of circulating plasma endocannabinoids

4.1.1 Chemicals, standards and laboratory material

Ammonium acetate (Am. Ac.), acetic acid, tert-butyl-methyl-ether (TBME), acetonitrile, and formic acid (FA) were from Merck (Darmstadt, Germany). 1-arachidonoyl glycerol (1-AG), 1-arachidonoyl glycerol-d5 (AG-d5), 2-arachidonoyl glycerol (2-AG), 2-arachidonoyl glycerol-d5 (2-AG-d5), 2-arachidonoyl glycerol-d8 (2-AG-d8), 2-linoleoyl glycerol (2-LG), 1-linoleoyl glycerol (1-LG), N-arachidonoyl ethanolamine or anandamide (AEA), N-arachidonoyl ethanolamine-d4 (AEA-d4), N-arachidonoyl ethanolamine-d8 (AEA-d8), N-docosatetraenoyl ethanolamine (DEA), N-dihomo- γ -linolenoyl ethanolamine (DGLEA), N-docosahexaenoyl ethanolamine (DHEA), N-docosahexaenoyl ethanolamine-d4 (DHEA-d4), N-linoleoyl ethanolamine (LEA), N-linoleoyl ethanolamine-d4 (LEA-d4), N-palmitoyl ethanolamine (PEA), N-palmitoyl ethanolamine-d4 (PEA-d4), N-palmitoleoyl ethanolamine (POEA), N-oleoyl ethanolamine (OEA), N-oleoyl ethanolamine-d4 (OEA-d4), N-stearoyl ethanolamine (SEA), N- α -linolenoyl ethanolamine (α -LEA), and N-eicosapentaenoyl ethanolamine (EPEA) were from Cayman Chemical (Ann Harbor, MI). 1-oleoyl glycerol (1-OG) and 2-oleoyl glycerol 2-OG were from Sigma-Aldrich (St. Louis, MO). 1-oleoyl glycerol-d5 (1-OG-d5) and 2-oleoyl glycerol-d5 (2-OG-d5) were from Toronto Research Chemicals (North York, ON, Canada). FIPI hydrochloride [CAS 939055-18-2], D609 [CAS 83373-60-8], edelfosine [CAS 77286-66-9] and GSK 264220A [CAS 685506-42-7] were from Tocris Bioscience (Bristol, UK). Orlistat (tetrahydrolipstatin) was from Cayman Chemical (Ann Harbor, MI). KT172, KT109 and RHC 80267

[CAS 83654-05-1] were from Sigma-Aldrich (St. Louis, MO). KIMAX 16 x 125 mm screw cap glass borosilicate tubes were from Kimble Chase (Mexico). Nunc 1.8 mL cryotube vials were from Thermo Fisher Scientific (Roskilde, Denmark). Ultrapure deionized water was produced by a Milli-Q Advantage A10 system from Millipore (Madrid, Spain).

The purity of the N-acyl ethanolamine (NAE) standards AEA, DEA, DGLEA, DHEA, DHEA, LEA, PEA, PEA, POEA, POEA, OEA, and SEA was >98 % as provided by the manufacturer. Purity of the monoacylglycerol (MG) standards 2-AG, 1-AG and 2-LG was >95%; and for 2-OG > 94%, 1-OG >99%, and 1-LG > 90%, respectively. The 2-MG standards were a combination of 90% isomer 2 and 10% isomer 1. The isomeric purity of the MG standards and their deuterated analogs was verified by injecting the individual standard solutions into the LC/MS-MS system with the following results: 91.2% 2-AG, 91.5% 2-AG-d5, 100% 1-AG, 100% 1-AG-d5, 97.3% 2-OG, 94.3% 2-OG-d5, 100% 1-OG, 88.0% 1-OG-d5, 98.7% 2-LG, 100% 1-LG. The isotopic purity of the deuterated analogs of NAEs and MGs was > 99% for all compounds. Stock and working standard solutions were prepared in acetonitrile and stored at -20°C. Whilst working standard solutions of up to 10 µg/mL were stable for protracted periods of time, a limited solubility was observed at a higher concentration (1 mg/mL) of stock solutions of saturated and monounsaturated NAEs and MGs after conservation at -20°C. Two mixtures of internal standard (ISTD) were used: ISTD mix 1 prepared at 0.01 µg/mL AEA-d4, 0.01 µg/mL DHEA-d4, 0.02 µg/mL LEA-d4, 0.04 µg/mL PEA-d4, 0.04 µg/mL OEA-d4, 0.2 µg/mL 2-AG-d5, 1 µg/mL 2-OG-d5, and ISTD mix 2 prepared at 5.0 µg/mL 2-AG-d8, 0.25 µg/mL AEA-d8. The two mixes of ISTD were spiked into the plasma samples at a fixed volume of 25 µL. The structures of the eCB analytes (NAEs and 1/2-MGs) and deuterated analogs are represented in **Figures 9** and **10**.

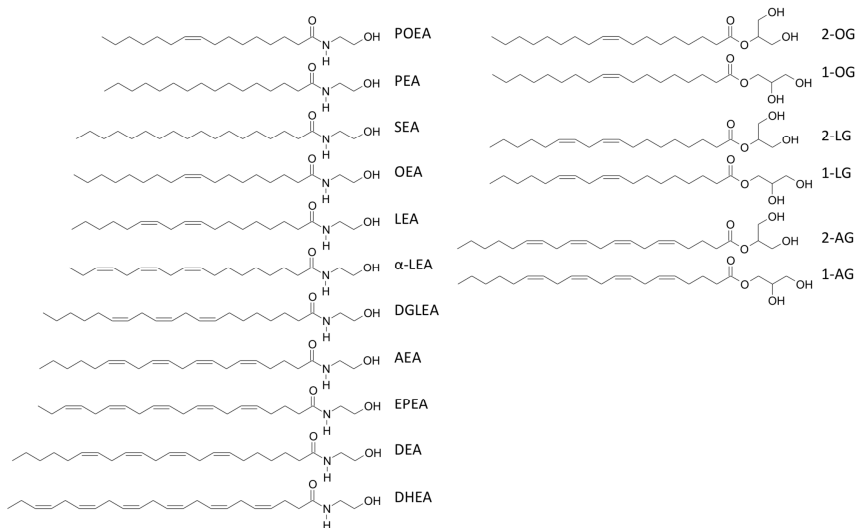


Figure 9. Structures of N-acylethanolamines (NAEs) and 2/1-monoacylglycerols (2-MGs). *J Lipid Res.* 2014;55:966-77

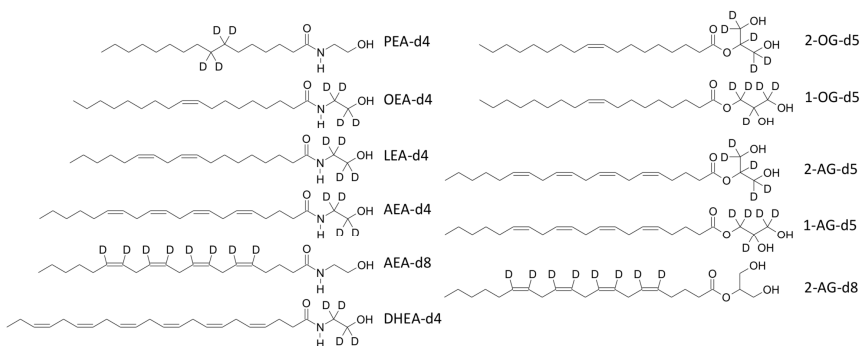


Figure 10. Structures of the deuterated analogs of N-acylethanolamines (NAEs) and 2/1-monoacylglycerols (2-MGs). *J Lipid Res.* 2014;55:966-77

4.1.2 Human subjects

Three human male volunteers were recruited for the procurement of fresh blood samples following protocol MUESBIOL/1 (“Protocol for the collection of biological samples for biomedical research studies”). Twenty five female healthy control volunteers of BMI <25 kg/m² were recruited for the procurement of fresh blood samples following the TANOBE protocol. Both protocols have been approved by the Ethical Committee of Parc de Salut Mar Barcelona (CEIC-PSMAR) and comply with the Declaration of Helsinki. An informed consent was obtained from the human subjects.

4.1.3 Sample preparation

Blood freshly extracted from human volunteers was collected in 10 mL K2E 18.0 mg (EDTA) BD Vacutainer tubes and centrifuged immediately for 15min at 1700 g in a refrigerated centrifuge (4°C). Plasma was then immediately separated from the blood and distributed in aliquots for further processing or stored at -80°C. Discarded human plasma batches from the Blood Bank of Hospital del Mar of Barcelona were used for the validation experiments.

Plasma samples were thawed in less than 30 min at room temperature and processed on ice. Aliquots of 0.5 mL were transferred into glass borosilicate tubes, spiked with 25 µL of ISTD mix 1 or mix 2, diluted up to 1 mL with 0.1M Ammonium Acetate buffer (pH 4.0) extracted with 6 mL of TBME and centrifuged (1700g, 5 min) at room temperature. The organic phase was transferred to clean tubes, evaporated (40°C, 20 min) under a stream of nitrogen, and extracts were reconstituted

in 100 μL of a mixture of water:acetonitrile (10:90, v/v) with 0.1% FA (v/v) and transferred to HPLC vials. Twenty μL were injected into the liquid chromatography–mass spectrometry (LC-MS-MS) system.

4.1.4 Liquid-chromatography/Mass Spectrometry conditions

An Agilent 6410 triple quadrupole (Agilent Technologies, Wilmington, DE) equipped with a 1200 series binary pump, a column oven and a cooled autosampler (4°C) was used. Chromatographic separation was carried out with a Waters C18-CSH column (3.1 x 100 mm, 1.8 μm particle size) maintained at 40°C with a mobile phase flow rate of 0.4 mL/min. The composition of the mobile phase was: A: 0.1% (v/v) FA in water; B: 0.1% (v/v) FA in acetonitrile. The initial conditions were 40% B. The gradient was first increased linearly to 90% B over 4 minutes, then increased linearly to 100% B over 5 minutes and maintained at 100% B for 3 minutes, to return to initial conditions for a further 4 minutes with a total run time of 16 minutes. The ion source was operated in the positive electrospray mode. Desolvation gas temperature of 350°C and a gas flow rate of 10 L/min were used. The pressure of the nebulizer was set at 40 psi and the capillary voltage at 4,000 V. The multiple reaction monitoring mode (MRM) was employed for quantification. The experimental mass spectrometry conditions for each compound are listed in **Tables 1 and 2**.

Table 1. Experimental LC/MS-MS parameters for the analyte detection

Analyte	Mw	RT	CV %	P	Q	I	F	CE	IS	RF
2-AG	378.6	7.65	0.08	379	287	269, 203	135	12	2-AG-d5	1.00
1-AG	378.6	7.77	0.30	379	287	269, 203	135	12	2-AG-d5	1.00
2-LG	354.5	7.76	0.06	355	263	245, 337	135	12	2-OG-d5	0.79
1-LG	354.5	7.94	0.08	355	263	245, 337	135	12	2-OG-d5	0.79
2-OG	356.5	8.61	0.41	357	265	247, 339	135	12	2-OG-d5	1.00
1-OG	356.5	8.82	0.08	357	265	247, 339	135	12	2-OG-d5	1.00
AEA	347.5	7.22	0.07	348	62	44, 287	135	12	AEA-d4	1.00
DEA	375.6	7.99	0.08	376	62	44	135	12	AEA-d4	1.26
DGLEA	349.6	7.61	0.08	350	62	44	135	12	AEA-d4	1.68
DHEA	371.6	7.11	0.07	372	62	44	135	12	DHEA-d4	1.00
EPEA	345.5	6.66	0.13	346	62	44	135	12	AEA-d4	1.00
LEA	323.5	7.26	0.07	324	62	44	135	12	LEA-d4	1.00
α -LEA	321.5	6.66	0.11	322	62	44	135	12	LEA-d4	1.00
OEA	325.5	8.05	0.06	326	62	44, 309	135	12	OEA-d4	1.00
PEA	299.5	7.81	0.07	300	62	44, 283	135	12	PEA-d4	1.00
POEA	297.5	6.94	0.08	298	62	44	135	12	PEA-d4	1.00
SEA	327.5	9.11	0.07	328	62	44, 311	135	12	OEA-d4	1.00

Molecular weight (MW); retention time (RT, min); coefficient of variation of the retention time (CV %); precursor ion (P, m/z); quantifier product ion (Q, m/z); identifier/s product ion/s (I, m/z); fragmentor (F, V); collision energy (CE, eV); internal standard (IS); response factor of the analyte versus the internal standard (RF); *J Lipid Res.* 2014;55:966-77.

Table 2. Experimental LC/MS-MS parameters for the deuterated analogs detection

Deuterated analog	MW	RT	Q1	Q3	F	CE
2-AG-d5	383.6	7.63	384.3	287	135	12
1-AG-d5	383.6	7.77	384.3	287	135	12
2-AG-d8	386.6	7.59	387.5	295	135	12
2-OG-d5	361.6	8.59	362.2	265.3	135	12
1-OG-d5	361.6	8.79	362.2	265.3	135	12
AEA-d4	351.6	7.21	352.2	66	135	12
AEA-d8	355.6	7.19	356.2	62	135	12
DHEA-d4	375.6	7.09	376.3	66	135	12
LEA-d4	327.5	7.24	328.5	66	135	12
OEA-d4	329.6	8.04	330.4	66	135	12
PEA-d4	303.5	7.79	304.4	66	135	12

Molecular weight (MW); retention time (RT, min); precursor ion (Q1, m/z); product ion (Q3, m/z); fragmentor (F, V); collision energy (CE, eV); *J Lipid Res.* 2014;55:966-77.

4.1.5 Method development and validation

4.1.5.1 Linearity

The linearity of the method was assessed for seven surrogated analytes by construction of calibration curves using plasma samples spiked with deuterated analogs of NAE and MG. Analysis was performed in quadruplicate for the following surrogated analytes: AEA-d4, LEA-d4, PEA-d4, OEA-d4, DHEA-d4, 2-AG-d5, and 2-OG-d5. The ISTD were 2-AG-d8 and AEA-d8 (ISTD mix 2), which have additional deuterium atoms in their structure. 2-AG-d8 was used as ISTD of 2-MG, and AEA-d8 as ISTD of NAE. The regression analyses of the calibrations curves were performed with SPSS 12.0 with a 1/x weighting factor.

4.1.5.2 Quantification calculations

Experimental LC/MS-MS parameters for the detection of analytes and the deuterated analogs are presented in Tables 1 and 2. The quantification of the surrogated analytes was calculated by interpolation of the response ratios on the calibration curves. The quantification of the authentic analytes was carried out by isotope dilution with the following formula:

$$[\text{eCB}] \text{ ng/mL} = (\text{ng ISTD} \times \text{analyte response}) / (\text{ISTD response} \times \text{RF} \times \text{mL aliquot volume})$$

The response factor (RF) was calculated as the ratio of the response area of the analyte divided by the response area of its ISTD for a standard solution mix directly injected without extraction into the LC/MS-MS system and in which equal amounts of the analyte and ISTD were present. For some analytes a deuterated form was not commercially available so a deuterated analog of another NAE or MG with a similar structure was used as ISTD. ISTD mix 1 was used for the quantification of authentic analytes. This fit-for-purpose approach could be employed due to the fact that the basic structure of the NAEs and the MGs is the same, the only difference being the length of the hydrocarbon chain and number and position of double bonds. For some analytes the RF was considered 1.0 since the differences in the absolute response were less than 10% (Table 1). We found that the responses of 2-AG-d8 and AEA-d8 were considerably lower than their non-deuterated forms (approximately ten-fold) although as they were not used in the isotope dilution quantification method calculations were not affected. The decreased response was probably due to the different position of the deuterium atoms in the structure of the d8 analog (and next to the double bonds) compared to the

d4 and d5 analogs (Figure 10). In our LC/MS-MS conditions, responses of the 1-MG and 2-MG isomers were the same.

4.1.5.3 Limits of detection and quantification

The mathematical estimates of the limits of detection (LOD) and lower limits of quantification (LLOQ) of the surrogated analytes were inferred from the equations of the curves by the following formulas:

$$\text{LOD ng/mL} = (\text{standard deviation of the replicates of the lowest concentration calibrator} / \text{slope}) \times 3$$

$$\text{LLOQ ng/mL} = (\text{standard deviation of the replicates of the lowest concentration calibrator} / \text{slope}) \times 10$$

Additionally, the lower limits of quantification (LLOQ) of the surrogated analytes were verified experimentally by a six replicate analysis of plasma spiked with d4 or d5 deuterated forms of NAE and 2-MG at the following concentrations: PEA-d4 0.1 ng/mL, OEA-d4 0.1 ng/mL, LEA-d4 0.1 ng/mL, AEA-d4 0.02 ng/mL, DHEA-d4 0.02 ng/mL, 2-AG-d5 0.75 ng/mL, 2-OG-d5 2.5 ng/mL. The samples were further spiked with ISTD mix 2, which contained 2-AG-d8 and AEA-d8 and analyzed by LC/MS-MS. The ratio of the surrogated analytes and their ISTD was calculated. A coefficient of variation of the ratios of less than 20% and a signal to noise ratio greater than 3 were considered acceptable. A dilution integrity experiment was carried out for lower sample volumes down to 50 μL , with no significant differences in concentration. However, the standard volume of the method was set at 0.5 mL in order to be able to quantify the eCBs and eCB-like compounds with lower endogenous concentrations.

4.1.5.4 Accuracy and imprecision

The within-day and between-day accuracy and imprecision of the method were evaluated by the quadruplicate analysis of quality control samples (QCs) at three concentration levels (QC-L, QC-M, and QC-H) over a three day validation protocol. The QCs were prepared by spiking a batch of plasma on top of its basal eCB and eCB-like concentrations. QC-L was spiked at 0.05 ng/mL POEA, DGLEA, EPEA, ALA, LEA, AEA, DEA, DHEA, 1 ng/mL 2-AG, PEA, OEA, SEA and 5 ng/mL 2-OG, 2-LG. QC-M was spiked at 0.5 ng/mL POEA, DGLEA, EPEA, LEA, α -LEA, AEA, DEA, DHEA, 5 ng/mL 2-AG, PEA, OEA, SEA and 50 ng/mL of 2-OG, 2-LG. QC-H was spiked at 2.5 ng/mL POEA, DGLEA, EPEA, LEA, α -LEA, AEA, DEA, DHEA, 25 ng/mL 2-AG, PEA, OEA, SEA and 250 ng/mL 2-OG, 2-LG. Aliquots of each QC were distributed into cryotubes and stored at -80C until analysis. The samples were randomly analyzed in order to assess carry over. Aliquots of 0.5 mL of the QC samples were spiked with ISTD mix 1 at the following amounts of deuterated analogs: 0.25 ng AEA-d4, 0.25 ng DHEA-d4, 0.50 ng LEA-d4, 1 ng PEA-d4 and OEA-d4, 5 ng 2-AG-d5 and 25 ng 2-OG-d5 and analyzed by LC/MS-MS. The quantification was done by isotope dilution.

Accuracy was calculated as the percentage (%) of difference between the observed concentration and the nominal concentration. The nominal concentration was calculated as the expected concentration on day 1 of the QC sample after the spiking process, taking into account the basal EC and ERC concentrations. A percentage of difference less than 15% for QC-M, QC-H and less than 20% for QC-L was considered acceptable. Imprecision was calculated as the standard error deviation

(RSD) of the QC sample replicates. An RSD less than 15% for QC-M, QC-H and less than 20% for QC-L was considered acceptable.

4.1.5.5 Recovery and matrix effect

Recovery and matrix effect were evaluated in plasma from six different sources with deuterated analogs as surrogated analytes analyzed in triplicate. Firstly, each batch of plasma was divided into two pools, one pool was spiked with ISTD mix 1 and mix 2 and extracted, while the other pool was spiked with ISTD mix 1 and mix 2 after extraction. Secondly, ISTD mix 1 and mix 2 were also spiked into clean glass tubes, evaporated and reconstituted. Finally, extracted samples and pure standards were analyzed by LC/MS-MS. Recovery was calculated as the response of the SA of samples spiked before extraction vs. samples spiked after extraction. The matrix effect was calculated as the response of the surrogated analytes of samples spiked after extraction vs. the pure standards. Additionally, the coefficient of variation (CV %) of the ratio of the surrogated analytes with the ISTD of the six plasma sources was calculated.

4.1.5.6 Stability of the analytes on re-injection

The stability of the reconstituted extract solutions on HPLC vials was tested with the re-injection of a batch in which the vials were kept at 4°C for 24h and another batch with the vials kept at -20°C for ten days.

4.1.6 Chemical and biological stability of 2-monoacylglycerols

4.1.6.1 Stability of the isomers 1 and 2 of monoacylglycerols in the biological matrix

The stability of the isomers 1 and 2 of MG in the biological matrix was assessed by measuring the ratio between the isomers after preservation of the plasma at different times and temperatures. The rate of isomerization (or acyl migration) was measured in two experiments: in a) one batch of human plasma from the blood bank was spiked with 2-OG-d5 and 2-AG-d5 and another batch was spiked with 1-OG-d5 and 1-AG-d5. Samples were analyzed by LC/MS-MS and the ratios of the 1 and 2 isomers of both batches were calculated. The spiked standards, dissolved in mobile phase, were also injected directly into the LC/MS-MS system and the isomer ratio was calculated in a) a set of freshly obtained plasma samples from human volunteers incubated 2h at 4°C, and b) another set incubated 2h at room temperature. The two sets of samples were analyzed by LC/MS-MS and the ratios of endogenous 1 and 2 MG isomers were calculated.

4.1.6.2 Inhibition experiments of the ex-vivo generation of monoacylglycerols (MG) from plasma

Blood was obtained from human volunteers and processed immediately. The rate of production of MG from the separated plasma was assessed by eCB analysis after incubation 2h at room temperature under agitation. Basal eCB levels (time 0) were estimated by immediate eCB analysis. A set of potential inhibitors of MG production were tested by spiking the plasma before incubation 2h at room temperature at

different concentrations of inhibitors. On several experiments the following phospholipase and lipase inhibitors were tested: edelfosine, D609, FIPI, Orlistat, RHC 80267, KT172, KT109 and GSK 264220A. Stock inhibitor solutions were prepared in ethanol except D609 that was prepared in water. The volume of spiking solution added was less than 2% with respect to the plasma aliquot volume. Plasma was distributed into cryotubes for the incubation experiments. Edelfosine is a phosphatidylinositol phospholipase C inhibitor ($IC_{50} = 9.6\mu M$). D609 is a phosphatidyl choline-specific phospholipase C inhibitor ($K_i=6.4\mu M$). FIPI is a phospholipase D2 and D1 inhibitor ($IC_{50} = 20\text{ nM}$, 25 nM). Orlistat is a gastric and pancreatic lipase inhibitor and a non-selective $DAGL\alpha$ and $DAGL\beta$ inhibitor ($IC_{50} = 60\text{ nM}$, 100 nM). RHC 80267 is a non-selective $DAGL$ inhibitor ($IC_{50} = 4\mu M$). KT172 and KT109 are selective $DAGL\beta$ inhibitors ($IC_{50} = 60\text{ nM}$, 42 nM , respectively) and also $DAGL\alpha$ inhibitors ($IC_{50} = 0.14\mu M$, $2.3\mu M$, respectively). GSK 264220A is an endothelial lipase and a lipoprotein lipase inhibitor ($IC_{50} = 0.13\mu M$, $0.10\mu M$, respectively). The effect of the blood collection tube on the MG production was assessed on EDTA (K2E 18 mg) or Heparin (LH, 170 I.U) BD Vacutainer 10 mL tubes with or without the presence of the inhibitor. All the inhibitors were tested with EDTA-plasma while Orlistat and GSK 264220A were additionally tested on heparin-plasma. The estimation of the IC_{50} of Orlistat for the generation of 2-AG, 2-LG and 2-OG was done in EDTA-plasma samples from three human volunteers with the following added concentrations of Orlistat: 0, 50, 150, 450, 900, 1500, and 2500 nM. Control plasma samples were kept at $4^{\circ}C$ for 2h until analysis. The percentage of inhibition was calculated with respect to the levels at concentration of inhibitor 0 of each plasma source. The data was modeled by the software GraphPad Prism 5 with the inhibition model: \log [inhibitor] vs. % inhibition and the IC_{50} for 2-AG, 2-LG and OG were calculated.

4.1.6.3 Stabilization of monoacylglycerol (MG) measures in plasma with Orlistat

Blood extracted from 25 human female volunteers was collected in 10 mL K2E 18.0 mg (EDTA) BD Vacutainer tubes, centrifuged immediately at 1700 g in a refrigerated centrifuge (4°C). Plasma of each volunteer was separated immediately from the blood and two equal 0.6 mL aliquots were obtained. One aliquot was spiked at 3.35 µM with 5 µL of Orlistat solution (200 µg/mL, ethanol). Both aliquots were stored at -80°C until eCB analysis with our standard procedure.

4.2 Quantification of endocannabinoids in animal models

The developed methodology for eCB quantification in plasma has been adapted for eCB quantification in animal models. The eCB quantification in plasma of rat or mice is the same as the method in human. In regards to mice the only difference is the volume of plasma for the analysis (due to the lower volume of plasma available), which is typically 100 µL. To maintain the proportions of organic and aqueous phases and to be able to separate the phases, and additional amount of dilution buffer (Am. Ac. 0.1M pH 4.0) is added for lower plasma volumes.

The methodology has been adapted for eCB quantification in brain tissue. The method of analysis by LC/MS-MS for brain tissue is the same as the method in plasma. The difference is the inclusion of a homogenization step and the spiking with a higher amount of internal

standard. For a proper quantification, the amount of internal standard added during extraction needs to be of a similar magnitude of the expected amounts of endogenous eCBs in tissue, which have very different ranges in plasma or brain. In brain of mice for instance 2-AG levels are typically 10 nmol/g tissue, while AEA levels are 30 pmol/g tissue, and this can vary depending on the brain region [141]. In human plasma 2-AG and AEA concentrations reported are in the order of 1-2 pmol/mL for both compounds [138].

Brain tissues are kept at -80°C or in dry ice until homogenization and the homogenization is done on ice, using a glass homogenizer. The homogenization step needs to be fast to avoid the ex-vivo generation of eCBs, and it typically takes 5 min to process one sample. The homogenization is done with 0.02%(v/v) trifluoroacetic acid in water (pH 3.0) and homogenates are extracted in tert-butyl-methyl ether like the plasma samples.

4.3 The endocannabinoid system, weight categories and olfaction

4.3.1 Human subjects. Characteristics of the human sample

The study sample was made up of 161 females (aged 18-65 years) with body mass indices (BMI) ranging from under-weight to morbid obesity. The characteristics of the study subjects are presented in **Table 3**. Seven centers, all involved in the CIBERObn (Spanish Biomedical Research Centre in Physiopathology of Obesity and Nutrition, www.ciberobn.com), participated. Only women were selected for this study. The population of subjects from the present study comes from a

larger clinical cohort for the study of eating disorders in women. Obese participants ($\text{BMI} > 30 \text{ Kg/m}^2$) were patients who had been consecutively referred to the clinics mentioned above. Recruitment of the non-obese participants ($\text{BMI} < 30 \text{ Kg/m}^2$) took place by means of word-of-mouth and advertisements at local universities. The selection was based on BMI. Exclusion criteria included: a) being male, b) a history of chronic medical illness, c) the use of psychoactive medication and drugs, d) Age under 18 or over 65 years. Subjects diagnosed with eating disorders, such as anorexia, bulimia, or binge eating disorder, were excluded from this sample. Enrolment in the study was between January 2010 and September 2012. All participants gave written and signed informed consent, the study was conducted according to the Declaration of Helsinki and the Ethics Committee of all the institutions involved [Comissió Deontològica de la Universitat Jaume I, Subcomisión Clínica del Hospital Universitario “Virgen de la Victoria”, Málaga, Comité Etic de Investigacio Clinica Hospital Universitari de Girona Doctor Josep Trueta (048/10), Comité Etico de Investigacion Clinica del Consorci Mar Parc de Salut de Barcelona-Parc de Salut Mar (2010/3914/I), Comité de Etica de la Investigación Universidad de Navarra (110/2010) and Comité Etico de Investigación Clínica del Hospital Universitari de Bellvitge (307/06)] approved the study.

Table 3. Characteristics of the study subjects

	UW (n=18) BMI<19 kg/m ²	NW (n=70) 19≤BMI<25	OW (n=13) 25≤BMI<30	OB (n=26) 30≤BMI<40	MO (n=34) BMI≥40 kg/m ²
Age (yrs)	24.0 (7.45)	27.4 (7.36)	33.4 (7.64)	47.3 (11.1)	43.5 (11.2)
Height (cm)	164 (7.99)	166 (6.40)	162 (4.11)	161 (6.27)	161 (7.36)
Weight (Kg)	48.9 (5.20)	59.9 (6.31)	70.9 (4.67)	92.0 (8.44)	122 (17.8)
BMI (Kg/m²)	18.1 (0.64)	21.7 (1.62)	26.9 (0.94)	35.5 (2.53)	46.7 (5.10)
% fat mass	18.7 (4.06)	27.0 (4.48)	33.6 (3.59)	42.1 (6.14)	46.4 (4.19)
LDL-C (mg/dL)	84.5 (28.9)	92.7 (23.8)	106 (26.1)	116 (33.5)	107 (24.7)
HDL-C (mg/dL)	55.4 (16.0)	58.1 (10.3)	58.5 (16.0)	47.6 (7.39)	43.8 (8.98)
Total-C (mg/dL)	154 (43.1)	165 (31.0)	180 (36.8)	187 (37.8)	179 (33.7)
Triglycerides (mg/dL)	59.4 (25.1)	66.5 (24.8)	67.2 (25.2)	107 (35.0)	129 (60.2)
Glucose (mg/dL)	80.7 (15.3)	82.9 (20.4)	80.2 (11.4)	101 (25.2)	98.7 (21.9)
Smokers (%)	31.6	33.9	30.8	20.0	28.1
Menopausia (%)	0	1.50	0	45.5	37.9
Use of oral contraceptives	27.8	26.9	20.0	4.00	10.3

Data are mean (standard deviation) or percentage (%); under-weight (UW); normal-weight (NW); over-weight (OW); obese (OB); morbidly obese (MO); body mass index (BMI); low density lipoprotein cholesterol (LDL-C); high density lipoprotein cholesterol (HDL-C); total cholesterol (Total-C)

4.3.2 Endocannabinoid quantification, anthropometry and lipid profile

Endocannabinoid quantification in plasma of the participants was done as described in section 4.1.3

The following anthropometric measures were considered: height (m), weight (kg), BMI (kg/m²), and %body fat. Body composition was assessed using a Tanita Multi-Frequency Body Composition Analyzer MC-180MA (Tanita Corp., Tokyo, Japan). Tanita uses the non-invasive technique of bioelectrical impedance analysis (BIA) that predicts from a series of equations total body water content and free fat mass, from which fat mass can be calculated.

EDTAK2 plasma glucose, total cholesterol (Total-C), and triglycerides were determined by enzymatic methods, high-density lipoprotein cholesterol (HDL-C) by an accelerator selective detergent method in a PENTRA-400 autoanalyzer (ABX-HORIBA Diagnostics, Montpellier, France). Low-density lipoprotein cholesterol (LDL-C) was calculated by the Friedewald equation whenever triglycerides were <300 mg/dL.

4.3.3 Olfactory capacity tests

Olfactory capacity was assessed by the “Sniffin’Sticks” test (Burghart Messtechnik GmbH, Wedel, Germany), which evaluates chemosensory performance based on pen-like odor-dispensing devices (**Figure 11**). The test has been previously described and validated [137]

and it is deemed suitable for the routine clinical assessment of olfactory performance. It is made up of three sub-tests: odor threshold (OT), odor discrimination (OD), and odor identification (OI). OT is the lowest concentration of a certain odor compound that is perceivable by the human sense of smell. OD and OI show the capacity to differentiate and identify odorants, respectively. OD and OI are more related to cognitive aspects of olfaction, while OT is more sensorial [134]. OT was assessed with n-butanol, while OD and OI were assessed with sixteen common fragrances, such as peppermint, orange, leather, cinnamon, banana, garlic, lemon, rose, coffee, apple, clove, pineapple, aniseed and fish [137]. Subjects were assessed individually in a well-ventilated room and they wore eye masks to perform the test. Subjects were requested not to smoke, chew gum or having eaten any products during the previous one hour at the start of the test. The tests were performed in the time period after breakfast and before lunch and on the same day that blood was collected for eCB analysis. A trained researcher carried out the tests in the following order: OT, OD and OI.

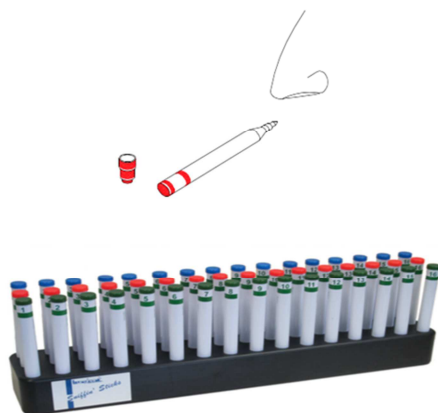


Figure 11. Sniffin' Sticks test battery

4.3.3.1 Olfactory threshold (OT) test

Using a triple-forced choice paradigm, detection thresholds were measured by employing a single staircase method. Three pens were presented in a randomized order, two pens contained odorless samples, and the third contained an odorant sample at a particular dilution. A total of 16 odor concentrations were tested. The task of the subject was to indicate which pen contained the odorant. Concentration of the odorant was augmented if the subject chose an odorless pen and reduced if the correct pen was recognized twice, which triggered a reversal of the staircase. The mean of the last four staircase reversal points of a total of seven reversals was used as the threshold estimate. The range of this score is from 0 to 16 points. The higher is the score the higher is olfactory threshold capacity.

4.2.3.2 Olfactory discrimination (OD) test

The subjects were asked to discriminate between 16 triplets of odors. In each group two odors were identical and one odor was different and the task was to recognize the pen in which the odor was different. The total score was the sum of correct responses, which can range from 0 to 16 points. The higher is the score the higher is olfactory discrimination capacity.

4.2.3.3 Olfactory identification (OI) test

A pen with an odor was presented to the subject. Subjects were asked to identify the odor, by choosing it in a card from a list of four descriptors, only one of which correctly identified the odor. For this

purpose the eye mask was removed (only for reading the card). The total score was the sum of correct responses, which can range from 0 to 16 points. The higher is the score the higher is olfactory identification capacity.

4.3.3.4 Threshold-discrimination-identification (TDI) score

The sum of the scores from the three olfactory subtests (OT, OD, and OI) results in the composite olfactory threshold-discrimination-identification (TDI) score, which can range from 0 to 48 points. The higher is the score the higher is olfactory capacity. TDI declines with age, the strongest decrease is observed in individuals >55 years [132]. Normosmia, or normal olfactory function is defined for TDI scores higher than 30.3 points, hyposmia, or decrease in olfactory capacity is defined for TDI scores lower than 30.3, and anosmia, or functional loss of olfactory capacity is defined for TDI scores lower than 16.5.

4.3.4 Statistical analysis

Characteristics of the five BMI sample groups are presented by the mean and the standard deviation. Boxplots (Tukey) were generated with software GraphPad Prism 5. Statistical analysis was performed with the software packages SPSS (version 18) and R (version 3.2.1). ANCOVA models were employed to compare the BMI groups with respect to eCB concentrations and olfactory scores adjusting for age and for the post-hoc pairwise comparisons in the framework of this model, the Tukey test was used. The correlations between the olfactory variables, on one hand, and the other study variables, on the other hand, were estimated

using Pearson's correlation coefficient. In addition, the association of TDI scores with BMI, %body fat and 2-AG was studied by means of ANCOVA models that controlled for age, smoking (yes/no), menstruation (normal/irregular/menopause), and the use of contraceptives (yes/no) as all these variables could affect olfactory capacity. Both the estimated parameter (B) of each variable of interest and the coefficient of determination (R^2), which represents the percentage of variability of TDI explained by the models, are presented.

5. RESULTS AND DISCUSSION

5.1 Quantification of circulating plasma endocannabinoids

5.1.1 Method development

Whilst some solid phase extraction methods were tried recovery was difficult to optimize due to the varying structures of the analyzed compounds (NAEs and MGs). The liquid-liquid extraction methods provided the best overall recoveries. In order to assess a method to stabilize the original isomeric ratio after the extraction and evaporation steps, 0.5 mL plasma samples were spiked with the deuterated analog isomers 2-AG-d5 and 2-OG-d5, and extracted and analyzed by LC/MS-MS to evaluate the generation of 1-AG-d5 and 1-OG-d5 by chemical isomerization (acyl migration) (**Table 4**).

Table 4. Stability of the isomerization upon extraction from the biological matrix

Extraction solvent	Ratio	
	2-AG-d5 (ISO1/ISO2)	2-OG-d5 (ISO1/ISO2)
Spiked plasma		
TBME:water (6:1, v/v) ^a	0.59	0.32
TBME:water (6:1, v/v) ^b	0.53	0.20
TBME:Am. Ac. 0.1M, pH 4.0 (6:1, v/v) ^a	0.10	0.09
Toluene:water (6:1, v/v) ^a	1.40	0.47
Standard solution	0.06	0.05

The stability of the isomerization of isomer 2 to isomer 1 during extraction and evaporation steps was assessed by analyzing the ratio (ISO1/ISO2) of plasma spiked with standard solutions of 2-AG-d5 and 2-OG-d5 subjected to liquid-liquid extraction compared with standard solutions dissolved in mobile phase injected directly into the LC/MS/MS system; Isomer 1 (ISO1); Isomer 2 (ISO2).

^a Reused clean tubes; ^b New silanized tubes. *J Lipid Res.* 2014;55:966-77

Several liquid-liquid extraction methods were tested: TBME or toluene as extraction solvents, Ammonium acetate buffer 0.1M at pH 4.0 or water as aqueous solvents, and new silanized borosilicate glass tubes (or clean re-used tubes) to test for the activity of catalytic silanols. Aqueous solvents were used to reduce viscosity and control plasma pH. Elevated temperatures, presence of serum albumin in the sample, and high pH values have been reported to accelerate 2-AG/1-AG acyl migration [139,140,142]. It is worth noting that commercially available solutions of 2-AG and other 2-MG usually contain 5% to 10% of 1-MG. It seems, therefore, impossible to completely avoid 2-MG/1-MG isomerization. The solvent that best preserved the original deuterated MG isomeric ratio of the sample after extraction was a mixture 6:1 TBME: 0.1 M Am. Ac. buffer pH 4.0. In our experimental conditions we observed that TBME preserved the 2-MG/1-MG ratio better than toluene, which was the solvent of choice for other authors [138,140]. However, this is most likely due to the longer evaporation time of toluene compared to TBME, which in our experiment was relevant due to the amount of solvent used (6 mL) in the liquid-liquid extraction. The standard solutions were prepared in acetonitrile since methanol and other protic solvents promote the isomerization of isomer 2 into isomer 1 of MG [139]. No differences were observed between extraction tubes that were clean, re-used ones or new silanized tubes.

We found optimal recoveries and peak shapes with the reconstitution of the extract in a mix of water:acetonitrile (10:90) with 0.1% FA. The eCB and eCB-like profile was separated by reverse phase gradient chromatography in a C18 column (**Figure 12**) since with a C8 column complete separation of the MG isomers was not possible.

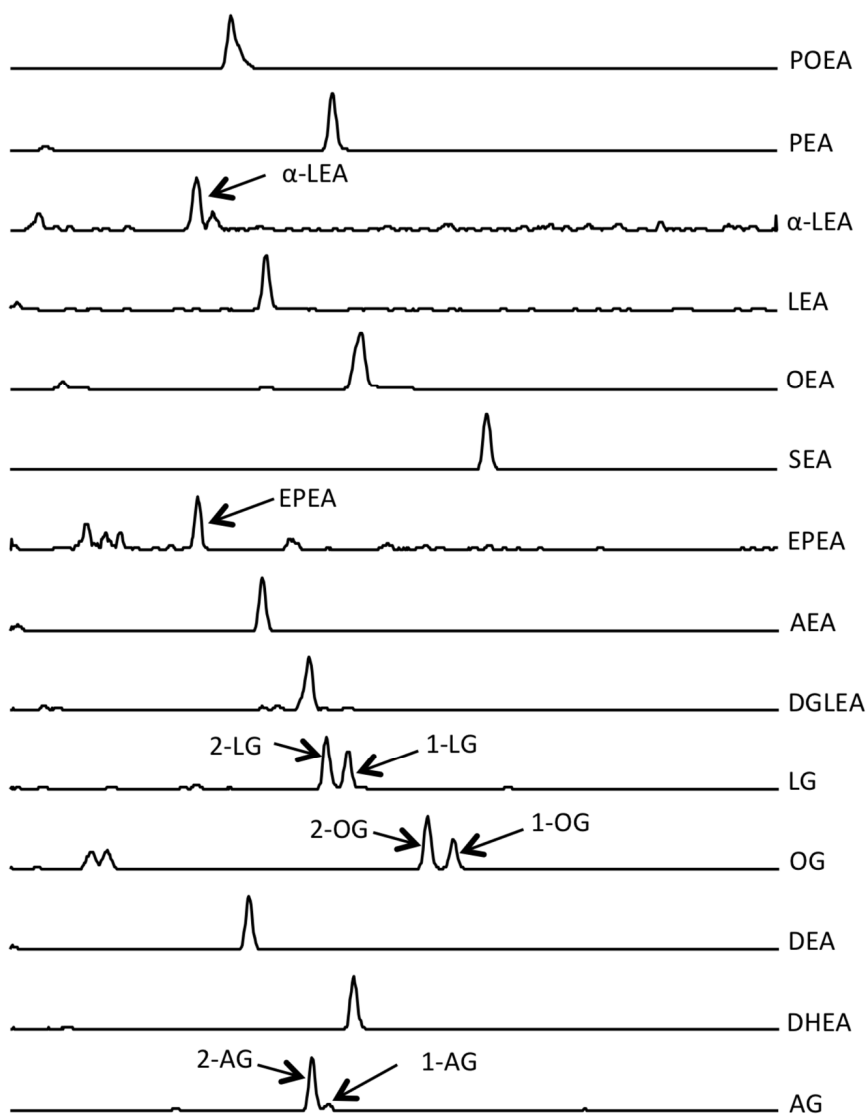


Figure 12. LC/MS-MS chromatogram of the endocannabinoid profile of a human plasma sample. *J Lipid Res.* 2014;55:966-77

Acetonitrile was used as the organic mobile phase as we observed that methanol also promoted 2-MG /1-MG isomerization, if present in the mobile phase. FA at 0.1% v/v was employed as an additive of the mobile

phase to promote the positive ionization of NAE and MG. The parent ion adducts selected for fragmentation in the mass spectrometer were in the form of $[M+H]^+$. The product ion m/z 62, which corresponds to ethanolamine, is characteristically generated by fragmentation of NAE while a neutral loss of mass 92, which corresponds to glycerol, is common to the fragmentation of MG. The specific MRM transitions are listed in Tables 1 and 2. The method is selective and specific for each analyte with no cross contamination between MRM channels and, in most cases, a single chromatographic peak corresponding to the endogenous analyte was found throughout the acquisition time. The variation in retention time of the individual analytes in a typical batch analysis was less than 0.5%. The retention time and product ion spectra of the endogenous analytes in the matrix matched the ones of the authentic standards.

The quantification of endocannabinoids, as for all endogenous analytes, is challenging due to the absence of a blank matrix. Some authors have developed strategies of depletion of the analytes by processing the plasma using five cycles of activated charcoal [138]. Other authors have used a surrogated analysis approach [143] or carried out quantification by isotope dilution [144,145]. It is to be noted that eCB depleted plasma still contains MG, probably due to its high concentrations [138]. In this work we have assessed the linearity, LOD, LLOQ, recovery, matrix effect, and MG acyl migration stability of the method using deuterated analog forms as surrogated analytes and internal standards (ISTD). Our approach is valid since the original unaltered matrix can be used and, theoretically, the deuterated forms have the same properties as the authentic analytes. However, there is a limited number of deuterated analogs of eCBs and eCB-like compounds, and in order to use this approach different deuterated analog versions for each analyte are necessary. For this reason, in the analysis of samples of clinical studies

(inhibition experiments), and in determining the accuracy and imprecision of the method, quantification was carried out with isotope dilution as described in the methods section.

5.1.2 Method validation

Recoveries were high (>80%) for all the analytes, matrix effect was substantial (40%) in some analytes such as 2-OG-d5. Minimal differences in the matrix effect of the six plasma sources were, however, observed because it was compensated by the use of deuterated analogs with similar ISTD structure (**Table 5**).

Table 5. Recovery and matrix interference of the surrogated analytes in plasma of six different sources

Surrogate analyte	ISTD	Recovery (%)	Matrix effect (%)	CV (%)
PEA-d4	OEA-d4	96 ± 11	-26 ± 4.7	3.0
LEA-d4	OEA-d4	96 ± 7.1	-19 ± 4.8	3.0
OEA-d4	PEA-d4	95 ± 8.4	-19 ± 5.8	3.4
AEA-d4	AEA-d8	95 ± 7.9	-15 ± 4.9	3.5
DHEA-d4	AEA-d4	89 ± 7.6	-11 ± 6.0	2.9
AEA-d8	AEA-d4	84 ± 8.7	-8.0 ± 5.0	4.2
2-OG-d5	2-AG-d5	84 ± 8.0	-40 ± 5.8	7.9
2-AG-d5	2-AG-d8	85 ± 7.8	-27 ± 4.0	3.9
2-AG-d8	2-AG-d5	81 ± 6.8	-16 ± 4.3	4.9

Mean ± standard deviation of the recovery (%) and matrix effect (%) of the surrogate analytes in plasma of six different sources and analyzed in triplicate; coefficient of variation (CV %) of the ratio of the surrogated analytes with the internal standard (ISTD) of the six plasma sources. *J Lipid Res.* 2014;55:966-77

The method is linear for the eCBs and eCB-like compounds whose quantification was standardized. Results, which include the mathematically derived LOD and LLOQ, are shown in **Tables 6A, 6B** and **6C**. The LLOQ of the method verified experimentally are the following: 0.02 ng/mL for AEA, DEA, DGLEA, EPEA, α -LEA, DHEA and POEA, 0.1 ng/mL for LEA, 0.5 ng/mL for OEA and SEA, 0.75 ng/mL for 2-AG, 1 ng/mL for PEA, 2.5 ng/mL for 2-OG and 2-LG. The LLOQ of PEA, OEA, and SEA were set at a higher concentration than their mathematical LLOQ due to small basal contaminant concentrations found in the solvents and glassware as reported by other authors [138] [146]. No significant carry-over was detected. No differences in the concentration values were found after re-injecting vials kept at 4°C for 24h. Vials kept at minus 20°C were stable for all analytes except SEA.

Table 6A. Calibration curve and linearity parameters of the surrogate analytes

Surrogate analyte	ISTD	NC	MC	STDR	accuracy	CV	slope	intercept	r ²	LOD	LLOQ
2-AG-d5	2-AG-d8	1.00	1.10	0.080	101.1	7.0	0.0620 ± 0.0011	-0.0173 ± 0.0126	0.995	0.25	0.77
		12.5	11.1	0.300	91.4	2.7					
		25.0	25.4	0.396	101.2	1.6					
		38.0	39.2	1.90	101.0	4.8					
		50.0	49.8	3.64	102.5	7.3					
2-OG-d5	2-AG-d8	2.50	2.60	0.24	103.9	9.1	0.0472 ± 0.0008	-0.0150 ± 0.0305	0.995	0.78	2.37
		62.5	58.9	4.86	94.3	8.2					
		125	126	16.2	100.9	12.8					
		190	190	9.04	99.8	4.8					
		250	253	13.0	101.1	5.1					
AEA-4	AEA-d8	0.05	0.05	0.006	98.4	12	0.3626 ± 0.0033	0.0007 ± 0.0025	0.999	0.02	0.06
		1.25	1.26	0.087	100.4	6.9					
		2.50	2.56	0.143	102.3	5.6					
		3.80	3.82	0.098	100.5	2.6					
		5.00	4.92	0.082	98.4	1.7					

Internal standard (ISTD); nominal spiked concentration in ng/mL (NC); measured concentration in ng/mL (MC); standard deviation of the residuals (STDR); accuracy in %, coefficient of variation in % (CV); slope (mean ± SD); intercept (mean ± SD), correlation coefficient (r²); limit of detection (LOD); lower limit of quantification (LLOQ). *J Lipid Res.* 2014;55:966-77

Table 6B. Calibration curve and linearity parameters of the surrogate analytes

Surrogate analyte	ISTD	NC	MC	STDR	accuracy	CV	slope	intercept	r ²	LOD	LLOQ
DHEA-d4	AEA-d8	0.05	0.05	0.004	99.2	8.7	0.2567 ± 0.0022	0.0008 ± 0.0017	0.999	0.01	0.04
		1.25	1.26	0.065	100.6	5.2					
		2.50	2.51	0.180	100.5	7.2					
		3.80	3.84	0.029	101.0	0.8					
		5.00	4.95	0.090	98.9	1.8					
LEA-d4	AEA-d8	0.05	0.05	0.002	98.5	5.0	0.6460 ± 0.0058	0.0029 ± 0.0044	0.999	0.01	0.02
		1.25	1.26	0.079	101	6.3					
		2.50	2.53	0.147	101	5.8					
		3.80	3.84	0.109	101	2.8					
		5.00	4.92	0.108	98.4	2.2					

Internal standard (ISTD); nominal spiked concentration in ng/mL (NC); measured concentration in ng/mL (MC); standard deviation of the residuals (STDR); accuracy in %, coefficient of variation in % (CV); slope (mean ± SD); intercept (mean ± SD), correlation coefficient (r²); limit of detection (LOD); lower limit of quantification (LLOQ). *J Lipid Res.* 2014;55:966-77

Table 6C. Calibration curve and linearity parameters of the surrogate analytes

Surrogate analyte	ISTD	NC	MC	STDR	accuracy	CV	slope	intercept	r ²	LOD	LLOQ
OEA-d4	AEA-d8	2.50	2.24	0.02	89.6	0.8	0.7761 ± 0.0171	-1.3384 ± 0.2568	0.991	0.06	0.19
		12.5	13.9	1.36	111	9.8					
		25.0	25.8	0.56	103	2.2					
		38.0	37.8	3.38	99.5	8.9					
		50.0	48.2	2.75	96.4	5.7					
PEA-d4	AEA-d8	2.50	2.18	0.013	87.3	0.6	0.9274 ± 0.0194	-1.5493 ± 0.2909	0.992	0.04	0.13
		12.5	14.2	1.63	113	11.5					
		25.0	26.1	0.88	104	3.4					
		38.0	37.8	1.05	99.6	2.8					
		50.0	47.7	1.67	95.5	3.5					

Internal standard (ISTD); (NC) nominal spiked concentration in ng/mL (NC); measured concentration in ng/mL (MC); standard deviation of the residuals (STDR); accuracy in %, coefficient of variation in % (CV); slope (mean ± SD); intercept (mean ± SD), correlation coefficient (r²); limit of detection (LOD); lower limit of quantification (LLOQ). *J Lipid Res.* 2014;55:966-77

Within run and between run accuracy and imprecision values of NAE and MG are presented in **Table 7** and fit current standard requirements for analytical method validation. With respect to the MG, we found decreases in the concentration of the separate 2-MG isomers from day 2 of the validation protocol due to acyl migration during conservation of the plasma. This is explained in the section on stability of the isomeric ratio of MG. The method is deemed fit for the determination of the eCB and eCB-like profile in human plasma samples.

RESULTS AND DISCUSSION

Table 7. Imprecision and accuracy

	Within run						Between run					
	Imprecision (%)			Accuracy (%)			Imprecision (%)			Accuracy (%)		
	QC-L	QC-M	QC-H	QC-L	QC-M	QC-H	QC-L	QC-M	QC-H	QC-L	QC-M	QC-H
2-AG	8.7	9.0	7.2	88.7	91.0	75.6	11.0	18.4	14.8	88.4	71.7	83.3
2/1-AG	6.7	5.7	5.7	96.9	96.4	93.5	7.4	14.3	8.2	88.7	93.2	103
2-LG	11.0	12.8	5.9	95.8	91.3	77.2	16.2	18.2	19.5	80.2	76.3	83.2
2/1-LG	5.4	8.5	5.7	94.9	101	105	11.2	4.8	9.6	91.4	101	110
2-OG	10.6	7.6	8.6	86.9	92.9	83.2	10.6	18.3	8.2	88.4	77.5	89.5
2/1-OG	9.7	8.7	6.9	95.3	89.9	97.0	12.1	11.2	5.6	90.8	85.1	104
AEA	4.6	6.1	4.3	92.9	88.7	89.6	9.8	10.2	4.8	92.1	92.9	89.4
DEA	4.5	6.1	5.2	91.6	91.4	93.0	11.9	6.9	5.3	95.0	94.1	95.2
DGLEA	7.7	6.1	4.1	97.0	97.6	95.0	10.4	9.0	5.4	101	97.5	98.3
DHEA	4.7	8.8	3.0	94.6	92.1	90.6	10.2	9.3	4.6	90.9	94.5	93.7
EPEA	7.2	5.3	4.3	95.3	89.9	88.0	9.8	10.0	6.1	90.6	89.1	89.7
LEA	3.2	7.4	5.4	97.8	97.9	97.5	10.0	10.2	5.5	94.8	99.9	101
α -LEA	5.6	9.0	5.7	93.9	88.5	87.0	11.5	12.5	8.1	86.7	88.5	88.1
OEA	2.9	7.5	3.8	97.5	98.4	96.4	9.3	9.7	4.6	94.9	97.2	102
PEA	2.9	6.6	3.0	95.4	97.6	96.7	9.4	9.5	3.9	94.5	96.5	100
POEA	7.0	11.3	6.2	96.5	93.8	86.3	14.1	12.4	9.8	92.9	89.7	89.8
SEA	4.9	9.4	3.8	93.3	98.3	99.0	10.8	10.5	8.8	101	97.2	104

Data represent the mean values of QC sample replicates. *J Lipid Res.* 2014;55:966-77

5.1.3 Inhibition experiments of the ex vivo generation of 2-monoacylglycerols in plasma

Fanelli et al. [138] reported the generation of 2-AG in plasma in the absence of blood cells, with increases in 2/1-AG for plasma preserved for 4h at 4°C or room temperature. In the course of our MG stability experiments we observed approximately five fold increases in 2/1-LG and 2/1-OG concentrations in plasma preserved for just 2h at room temperature compared to plasma preserved at 4°C. In regards to 2/1-AG we observed differences in concentration when plasma was analyzed immediately after blood extraction *vs* some time afterwards (2h) or after a freezing/thawing step even though cold chain (4°C) was maintained. We therefore investigated in controlled experiments several phospholipase and lipase inhibitors for its capacity to inhibit ex-vivo monoacylglycerol (MG) production in plasma. 2-AG, and its precursors in the organism can be originated from multiple biosynthetic pathways and tissues, including blood cells. 2-AG is mainly originated from sequential hydrolysis of phosphatidylinositol (PI) phospholipids but it also can be originated from phosphatidylcholine (PC) phospholipids [147] (**Figure 13**). The diacylglycerol lipase (DAGL) α or β releases 2-AG from its main precursor, diacylglycerol (DAG) [148]. 2-AG and other 2-MGs also originate from fat digestion in the intestinal lumen, where dietary triacylglycerol is hydrolyzed in the sn-1 and sn-3 position by pancreatic lipase through a series of directed stepwise reactions to DAG, 2-MG, fatty acids, and glycerol. 2-MGs are readily adsorbed and re-synthesized to triacylglycerols through the MG pathway [45] [15,149,150]. In our attempt to discover the source of 2-AG originated ex-vivo from plasma we used several lipase inhibitors that included inhibitors of the biosynthesis of 2-AG precursors. In the inhibition experiments we initially

used an inhibitor of PI phospholipase C (PLC) (edelfosine), an inhibitor of phospholipase D1 and D2 (FIPI), and an inhibitor of PC phospholipase C (D609). We also used Orlistat, a potent non-specific inhibitor of DAGL α and DAGL β [151], which is also a gastric and pancreatic lipase inhibitor [152].

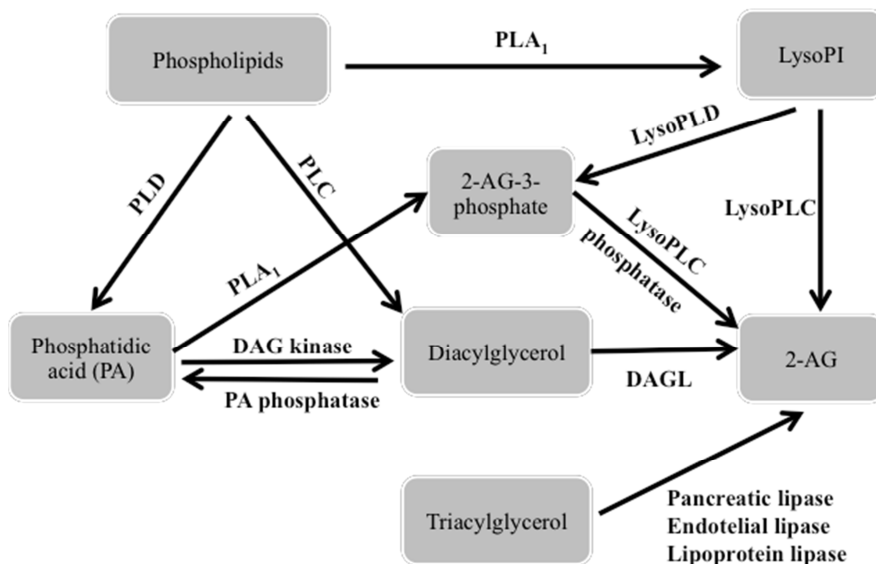


Figure 13. Schematic pathways on the biosynthesis of 2-arachidonoyl glycerol (2-AG). Phospholipase A1 (PLA₁); phospholipase D (PLD); phospholipase C (PLC); 2-arachidonoyl-sn-glycero-3-phosphoinositol (LysoPI); lysophospholipase D (LysoPLD); lysophospholipase C (LysoPLC); diacylglycerol lipase (DAGL); diacylglycerol kinase (DAG kinase); phosphatidic acid phosphatase (PA phosphatase). Adapted from *Curr Top Behav Neurosci.* 2009;1:3-35.

We found no inhibition activity for the phospholipase inhibitors D609, FIPI and edelfosine (IC₅₀>30 μ M, IC₅₀>125 nM, IC₅₀>50 μ M). On the other hand, we observed inhibition of the ex-vivo generation of 2-AG, 2-LG and 2-OG in plasma spiked with Orlistat. It is to be noted that the

artifactual generation of MG persisted even after immediate sample centrifugation that essentially eliminates all blood cells, which means that this MG buildup should be related to an enzymatic plasma activity. Since Orlistat is a general lipase inhibitor we also tested the inhibition activity of RHC 80267, another non-specific inhibitor of DAGL α [151] and KT172 and KT109, potent selective DAGL β inhibitors [19]. Neither of these compounds showed inhibition activity ($IC_{50} > 30 \mu M$, $IC_{50} > 15 \mu M$, $IC_{50} > 15 \mu M$), which means that the ex-vivo MG production in plasma is a mechanism independent of DAGL. Additionally, we investigated the effect of the blood collection tube on MG generation. We found that MG concentrations were higher in heparin-plasma than in EDTA-plasma. The differences were maintained either for samples analyzed immediately or after incubation at room temperature. Orlistat was able to inhibit MG production in plasma originated from both kind of tubes, but due to the higher MG buildup in heparin-plasma, a higher concentration of Orlistat was needed to achieve full inhibition. (**Table 8**).

Table 8. Stability of monoacylglycerol concentrations on different collection conditions

Blood Tube	Inhibitor in Plasma	2/1-AG		2/1-LG		2/1-OG	
		Time 0	Time, 2h at room temperature	Time 0	Time, 2h at room temperature	Time 0	Time, 2h at room temperature
EDTA	-	0.75 ± 0.21	8.51 ± 4.57	8.57 ± 2.23	102 ± 86.5	9.68 ± 2.28	115 ± 85.9
EDTA	+		1.13 ± 1.03		11.8 ± 5.1		15.6 ± 2.30
Heparin	-	2.82 ± 0.67	30.6 ± 23.0	83.7 ± 12.8	876 ± 729	72.3 ± 0.93	619 ± 475
Heparin	+		2.99 ± 0.05		65.3 ± 3.77		48.0 ± 1.20

Blood was collected in EDTA or heparin tubes. The separated plasma was analyzed immediately (time 0) or after incubation for 2h at room temperature with or without addition of Orlistat to the plasma collection tube. Orlistat was added at 3.5 μ M to EDTA-plasma and at 15 μ M to heparin-plasma. Data are presented as mean \pm SD of 2/1-MG concentrations (ng/mL) of plasma from one volunteer in an experiment performed in duplicate. *J Lipid Res.* 2014;55:966-77

Further, since heparin-plasma is commonly used for the assay of lipoprotein lipase due to its affinity for heparin [153], we also tested the inhibition activity of GSK 264220A, an endothelial lipase and a lipoprotein lipase inhibitor [154] but we found no inhibition ($IC_{50} > 15 \mu M$) on EDTA-plasma or heparin-plasma. The reason of the lower MG concentrations on EDTA plasma is probably due to the chelating effect of EDTA on the cofactors needed for MG biosynthesis. We recommend, therefore, the use of EDTA blood tubes for collection in addition to Orlistat. In a second set of experiments, EDTA-plasma of three human volunteers was used for the calculation of the IC_{50} of Orlistat for the ex-vivo generation of 2-AG, 2-LG and 2-OG. An inhibition model was obtained and the data is graphically presented in **Figure 14**. The IC_{50} of Orlistat with the mean, its 95% confidence interval and the coefficient of determination (R^2) of the inhibition model are as follows: 285.6 nM [212.4, 384.0] for 2-AG ($R^2=0.8809$), 146.1 nM [104.9, 203.4] for 2-LG ($R^2=0.9087$) and 148.7 nM [110.6, 200.0] for 2-OG ($R^2 = 0.9254$).

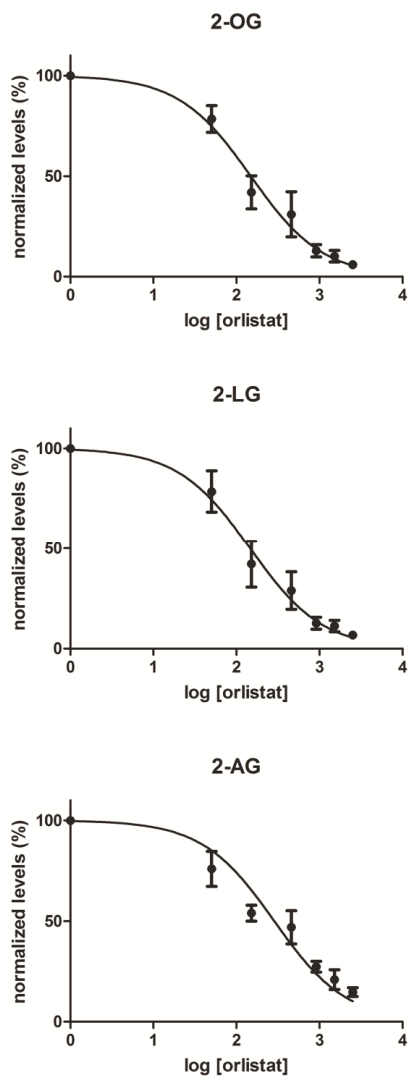


Figure 14. Inhibition model of ex vivo production of 2-MG in plasma with Orlistat. Plasma from freshly extracted blood was spiked with a range of concentrations of Orlistat, incubated at room temperature for 2 h, and analyzed by LC/MS-MS to detect the levels of 2-AG, 2-OG, and 2-LG. Values represent the normalized 2-MG levels of three different volunteers analyzed in triplicate. *J Lipid Res.* 2014;55:966-77

The ex-vivo generation of MG in plasma can be prevented by Orlistat. Since our MG assay was done at room temperature we tested in controlled conditions whether Orlistat addition to the plasma storage tube had any effect on MG measures when a typical clinical sample collection protocol was followed. For that, 25 female blood samples were collected and processed in a matter of weeks, maintaining the cold chain until finally stored at -80°C. ECB analysis took place several weeks after all samples had been collected and was done with our standard sample preparation procedure. The results are presented in **Table 9** and they show that Orlistat addition during the sample collection protocol lead to a significant reduction of all MG measures (36 to 59%, $p < 0.001$). The NAE, which are the other measures of our eCB and eCB-like analysis, were not affected by the addition of Orlistat. We think that differences may have arisen due to the enzymatic activity taking place in the freezing/thawing and processing steps. All the NAE and MG described in the method could be quantified in the 25 human female samples (Table 9) with the exception of EPEA that due to its low levels could only be quantified in 14 samples. In summary, data show that Orlistat addition as part of the sample collection protocol can be a tool to stabilize MG concentrations in plasma and this can aid in the harmonization of eCB and eCB-like measurements in clinical samples.

Table 9. Effect of Orlistat addition to plasma on endocannabinoid measures

	N	Measured concentration (ng/mL)		Change (%)	P
		Without Added Orlistat	With Added Orlistat		
2/1-AG	25	2.42 ± 1.10	0.89 ± 0.50	-59.0 ± 23.9	<0.001
2/1-LG	25	15.2 ± 8.48	7.76 ± 3.54	-47.2 ± 17.5	<0.001
2/1-OG	25	16.1 ± 10.4	8.93 ± 4.90	-35.9 ± 25.0	<0.001
AEA	25	0.40 ± 0.19	0.39 ± 0.19	-2.09 ± 9.58	0.225
DEA	25	0.12 ± 0.04	0.11 ± 0.04	0.45 ± 11.8	0.671
DGLEA	25	0.11 ± 0.03	0.12 ± 0.03	-0.33 ± 12.3	0.324
DHEA	25	0.45 ± 0.19	0.44 ± 0.21	-0.74 ± 10.9	0.801
EPEA	14	0.03 ± 0.01	0.03 ± 0.01	-8.67 ± 9.02	0.104
LEA	25	1.30 ± 0.38	1.23 ± 0.38	-4.05 ± 11.7	0.091
α-LEA	25	0.04 ± 0.01	0.04 ± 0.01	-4.39 ± 13.4	0.142
OEA	25	3.16 ± 1.26	3.10 ± 1.22	-1.72 ± 5.46	0.057
PEA	25	2.07 ± 0.67	2.06 ± 0.60	0.75 ± 9.20	0.774
POEA	25	0.18 ± 0.11	0.17 ± 0.10	-2.90 ± 12.0	0.491
SEA	25	1.18 ± 0.33	1.15 ± 0.32	-2.15 ± 8.81	0.214

Plasma of 25 female human volunteers was collected with or without Orlistat (3.4 μM) addition and stored at -80°C until EC analysis. Data are presented as mean ± SD. EPEA concentration was below the LLOQ for some of the samples. The effect of Orlistat addition to plasma on endocannabinoid measures was assessed by a paired-samples *t*-test. *J Lipid Res.* 2014;55:966-77

In summary the analysis of endocannabinoids (eCBs) is a challenging issue. To our knowledge this is the first time that an enzymatic activity inhibited by the lipase inhibitor Orlistat, and able to generate 2-arachidonoylglycerol (2-AG) and other 2-monoacylglycerols (2-MG) in plasma in the absence of cells has been reported. Our finding suggests that, as happens with eCB brain concentrations[141], peripheral eCB concentrations from clinical studies or animal models greatly depend on sample collection and sample time processing conditions that take place in the clinical and laboratory settings due to the natural presence of enzymatic activity in plasma. Because of the instability of eCB concentrations in blood and plasma, eCB studies need to follow strict harmonized sample collection and processing protocols in order to avoid artificial differences between samples. Finally, the collection of plasma samples with Orlistat may be a useful tool in the determination of real endogenous 2-MG concentrations. In addition to immediate centrifugation in refrigerated conditions, and separation of plasma from blood to avoid the release of N-acyl ethanolamines (NAE), such as anandamide (AEA) from blood cells, we also recommend the addition of Orlistat to plasma collecting tubes, maintaining the cold chain until storage and processing. Orlistat is inexpensive and thus may be a cost effective measure in order to aid in the harmonization of eCB and eCB-like measurements in clinical research. Data suggest that the ex-vivo generation of MG in plasma is a mechanism independent of diacylglycerol lipase (DAGL), since besides the general lipase inhibitor Orlistat, other specific or unspecific DAGL inhibitors do not inhibit MG generation and neither is the result of endothelial lipase or lipoprotein lipase activity. It goes beyond the scope of this work the full characterization of this enzymatic activity.

5.1.4 Stability of the isomeric ratio of monoacylglycerols

The results of the stability experiment of MG in plasma show that the chemical isomerization of isomer 2 to isomer 1 decreases with decreases in the preservation temperature of the plasma before analysis. However, isomerization is still observed, even if samples are stored at -80°C (**Table 10**). Furthermore, it has been reported that isomerization is also dependent on the amount of serum albumin present in the sample [142]. It is, therefore, possible that even when samples are subjected to the same storage conditions they could still have different chemical isomerization rates. Additionally, chemical isomerization takes place in plasma preserved for a very short time at room temperature.

We also investigated the endogenous origin of MG isomers in fresh plasma samples (**Table 11**). As has been previously suggested [140], our data support the hypothesis that 1-AG does not have an endogenous origin and is the result of chemical isomerization during sample storage and processing, since in fresh plasma samples we found that 1-AG was present at the same isomeric ratio as the pure standard mixture. On the other hand, we observed that 1-LG and 1-OG were present at substantial concentrations. 1-MGs originate from the *in vivo* isomerization of 2-MGs during digestion and absorption. It has been estimated that approximately 25% of 2-MGs are isomerized to the 1-MG form. However, 2-MG is the predominant form in which MGs are absorbed and re-synthesized to triacylglycerols while 1-MGs are eventually hydrolyzed by pancreatic lipase to free fatty acids and glycerol [15,149,150,155].

Table 10. Stability of the isomerization of spiked 2/1-AG-d5 and 2/1-OG-d5 in stored plasma

Spiked analyte	Ratio	Ratio			
		Time 0	Time, 30 min at room temperature	Time, 20 days at -20°C	Time, 20 days at -80°C
2-AG-d5	ISO1 / ISO2	0.08 ± 0.01	0.46 ± 0.06	0.84 ± 0.05	0.41 ± 0.01
1-AG-d5	ISO2 / ISO1	0.01 ± 0.01	0.04 ± 0.01	0.07 ± 0.01	0.03 ± 0.01
2-OG-d5	ISO1 / ISO2	0.08 ± 0.01	0.36 ± 0.06	0.58 ± 0.03	0.36 ± 0.06
1-OG-d5	ISO2 / ISO1	0.13 ± 0.03	0.13 ± 0.03	0.12 ± 0.04	0.13 ± 0.03

A pool of plasma was spiked separately with the deuterated analogs of the isomer 1 (ISO1) and isomer 2 (ISO2) of AG and OG. Aliquots were distributed in cryotubes and chemical stability of the isomer ratio (ISO1/ISO2 and ISO2/ISO1) was assessed upon conservation at time 0, 30 min at room temperature, 20 days at -20°C, or 20 days at -80°C. Data are presented as mean ± SD of replicate analysis. *J Lipid Res.* 2014;55:966-77

Table 11. Stability of the isomerization of endogenous 2/1-AG, 2/1-LG, and 2/1-OG in stored plasma

Endogenous analyte	Ratio ISO1 / ISO2	
	Time 2h at 4°C	Time 2h at room temperature
2/1-AG	0.09 ± 0.10	0.32 ± 0.24
2/1-LG	0.43 ± 0.13	0.76 ± 0.10
2/1-OG	0.28 ± 0.08	0.57 ± 0.06

The stability of the isomer 1/isomer 2 (ISO1/ISO2) ratio of endogenous 2/1-AG, 2/1-LG, and 2/1-OG was assessed in plasma of three different volunteers which was kept 2 h at 4°C or room temperature after extraction from the volunteer. Data are presented as mean ± SD of triplicate analyses. *J Lipid Res.* 2014;55:966-77

In summary we have validated a method for the determination of a range of MG and NAE in plasma. The developed method is able to preserve the original isomeric ratio of MG. We have found that the chemical isomerization of MG can only be avoided by an immediate processing (at cold temperature and acid pH) and analysis of samples. Due to the instability of MG to isomerization during conservation of the plasma we recommend to report MG concentrations as the sum of both isomers (isomer 1 and isomer 2).

5.2 Applicability of the endocannabinoid quantification method in clinical and translation studies

The developed methodology for endocannabinoids (eCB) and endocannabinoids related compounds quantification has been applied in the study discussed in section 5.3 of this thesis (Endocannabinoids, weight categories and olfaction). In addition, and in collaboration with other research groups, the methodology for eCB quantification has been applied in the following clinical and translational studies (**Tables 12A, 12B, 12C**) grouped as:

- (i) clinical and translational studies related to cognition and affective disorders.
- (ii) clinical and translational studies related with weight categories and cognition

Table 12A. Applicability of the endocannabinoid quantification method in clinical and translational studies related to cognition and affective disorders

Title	Authors	Journal	Tissue	Species
Differential role of anandamide and 2-arachidonoylglycerol in memory and anxiety-like responses.	Busquets-Garcia A, Puighermanal E, Pastor A , de la Torre R, Maldonado R, Ozaita A.	Biol Psychiatry. 2011;70: 479–486	Whole brain	Mice
Targeting the endocannabinoid system in the treatment of fragile X syndrome.	Busquets-Garcia A, Gomis-Gonzalez M, Guegan T, Agustin-Pavon C, Pastor A , Mato S, et al.	Nat Med. 2013;19: 603–607	Whole brain	Mice
Cognitive Impairment Induced by Delta9-tetrahydrocannabinol Occurs through Heteromers between Cannabinoid CB1 and Serotonin 5-HT2A Receptors	Viñals X, Moreno E, Lanfumey L, Cordoní A, Pastor A , la Torre de R, et al.	PLoS Biol. 2015;13: e1002194	Whole brain	Mice

Table 12B. Applicability of the endocannabinoid quantification method in clinical and translational studies related to cognition and affective disorders

Title	Authors	Journal	Tissue	Species
Sex differences in psychiatric comorbidity and plasma biomarkers for cocaine addiction in abstinent cocaine-addicted subjects in outpatient settings	Pedraz M, Araos P, García-Marchena N, Serrano A, Romero-Sanchiz P, Suarez J, et al.	Front Psychiatry. 2015;6: 17	Plasma	Human
Role of the endocannabinoid system in the emotional manifestations of osteoarthritis pain.	La Porta C, Bura SA, Llorente-Onaindia J, Pastor A , Navarrete F, García-Gutiérrez MS, et al.	Pain. 2015;156: 2001–2012	Amygdala, Hippocampus, Prefrontal cortex, Plasma	Mice, Human
Evaluation of plasma-free endocannabinoids and their congeners in abstinent cocaine addicts seeking outpatient treatment: impact of psychiatric co-morbidity.	Pavón FJ, Araos P, Pastor A , Calado M, Pedraz M, Campos-Cloute R, et al.	Addict Biol. 2013;18: 955–969	Plasma	Human

Table 12C. Applicability of the endocannabinoid quantification method in clinical and translational studies related with weight categories and cognition

Title	Authors	Journal	Tissue	Species
Moderate-vigorous physical activity across body mass index in females: moderating effect of endocannabinoids and temperament	Fernandez-Aranda F, Sauchelli S, Pastor A , Gonzalez ML, la Torre de R, Granero R, et al.	PloS One. 2014;9: e104534.	Plasma	Human
Modulation of the Endocannabinoids N-Arachidonylethanolamine (AEA) and 2-Arachidonylglycerol (2-AG) on Executive Functions in Humans	Fagundo AB, de la Torre R, Jiménez-Murcia S, Agüera Z, Pastor A , et al.	PLoS One. 2013 Jun 19;8(6):e66387.	Plasma	Human
Diet-dependent modulation of hippocampal expression of endocannabinoid signaling-related proteins in cannabinoid antagonist-treated obese rats.	Rivera P, Luque-Rojas MJ, Pastor A , Blanco E, Pavon FJ, Serrano A, et al.	Eur J Neurosci. 2013;37: 105–117	Hippocampus	Rat
Pharmacological blockade of the fatty acid amide hydrolase (FAAH) alters neural proliferation, apoptosis and gliosis in the rat hippocampus, hypothalamus and striatum in a negative energy context	Rivera P, Bindila L, Pastor A , Pérez-Martín M, Pavon FJ, Serrano A, et al.	Front Cell Neurosci. 982015;9:	Plasma	Rat

5.3 Endocannabinoids, weight categories and olfaction

The concentrations of eCBs and eCB-like compounds of each BMI sample group are presented in **Figures 15, 16, 17 and 18**. Plasma concentrations of 2-monoacylglycerols 2-AG, 2-LG and 2-OG were significantly elevated in obese and morbidly obese subjects, while plasma concentrations of N-acylethanolamines AEA, LEA and PEA were significantly lower in under-weight subjects.

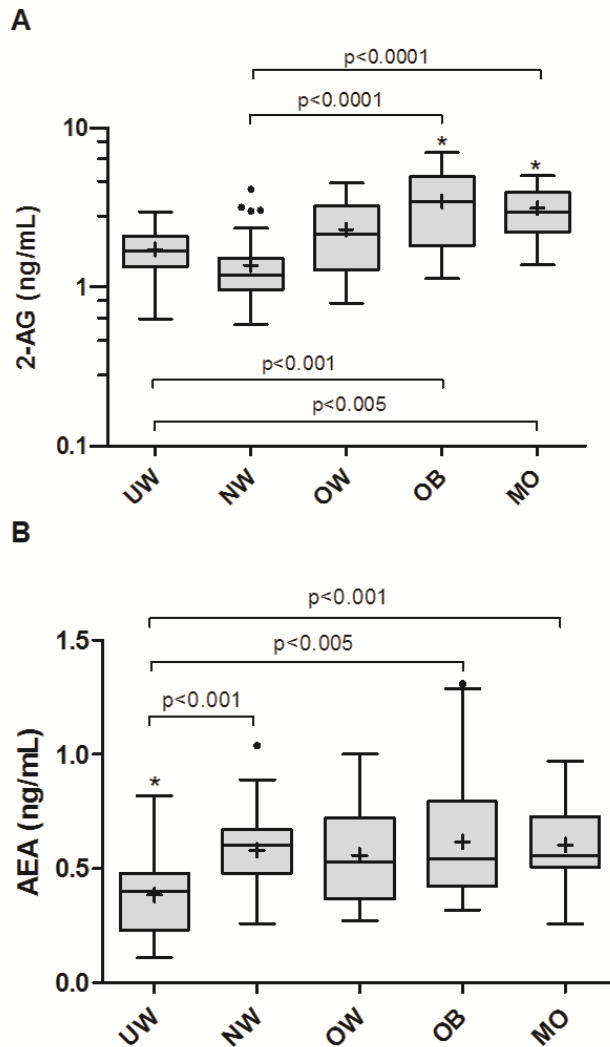


Figure 15. Endocannabinoid plasma concentrations. Box plots of plasma concentrations of 2-arachidonoyl glycerol (2-AG) (A), and anandamide (AEA) (B) of subjects from each of the body mass index (BMI) sub-groups. The median is represented as a line within the box plot and the mean is represented as a + sign. Significant differences ($p < 0.05$) in eCB concentrations between BMI subgroups are marked as asterisks (*). Outliers are represented as points.

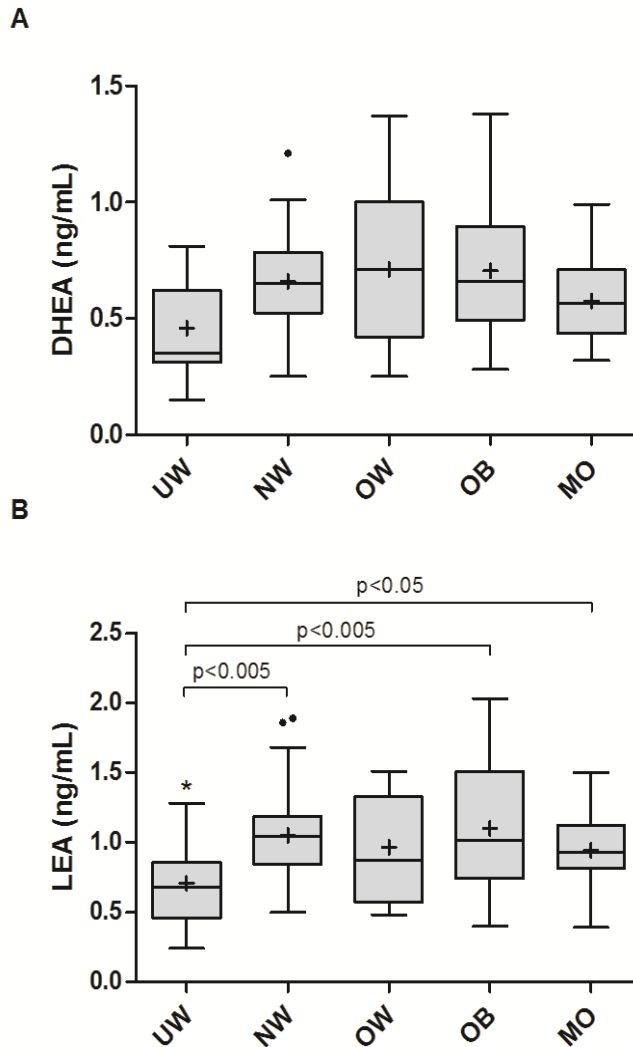


Figure 16. Endocannabinoid-like plasma concentrations. Box plots of plasma concentrations of N-docosahexaenoylethanolamine (DHEA) (A), and N-linoleoylethanolamine (B) of subjects from each of the body mass index (BMI) sub-groups. The median is represented as a line within the box plot and the mean is represented as a + sign. Significant differences ($p < 0.05$) in eCB concentrations between BMI subgroups are marked as asterisks (*). Outliers are represented as points.

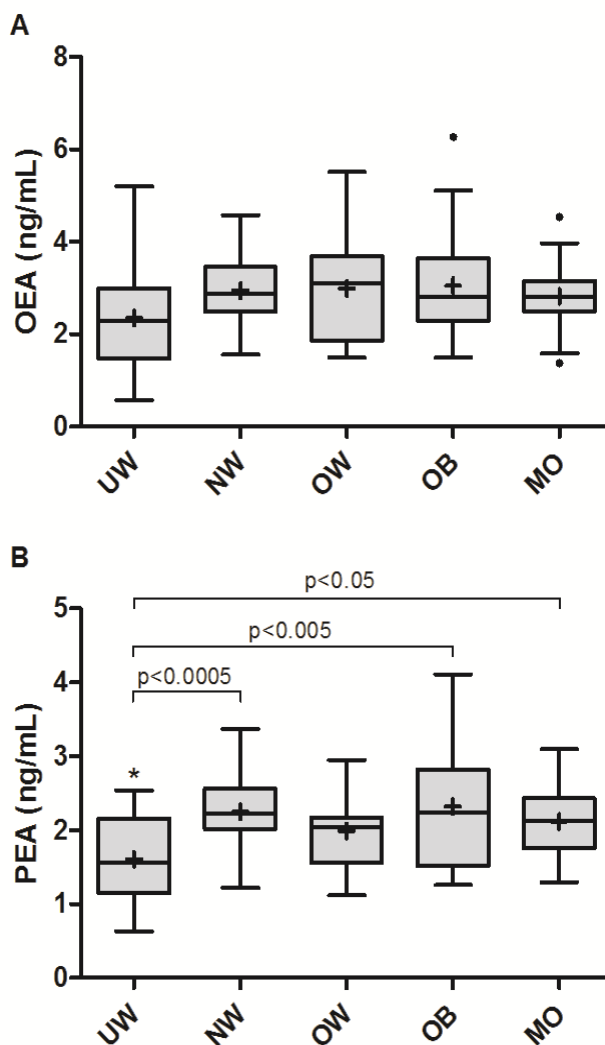


Figure 17. Endocannabinoid-like plasma concentrations. Box plots of plasma concentrations of N-oleoylethanolamine (OEA) (A), and N-palmitoylethanolamine (PEA) (B) of subjects from each of the body mass index (BMI) sub-groups. The median is represented as a line within the box plot and the mean is represented as a + sign. Significant differences ($p < 0.05$) in eCB concentrations between BMI subgroups are marked as asterisks (*). Outliers are represented as points.

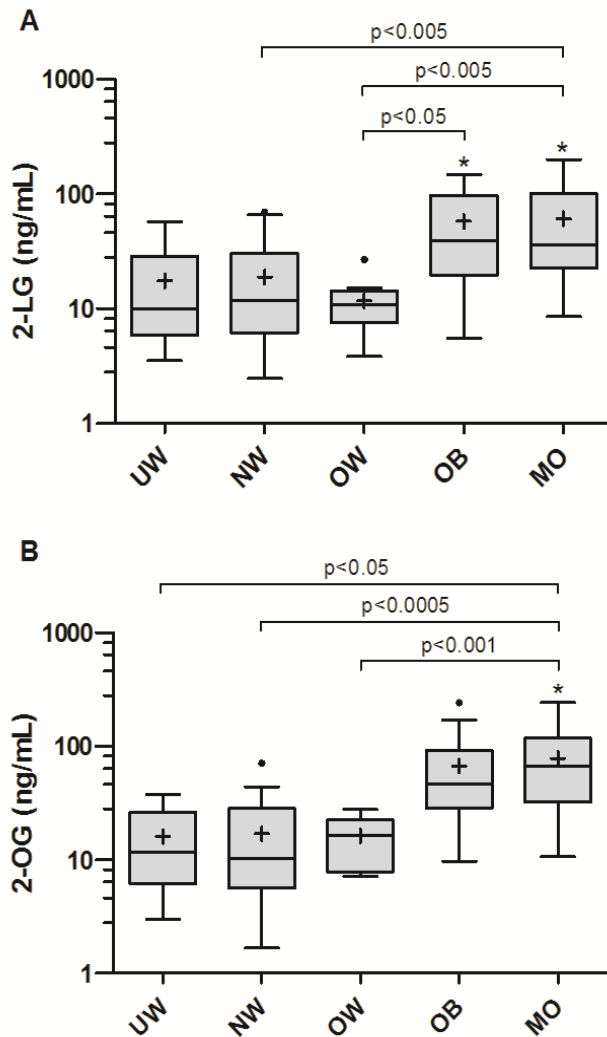


Figure 18. Endocannabinoid-like plasma concentrations. Box plots of plasma concentrations of 2-linoleoyl glycerol (2-LG) (A), and 2-oleoyl glycerol (2-OG) (B) of subjects from each of the body mass index (BMI) sub-groups. The median is represented as a line within the box plot and the mean is represented as a + sign. Significant differences ($p < 0.05$) in eCB concentrations between BMI subgroups are marked as asterisks (*). Outliers are represented as points.

Olfactory scores of each BMI sample group are presented in **Figures 19 and 20**. TDI scores are shown in relation to the TDI score of <30.3, typically used in clinics for hyposmia diagnostic [132]. TDI scores were significantly lower in obese and morbidly obese subjects. With respect to the olfactory sub-tests OT and OI scores were significantly lower in obese subjects but not in morbidly obese subjects.

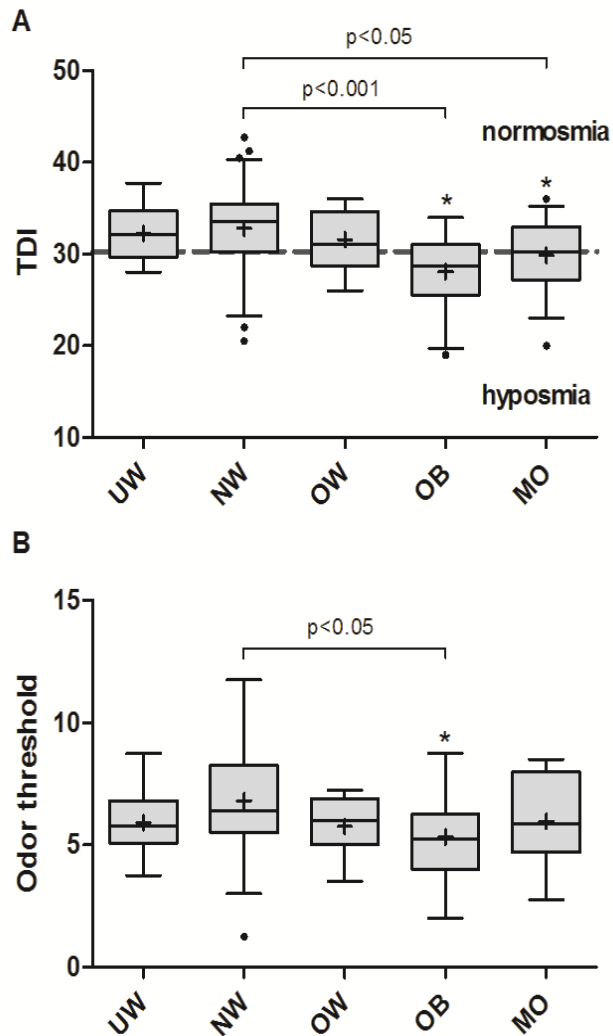


Figure 19. Olfactory scores. Box plots of odor threshold-discrimination-identification (TDI) scores (A), and odor threshold scores (B) of subjects from each of the body mass index (BMI) sub-groups. The median is represented as a line within the box plot and the mean is represented as a + sign. Significant differences ($p < 0.05$) in olfactory scores between BMI subgroups are marked as asterisks (*). Outliers are represented as points. Discontinuous line in (A) represents the TDI score of 30.3 that separates normosmia from hyposmia.

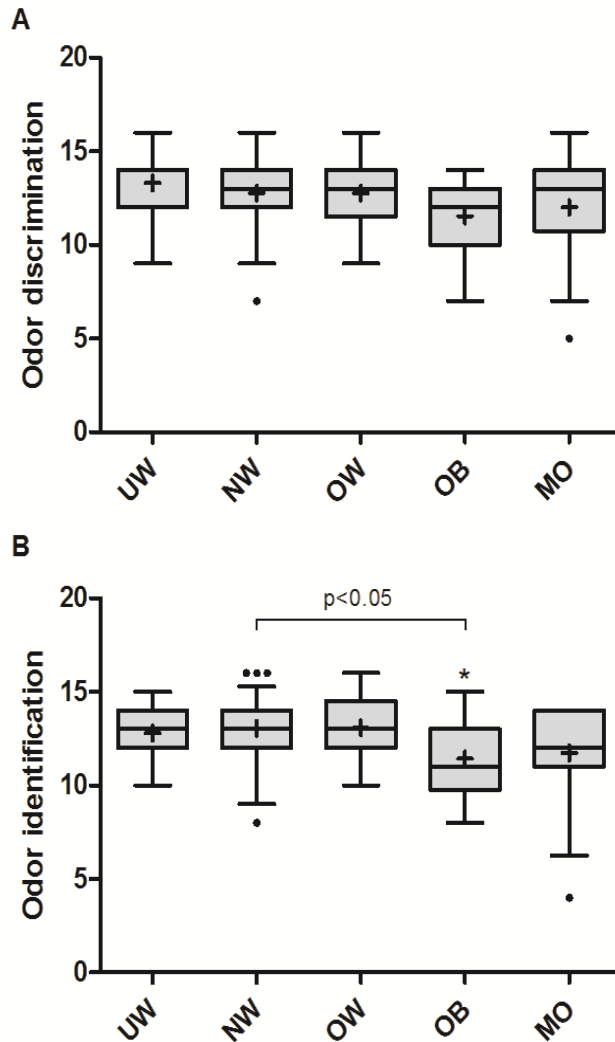


Figure 20. Olfactory scores. Box plots of odor discrimination scores- (A), and odor identification scores (B) of subjects from each of the body mass index (BMI) sub-groups. The median is represented as a line within the box plot and the mean is represented as a + sign. Significant differences ($p < 0.05$) in olfactory scores between BMI subgroups are marked as asterisks (*). Outliers are represented as points.

Next, we assessed the correlation of olfactory scores with the other study variables. TDI scores negatively correlated with age, BMI, %body fat, 2-AG, 2-LG, 2-OG, triglycerides and glucose (**Table 13**).

Table 13. Olfactory scores correlations

	Odor threshold	Odor discrimination	Odor identification	TDI
Age (yrs)	r=-0.16, p=0.049	r=-0.21, p=0.008	r=-0.25, p=0.002	r=-0.29, p<0.001
BMI (Kg/m ²)	r=-0.17, p=0.030	r=-0.20, p=0.011	r=-0.31, p<0.001	r=-0.32, p<0.001
%body fat	r=-0.21, p=0.009	r=-0.23, p=0.004	r=-0.27, p=0.001	r=-0.33, p<0.001
2-AG (ng/mL)	r=-0.23, p=0.004	r=-0.23, p=0.004	r=-0.23, p=0.003	r=-0.33, p<0.001
2-LG (ng/mL)	r=-0.15, p=0.063	r=-0.20, p=0.015	r=-0.20, p=0.017	r=-0.26, p=0.001
2-OG (ng/mL)	r=-0.14, p=0.080	r=-0.18, p=0.025	r=-0.18, p=0.024	r=-0.24, p=0.003
Triglycerides (mg/dL)	r=-0.10, p=0.209	r=-0.15, p=0.065	r=-0.18, p=0.025	r=-0.21, p=0.010
Glucose (mg/dL)	r=-0.08, p=0.307	r=-0.19; p=0.023	r=-0.21; p=0.009	r=-0.23; p=0.005

Odor threshold-discrimination-identification score (TDI), body mass index (BMI), 2-arachidonoylglycerol (2-AG), 2-linoleoylglycerol (2-LG), 2-oleoylglycerol (2-OG)

We noted that triglycerides and glucose did not correlate with OT. Since olfaction may be affected by many factors, we studied the association of TDI with the other study variables by means of ANCOVA models that controlled for age, smoking, menstruation, and the use of contraceptives. The variables of menstruation and the use of contraceptives were included in the models to take into account the effect of menopause, normal or irregular menstruation, and the use of contraceptives on olfaction. We found that lower TDI scores were independently associated with higher BMI [B=-0.09 (-0.17,-0.01; 95% CI), p=0.026, $R^2_{\text{model}} = 0.16$], higher %body fat [B=-9.97 (-18.0,-1.92 ; 95% CI), p=0.016, $R^2_{\text{model}} = 0.17$], and higher 2-AG circulating concentrations [B=-0.83 (-1.45,-0.20; 95% CI), p=0.010, $R^2_{\text{model}} = 0.17$].

Results of the present work show that obese subjects have a lower olfactory capacity than non-obese ones and that elevated circulating 2-AG concentrations associated to higher BMI are also linked to a lower olfactory capacity. In agreement with previous studies we show that eCBs AEA and 2-AG, and their respective congeners have a distinct profile in relation to body mass index.

Olfaction seems to be affected by the nutritional status [121]. The olfactory tests were performed in the time period between breakfast and lunch, and subjects could not have eaten on the previous hour at the start of test. A high hunger state increases olfactory sensitivity [156,157] and food palatability [156]. It is noteworthy that studies have reported differences in olfactory threshold under hunger or satiety between neutral and food odors [157,158] or in the pleasantness of odors [158]. Interestingly, in a recent study it was reported that obese subjects have a greater sensitivity and preference for the odor of chocolate than non-obese

subjects [159]. This is in contrast to our results in which we used the neutral odorant n-butanol for the OT test. These differences are possibly due to the different hedonic value of odors, especially the food-related ones. For instance, it also has been reported that obese subjects perceive the odor of black pepper oil as less pleasant than non-obese subjects [160].

Obese and morbidly subjects had a lower olfactory capacity than normal-weight subjects. OI and OT were the olfactory domains more affected by an increase of BMI. In this study we did not observe a worse olfactory capacity in morbid obese vs obese subjects as reported previously [116]. The decrease in olfactory capacity in obesity may be explained by a loss of olfactory neurons due to a high fat diet, as it has been observed in mice [161]. It is noteworthy that in mice models of diet-induced obesity, the levels of eCBs, the expression of eCB biosynthetic and inactivating enzymes and the expression of eCB receptors are altered in the hippocampus [162,163], a region that participates in the formation of odor memories, mediates hedonic aspects of eating, and influences cognitive processes. It has been hypothesized that a Western diet rich in saturated fat and sugar leads to obesity due to neurobiological changes in the hippocampus that affect cognitive function, specifically in memory and learning functions necessary for the inhibitory control in response to food cues [164]. Cognitive functions related to olfaction are also relevant in humans with regard to learning a flavor during ingestion [110]. Finally, it has been reported previously that 2-AG circulating levels inversely correlate with cognitive flexibility [165].

The over-activation of the eCB system in obesity may lead to changes in olfactory perception and eating behavior. A previous report has shown that cannabinoids decrease odor threshold and stimulate food

intake in fasted mice by means of olfactory processes [121]. In the present study, we found that a reduced olfactory capacity is related to high circulating 2-AG concentrations and high BMI. Permanent high eCB concentrations associated to obesity may lead to adaptive responses such as resistance to eCB signaling. For instance, a chronic exposure to a high-fat, palatable diet in mice has been shown to decrease the expression of the CB1 receptor in the nucleus accumbens shell, the hedonic “hotspot”, and in the hippocampus [166]. An alteration of reward pathways has been postulated as one possible cause for obesity [79]. In this work we did not quantify food enjoyment, but a loss of flavor due to a reduced olfactory capacity could shift the diet to eating more high caloric and palatable foods [111]. In addition, satiety mechanisms that rely on the olfactory system, such as olfactory sensory-specific satiety may be affected [167].

2-AG circulating concentrations, but not AEA ones, were inversely associated with olfactory capacity. 2-AG was also the eCB associated with obesity. Our results are in agreement with previous studies that relate 2-AG but not AEA with %visceral fat and dyslipidemia [93,96,97]. Notably, olfactory capacity was also inversely associated to %body fat. Although 2-AG and AEA are both agonists of CB1 receptors and they share the backbone of arachidonic acid in their structure they have different biosynthetic and degradation routes [30], which suggest they play a different modulatory role. With regard to the modulation of food intake by eCBs, an elegant experiment of Monteleone et. al. [168] showed an increase in 2-AG concentrations but not those of AEA associated to hedonic eating. We also note that although unrelated to differences in olfactory capacity, AEA concentrations were lower in healthy under-weight subjects. This is opposite to the eCB profile in anorexia, as anorexic subjects have elevated concentrations of AEA and unchanged concentrations of 2-AG [169]. Circulating concentrations of

eCB-related compounds mimicked the differential trend of eCBs AEA and 2-AG with regard to the BMI of the participants. The collective low concentrations of N-acylethanolamines AEA, LEA, and PEA in underweight subjects and the collective high concentrations of 2-monoacylglycerols 2-AG, 2-LG and 2-OG in obese and morbidly obese subjects suggest an up-regulation and/or down-regulation of the enzymes responsible for eCB biosynthesis and inactivation. With the exception of AEA and 2-AG, the rest of N-acylethanolamines and 2-monoacylglycerols do not bind to CB1 or CB2 receptors and have different molecular targets. However, they are biosynthesized and degraded by the same enzymes that metabolize AEA and 2-AG respectively [34]. In obese subjects, an up-regulation of diacylglycerol lipase α (DAGL α), the enzyme that biosynthesizes 2-AG and the other 2-acylglycerols, and a down-regulation of monoacylglycerol lipase (MAGL), the enzyme that degrades 2-AG and other 2-monoacylglycerols, have been reported [170]. Studies also have reported that a down-regulation of fatty acid amide hydrolase (FAAH), the enzyme that degrades AEA and other N-acylethanolamines, is associated to obesity [95,170,171]. In our study, however, we did not observe significant differences in N-acylethanolamine concentrations in obese subjects.

In summary we have shown that obese subjects have a lower olfactory capacity than non-obese ones and that elevated circulating 2-AG concentrations are linked to a lower olfactory capacity. In agreement with previous studies we showed that elevated 2-AG concentrations were linked to high BMI and obesity. Obese subjects had deficits in both odor threshold (OT) and odor identification (OI) capacity. A decrease in OI capacity may be related to cognitive deficits associated to obesity. Lower AEA and other NAE concentrations were associated to low BMI, while high 2-AG and other 2-MG concentrations were associated to high BMI,

suggesting a possible differential up-regulation or down-regulation of the enzymes that biosynthesize and inactivate NAE and 2-MG in these two extreme weight categories.

We cannot yet link a lower olfactory capacity as a result of a dysregulated eCB system in obesity since this is a cross-over study, and a cause-effect cannot be inferred from these data. This study has also other limitations that need to be addressed in future studies. One, the conclusions cannot be applied to the general population, and only to women. These findings should be replicated in men. Two, the relationship between plasma and brain eCB concentrations is unknown. We make the assumption that peripheral eCB concentrations are biomarkers of the state of the brain eCB system. The origin of plasma eCB is unknown and they may be originated in part from organ spillover. Three, the collection time for eCB analysis was different than the time that the olfactory tests were performed. Plasma for eCB analysis was collected after a 12h fast, while olfactory tests were performed in the time period between breakfast and lunch. Although subjects could not have eaten at the previous hour at the start of the test, the experimental conditions were not the same for these two biological factors, which are the eCB system and olfaction. And last, future studies should also include food-related odors due to their known effects on olfactory thresholds, and for the study of brain reward circuits and food enjoyment.

6. CONCLUSIONS

6.1 Method for the quantification of endocannabinoids in human plasma

1. We have validated a method for the determination of a range of endocannabinoids and endocannabinoid related compounds in human plasma following international quality standards requirements. This method has been adapted to other matrices and species.
2. Peripheral endocannabinoids (eCBs) concentrations from clinical studies or animal models greatly depend on sample collection and sample time processing conditions that take place in the clinical and laboratory settings due to the natural presence of enzymatic activity in plasma. We have been able to overcome and/or control most factors contributing to eCBs quantification variability.
 - a. We have been able to provide an approach to prevent the artefactual generation of 2-arachidonoylglycerol (2-AG) and other 2-monoacylglycerols (2-MG) in plasma consisting on the use of lipase inhibitor Orlistat to be added to samples freshly collected
 - b. The immediate centrifugation in refrigerated conditions of blood samples and separation of plasma from blood to avoid the release of N-acylethanolamines (NAE), such as anandamide (AEA) from blood cells is required.
 - c. The developed method is able to preserve the original isomeric ratio of monoacylglycerols (MG). We have found that the chemical isomerization of MG can only be

avoided by an immediate processing (at cold temperature and acid pH) and analysis of samples.

- d. Due to the instability of 2-monoacylglycerols (2-MG) to isomerization during conservation of the plasma it is recommended reporting MG concentrations as the sum of both isomers (isomer 1 and isomer 2).

6.2 Endocannabinoids, weight categories and olfaction

3. We have shown that obese subjects have a lower olfactory capacity than non-obese ones and that elevated circulating 2-AG concentrations are linked to a lower olfactory capacity.
4. In agreement with previous studies we showed that elevated 2-arachidonoylglycerol (2-AG) concentrations were linked to high BMI and obesity.
5. Lower anandamide (AEA) and other N-acylethanolamines (NAE) concentrations were associated to low BMI, while high 2-AG and other 2-monoacylglycerols (2-MG) concentrations were associated to high BMI, suggesting a possible differential up-regulation or down-regulation of the enzymes that biosynthesize and inactivate NAE and 2-MG in these two extreme weight categories.
6. Obese subjects have deficits in both odor threshold (OT) and odor identification (OI) capacity. A decrease in OI capacity may be related to cognitive deficits associated to obesity.

7. BIBLIOGRAPHY

1. Han X, Gross RW. Global analyses of cellular lipidomes directly from crude extracts of biological samples by ESI mass spectrometry: a bridge to lipidomics. *J Lipid Res.* 2003;44: 1071–1079. doi:10.1194/jlr.R300004-JLR200
2. Wenk MR. The emerging field of lipidomics. *Nat Rev Drug Discov.* 2005;4: 594–610. doi:10.1038/nrd1776
3. Shevchenko A, Simons K. Lipidomics: coming to grips with lipid diversity. *Nat Rev Mol Cell Biol.* 2010;11: 593–598. doi:10.1038/nrm2934
4. Piomelli D, Astarita G, Rapaka R. A neuroscientist's guide to lipidomics. *Nature Publishing Group.* 2007;8: 743–754. doi:10.1038/nm2233
5. Di Marzo V, Piscitelli F. The Endocannabinoid System and its Modulation by Phytocannabinoids. *Neurotherapeutics.* 2015. doi:10.1007/s13311-015-0374-6
6. Mechoulam R, Hanuš LO, Pertwee R, Howlett AC. Early phytocannabinoid chemistry to endocannabinoids and beyond. *Nature Publishing Group.* 2014;15: 757–764. doi:10.1038/nm3811
7. Pain S. A potted history. *Nature.* 2015;525: S10–1. doi:10.1038/525S10a
8. Kirkham TC, Williams CM. Endogenous cannabinoids and appetite. *Nutr Res Rev.* 2001;14: 65–86. doi:10.1079/NRR200118
9. Piomelli D. The molecular logic of endocannabinoid signalling. *Nat Rev Neurosci.* 2003;4: 873–884. doi:10.1038/nrn1247
10. Di Marzo V. The endocannabinoid system: its general strategy of action, tools for its pharmacological manipulation and potential therapeutic exploitation. *Pharmacol Res.* 2009;60: 77–84. doi:10.1016/j.phrs.2009.02.010
11. Castillo PE, Younts TJ, Chávez AE, Hashimoto-dani Y. Endocannabinoid signaling and synaptic function. *Neuron.* 2012;76: 70–81. doi:10.1016/j.neuron.2012.09.020

12. Savinainen JR, Saario SM, Laitinen JT. The serine hydrolases MAGL, ABHD6 and ABHD12 as guardians of 2-arachidonoylglycerol signalling through cannabinoid receptors. *Acta Physiol (Oxf)*. 2012;204: 267–276. doi:10.1111/j.1748-1716.2011.02280.x
13. Bisogno T, Melck D, De Petrocellis L, Di Marzo V. Phosphatidic acid as the biosynthetic precursor of the endocannabinoid 2-arachidonoylglycerol in intact mouse neuroblastoma cells stimulated with ionomycin. *J Neurochem*. 1999;72: 2113–2119.
14. Kobayashi T, Kishimoto M, Okuyama H. Phospholipases involved in lysophosphatidylinositol metabolism in rat brain. *J Lipid Mediat Cell Signal*. 1996;14: 33–37.
15. Mu H, Høy CE. The digestion of dietary triacylglycerols. *Progress in Lipid Research*. 2004;43: 105–133. doi:10.1016/S0163-7827(03)00050-X
16. Blankman JL, Cravatt BF. Chemical probes of endocannabinoid metabolism. *Pharmacol Rev*. 2013;65: 849–871. doi:10.1124/pr.112.006387
17. Rouzer CA, Marnett LJ. Endocannabinoid oxygenation by cyclooxygenases, lipoxygenases, and cytochromes P450: cross-talk between the eicosanoid and endocannabinoid signaling pathways. *Chem Rev*. 2011;111: 5899–5921. doi:10.1021/cr2002799
18. Alhouayek M, Muccioli GG. COX-2-derived endocannabinoid metabolites as novel inflammatory mediators. *Trends Pharmacol Sci*. 2014;35: 284–292. doi:10.1016/j.tips.2014.03.001
19. Hsu K-L, Tsuboi K, Adibekian A, Pugh H, Masuda K, Cravatt BF. DAGL β inhibition perturbs a lipid network involved in macrophage inflammatory responses. *Nat Chem Biol*. 2012;8: 999–1007. doi:10.1038/nchembio.1105
20. Nomura DK, Morrison BE, Blankman JL, Long JZ, Kinsey SG, Marcondes MCG, et al. Endocannabinoid Hydrolysis Generates Brain Prostaglandins That Promote Neuroinflammation. *Science*. 2011;334: 809–813. doi:10.1126/science.1209200
21. Mechoulam R, Parker LA. The endocannabinoid system and the brain. *Annu Rev Psychol*. 2013;64: 21–47. doi:10.1146/annurev-

psych-113011-143739

22. Bilkei-Gorzo A. The endocannabinoid system in normal and pathological brain ageing. *Philos Trans R Soc Lond, B, Biol Sci.* 2012;367: 3326–3341. doi:10.1098/rstb.2011.0388
23. Giuffrida A, Seillier A. New insights on endocannabinoid transmission in psychomotor disorders. *Prog Neuropsychopharmacol Biol Psychiatry.* 2012;38: 51–58. doi:10.1016/j.pnpbp.2012.04.002
24. Ashton CH, Moore PB. Endocannabinoid system dysfunction in mood and related disorders. *Acta Psychiatr Scand.* 2011;124: 250–261. doi:10.1111/j.1600-0447.2011.01687.x
25. Monteleone P. New frontiers in endocrinology of eating disorders. *Curr Top Behav Neurosci.* 2011;6: 189–208. doi:10.1007/7854_2010_87
26. Di Marzo V, Stella N, Zimmer A. Endocannabinoid signalling and the deteriorating brain. Nature Publishing Group. *Nature Publishing Group;* 2015;16: 30–42. doi:10.1038/nrn3876
27. Soltesz I, Alger BE, Kano M, Lee S-H, Lovinger DM, Ohno-Shosaku T, et al. Weeding out bad waves: towards selective cannabinoid circuit control in epilepsy. Nature Publishing Group. 2015;16: 264–277. doi:10.1038/nrn3937
28. Herkenham M, Lynn AB, Johnson MR, Melvin LS, de Costa BR, Rice KC. Characterization and localization of cannabinoid receptors in rat brain: a quantitative in vitro autoradiographic study. *J Neurosci.* 1991;11: 563–583.
29. Chávez AE, Chiu CQ, Castillo PE. TRPV1 activation by endogenous anandamide triggers postsynaptic long-term depression in dentate gyrus. *Nat Neurosci.* 2010;13: 1511–1518. doi:10.1038/nn.2684
30. Di Marzo V. Endocannabinoid signaling in the brain: biosynthetic mechanisms in the limelight. *Nat Neurosci.* 2011;14: 9–15. doi:10.1038/nn.2720
31. Nogueiras R, Diaz-Arteaga A, Lockie SH, Velásquez DA, Tschöp J, López M, et al. The endocannabinoid system: role in glucose and energy metabolism. *Pharmacol Res.* 2009;60: 93–98.

- doi:10.1016/j.phrs.2009.04.004
32. Basu S, Dittel BN. Unraveling the complexities of cannabinoid receptor 2 (CB2) immune regulation in health and disease. *Immunol Res.* 2011;51: 26–38. doi:10.1007/s12026-011-8210-5
 33. Bradshaw HB, Walker JM. The expanding field of cannabimimetic and related lipid mediators. *Br J Pharmacol.* 2005;144: 459–465. doi:10.1038/sj.bjp.0706093
 34. Fezza F, Bari M, Florio R, Talamonti E, Feole M, Maccarrone M. Endocannabinoids, related compounds and their metabolic routes. *Molecules.* 2014;19: 17078–17106. doi:10.3390/molecules191117078
 35. Hanus L, Gopher A, Almog S, Mechoulam R. Two new unsaturated fatty acid ethanolamides in brain that bind to the cannabinoid receptor. *J Med Chem.* 1993;36: 3032–3034.
 36. Sheskin T, Hanus L, Slager J, Vogel Z, Mechoulam R. Structural requirements for binding of anandamide-type compounds to the brain cannabinoid receptor. *J Med Chem.* 1997;40: 659–667. doi:10.1021/jm960752x
 37. Ben-Shabat S, Fride E, Sheskin T, Tamiri T, Rhee MH, Vogel Z, et al. An entourage effect: inactive endogenous fatty acid glycerol esters enhance 2-arachidonoyl-glycerol cannabinoid activity. *Eur J Pharmacol.* 1998;353: 23–31.
 38. Calignano A, La Rana G, Giuffrida A, Piomelli D. Control of pain initiation by endogenous cannabinoids. *Nature.* 1998;394: 277–281. doi:10.1038/28393
 39. Fu J, Gaetani S, Oveisi F, Verme Lo J, Serrano A, Rodriguez de Fonseca F, et al. Oleylethanolamide regulates feeding and body weight through activation of the nuclear receptor PPAR-alpha. *Nature.* 2003;425: 90–93. doi:10.1038/nature01921
 40. Verme Lo J, Fu J, Astarita G, La Rana G, Russo R, Calignano A, et al. The nuclear receptor peroxisome proliferator-activated receptor-alpha mediates the anti-inflammatory actions of palmitoylethanolamide. *Mol Pharmacol.* 2005;67: 15–19. doi:10.1124/mol.104.006353
 41. Borrelli F, Izzo AA. Role of acylethanolamides in the

- gastrointestinal tract with special reference to food intake and energy balance. *Best Pract Res Clin Endocrinol Metab.* 2009;23: 33–49. doi:10.1016/j.beem.2008.10.003
42. O'Sullivan SE. Cannabinoids go nuclear: evidence for activation of peroxisome proliferator-activated receptors. *Br J Pharmacol.* 2007;152: 576–582. doi:10.1038/sj.bjp.0707423
43. Grygiel-Górniak B. Peroxisome proliferator-activated receptors and their ligands: nutritional and clinical implications--a review. *Nutr J.* 2014;13: 17. doi:10.1186/1475-2891-13-17
44. Stienstra R, Duval C, Müller M, Kersten S. PPARs, Obesity, and Inflammation. *PPAR Res.* 2007;2007: 95974. doi:10.1155/2007/95974
45. Hansen KB, Rosenkilde MM, Knop FK, Wellner N, Diep TA, Rehfeld JF, et al. 2-Oleoyl glycerol is a GPR119 agonist and signals GLP-1 release in humans. *J Clin Endocrinol Metab.* 2011;96: E1409–E1417. doi:10.1210/jc.2011-0647
46. Syed SK, Bui HH, Beavers LS, Farb TB, Ficorilli J, Chesterfield AK, et al. Regulation of GPR119 receptor activity with endocannabinoid-like lipids. *Am J Physiol Endocrinol Metab.* 2012;303: E1469–E1478. doi:10.1152/ajpendo.00269.2012
47. Barrera JG, Sandoval DA, D'Alessio DA, Seeley RJ. GLP-1 and energy balance: an integrated model of short-term and long-term control. *Nat Rev Endocrinol.* 2011;7: 507–516. doi:10.1038/nrendo.2011.77
48. Pertwee RG, Howlett AC, Abood ME, Alexander SPH, Di Marzo V, Elphick MR, et al. International Union of Basic and Clinical Pharmacology. LXXIX. Cannabinoid receptors and their ligands: beyond CB₁ and CB₂. *Pharmacol Rev.* 2010;62: 588–631. doi:10.1124/pr.110.003004
49. Zygmunt PM, Petersson J, Andersson DA, Chuang H, Sjørgård M, Di Marzo V, et al. Vanilloid receptors on sensory nerves mediate the vasodilator action of anandamide. *Nature.* 1999;400: 452–457. doi:10.1038/22761
50. Caterina MJ, Schumacher MA, Tominaga M, Rosen TA, Levine JD, Julius D. The capsaicin receptor: a heat-activated ion channel

- in the pain pathway. *Nature*. 1997;389: 816–824.
doi:10.1038/39807
51. Vinuesa AG, Sancho R, García-Limones C, Behrens A, Dijke ten P, Calzado MA, et al. Vanilloid receptor-1 regulates neurogenic inflammation in colon and protects mice from colon cancer. *Cancer Res*. 2012;72: 1705–1716. doi:10.1158/0008-5472.CAN-11-3693
 52. Ryberg E, Larsson N, Sjögren S, Hjorth S, Hermansson N-O, Leonova J, et al. The orphan receptor GPR55 is a novel cannabinoid receptor. *Br J Pharmacol*. 2007;152: 1092–1101. doi:10.1038/sj.bjp.0707460
 53. Oka S, Toshida T, Maruyama K, Nakajima K, Yamashita A, Sugiura T. 2-Arachidonoyl-sn-glycero-3-phosphoinositol: a possible natural ligand for GPR55. *J Biochem*. 2009;145: 13–20. doi:10.1093/jb/mvn136
 54. Gasperi V, Dainese E, Oddi S, Sabatucci A, Maccarrone M. GPR55 and its interaction with membrane lipids: comparison with other endocannabinoid-binding receptors. *Curr Med Chem*. 2013;20: 64–78.
 55. Hanus L, Abu-Lafi S, Fride E, Breuer A, Vogel Z, Shalev DE, et al. 2-arachidonoyl glyceryl ether, an endogenous agonist of the cannabinoid CB1 receptor. *Proc Natl Acad Sci USA*. 2001;98: 3662–3665. doi:10.1073/pnas.061029898
 56. Porter AC, Sauer J-M, Knierman MD, Becker GW, Berna MJ, Bao J, et al. Characterization of a novel endocannabinoid, virodhamine, with antagonist activity at the CB1 receptor. *J Pharmacol Exp Ther*. 2002;301: 1020–1024.
 57. Oka S, Tsuchie A, Tokumura A, Muramatsu M, Suhara Y, Takayama H, et al. Ether-linked analogue of 2-arachidonoylglycerol (noladin ether) was not detected in the brains of various mammalian species. *J Neurochem*. 2003;85: 1374–1381.
 58. Richardson D, Ortori CA, Chapman V, Kendall DA, Barrett DA. Quantitative profiling of endocannabinoids and related compounds in rat brain using liquid chromatography-tandem electrospray ionization mass spectrometry. *Anal Biochem*. 2007;360: 216–226. doi:10.1016/j.ab.2006.10.039

59. Huang SM, Bisogno T, Trevisani M, Al-Hayani A, De Petrocellis L, Fezza F, et al. An endogenous capsaicin-like substance with high potency at recombinant and native vanilloid VR1 receptors. *Proc Natl Acad Sci USA*. 2002;99: 8400–8405. doi:10.1073/pnas.122196999
60. Chu CJ, Huang SM, De Petrocellis L, Bisogno T, Ewing SA, Miller JD, et al. N-oleoyldopamine, a novel endogenous capsaicin-like lipid that produces hyperalgesia. *J Biol Chem*. 2003;278: 13633–13639. doi:10.1074/jbc.M211231200
61. Ji D, Jang C-G, Lee S. A sensitive and accurate quantitative method to determine N-arachidonoyldopamine and N-oleoyldopamine in the mouse striatum using column-switching LC-MS-MS: use of a surrogate matrix to quantify endogenous compounds. *Anal Bioanal Chem*. 2014;406: 4491–4499. doi:10.1007/s00216-014-7816-6
62. Marinelli S, Di Marzo V, Florenzano F, Fezza F, Viscomi MT, van der Stelt M, et al. N-arachidonoyl-dopamine tunes synaptic transmission onto dopaminergic neurons by activating both cannabinoid and vanilloid receptors. *Neuropsychopharmacology*. 2007;32: 298–308. doi:10.1038/sj.npp.1301118
63. Verhoeckx KCM, Voortman T, Balvers MGJ, Hendriks HFJ, M Wortelboer H, Witkamp RF. Presence, formation and putative biological activities of N-acyl serotonins, a novel class of fatty-acid derived mediators, in the intestinal tract. *Biochim Biophys Acta*. 2011;1811: 578–586. doi:10.1016/j.bbali.2011.07.008
64. Tan B, O'Dell DK, Yu YW, Monn MF, Hughes HV, Burstein S, et al. Identification of endogenous acyl amino acids based on a targeted lipidomics approach. *J Lipid Res*. 2010;51: 112–119. doi:10.1194/jlr.M900198-JLR200
65. Kohno M, Hasegawa H, Inoue A, Muraoka M, Miyazaki T, Oka K, et al. Identification of N-arachidonylglycine as the endogenous ligand for orphan G-protein-coupled receptor GPR18. *Biochem Biophys Res Commun*. 2006;347: 827–832. doi:10.1016/j.bbrc.2006.06.175
66. Boger DL, Henriksen SJ, Cravatt BF. Oleamide: an endogenous sleep-inducing lipid and prototypical member of a new class of biological signaling molecules. *Curr Pharm Des*. 1998;4: 303–314.

67. Obesity: preventing and managing the global epidemic. Report of a WHO consultation. World Health Organization technical report series. 2000 pp. i–xii– 1–253.
68. Haslam DW, James WPT. Obesity. *Lancet*. 2005;366: 1197–1209. doi:10.1016/S0140-6736(05)67483-1
69. Kelly T, Yang W, Chen C-S, Reynolds K, He J. Global burden of obesity in 2005 and projections to 2030. *Int J Obes Relat Metab Disord*. 2008;32: 1431–1437. doi:10.1038/ijo.2008.102
70. Wajchenberg BL. Subcutaneous and visceral adipose tissue: their relation to the metabolic syndrome. *Endocrine Reviews*. 2000;21: 697–738. doi:10.1210/edrv.21.6.0415
71. Galgani J, Ravussin E. Energy metabolism, fuel selection and body weight regulation. *Int J Obes Relat Metab Disord*. 2008;32: S109–S119. doi:10.1038/ijo.2008.246
72. Dahlman I, Arner P. Obesity and polymorphisms in genes regulating human adipose tissue. *Int J Obes Relat Metab Disord*. 2007;31: 1629–1641. doi:10.1038/sj.ijo.0803657
73. Marti A, Moreno-Aliaga MJ, Hebebrand J, Martínez JA. Genes, lifestyles and obesity. *Int J Obes Relat Metab Disord*. 2004;28: S29–S36. doi:10.1038/sj.ijo.0802808
74. Morton GJ, Cummings DE, Baskin DG, Barsh GS, Schwartz MW. Central nervous system control of food intake and body weight. *Nature*. 2006;443: 289–295. doi:10.1038/nature05026
75. Broberger C. Brain regulation of food intake and appetite: molecules and networks. *J Intern Med*. 2005;258: 301–327. doi:10.1111/j.1365-2796.2005.01553.x
76. Rolls ET. Taste, olfactory and food texture reward processing in the brain and obesity. *Int J Obes Relat Metab Disord*. Nature Publishing Group; 2010;35: 550–561. doi:10.1038/ijo.2010.155
77. Morton GJ, Meek TH, Schwartz MW. Neurobiology of food intake in health and disease. *Nature Publishing Group*. 2014;15: 367–378. doi:10.1038/nrn3745
78. Murphy KG, Bloom SR. Gut hormones and the regulation of energy homeostasis. *Nature*. 2006;444: 854–859.

- doi:10.1038/nature05484
79. Kenny PJ. Reward Mechanisms in Obesity: New Insights and Future Directions. *Neuron*. 2011;69: 664–679.
doi:10.1016/j.neuron.2011.02.016
 80. Wang G-J, Volkow ND, Fowler JS. The role of dopamine in motivation for food in humans: implications for obesity. *Expert Opin Ther Targets*. 2002;6: 601–609.
doi:10.1517/14728222.6.5.601
 81. Kringelbach ML. Food for thought: hedonic experience beyond homeostasis in the human brain. *Neuroscience*. 2004;126: 807–819. doi:10.1016/j.neuroscience.2004.04.035
 82. Zheng H, Lenard NR, Shin AC, Berthoud H-R. Appetite control and energy balance regulation in the modern world: reward-driven brain overrides repletion signals. *Nature Publishing Group*; 2009;33: S8–S13. doi:10.1038/ijo.2009.65
 83. Small DM. Individual differences in the neurophysiology of reward and the obesity epidemic. *Nature Publishing Group*; 2009;33: S44–S48. doi:10.1038/ijo.2009.71
 84. Berridge KC. ‘Liking’ and ‘wanting’ food rewards: Brain substrates and roles in eating disorders. *Physiology & Behavior*. 2009;97: 537–550. doi:10.1016/j.physbeh.2009.02.044
 85. Cota D, Marsicano G, Tschöp M, Grübler Y, Flachskamm C, Schubert M, et al. The endogenous cannabinoid system affects energy balance via central orexigenic drive and peripheral lipogenesis. *J Clin Invest*. 2003;112: 423–431.
doi:10.1172/JCI17725
 86. Kirkham TC. Cannabinoids and appetite: food craving and food pleasure. *Int Rev Psychiatry*. 2009;21: 163–171.
doi:10.1080/09540260902782810
 87. Di Marzo V, Ligresti A, Cristino L. The endocannabinoid system as a link between homeostatic and hedonic pathways involved in energy balance regulation. *Nature Publishing Group*; 2009;33: S18–S24. doi:10.1038/ijo.2009.67
 88. Pagotto U, Marsicano G, Cota D, Lutz B, Pasquali R. The Emerging Role of the Endocannabinoid System in Endocrine

- Regulation and Energy Balance. *Endocrine Reviews*. 2006;27: 73–100. doi:10.1210/er.2005-0009
89. DiPatrizio NV, Astarita G, Schwartz G, Li X, Piomelli D. Endocannabinoid signal in the gut controls dietary fat intake. *Proceedings of the National Academy of Sciences*. 2011;108: 12904–12908. doi:10.1073/pnas.1104675108
90. Rodríguez de Fonseca F, Navarro M, Gómez R, Escuredo L, Nava F, Fu J, et al. An anorexic lipid mediator regulated by feeding. *Nature*. 2001;414: 209–212. doi:10.1038/35102582
91. Fu J, Astarita G, Gaetani S, Kim J, Cravatt BF, Mackie K, et al. Food intake regulates oleoylethanolamide formation and degradation in the proximal small intestine. *J Biol Chem*. 2007;282: 1518–1528.
92. Schwartz GJ, Fu J, Astarita G, Li X, Gaetani S, Campolongo P, et al. The Lipid Messenger OEA Links Dietary Fat Intake to Satiety. *Cell Metabolism*. 2008;8: 281–288. doi:10.1016/j.cmet.2008.08.005
93. Blüher M, Engeli S, Klötting N, Berndt J, Fasshauer M, Batkai S, et al. Dysregulation of the peripheral and adipose tissue endocannabinoid system in human abdominal obesity. *Diabetes*. 2006;55: 3053–3060. doi:10.2337/db06-0812
94. Di Marzo V. The endocannabinoid system in obesity and type 2 diabetes. *Diabetologia*. 2008;51: 1356–1367. doi:10.1007/s00125-008-1048-2
95. Engeli S, Böhnke J, Feldpausch M, Gorzelniak K, Janke J, Batkai S, et al. Activation of the peripheral endocannabinoid system in human obesity. *Diabetes*. 2005;54: 2838–2843.
96. Côté M, Matias I, Lemieux I, Petrosino S, Alméras N, Després J-P, et al. Circulating endocannabinoid levels, abdominal adiposity and related cardiometabolic risk factors in obese men. *Int J Obes (Lond)*. 2007;31: 692–699. doi:10.1038/sj.ijo.0803539
97. Di Marzo V, Côté M, Matias I, Lemieux I, Arsenault BJ, Cartier A, et al. Changes in plasma endocannabinoid levels in viscerally obese men following a 1 year lifestyle modification programme and waist circumference reduction: associations with changes in metabolic risk factors. *Diabetologia*. 2009;52: 213–217.

doi:10.1007/s00125-008-1178-6

98. Silvestri C, Ligresti A, Di Marzo V. Peripheral effects of the endocannabinoid system in energy homeostasis: Adipose tissue, liver and skeletal muscle. *Rev Endocr Metab Disord.* 2011;12: 153–162. doi:10.1007/s11154-011-9167-3
99. Fellow FJB-SPSR, fellow JSPPP, Leader ANPG, de Fonseca MD Group Leader FR. *Best Practice & Research Clinical Endocrinology & Metabolism.* Best Pract Res Clin Endocrinol Metab. Elsevier Ltd; 2009;23: 87–102. doi:10.1016/j.beem.2008.10.012
100. Vettor R, Pagano C. The role of the endocannabinoid system in lipogenesis and fatty acid metabolism. *Best Pract Res Clin Endocrinol Metab.* 2009;23: 51–63.
101. Poirier B, Bidouard J-P, Cadrouvele C, Marniquet X, Staels B, O'Connor SE, et al. The anti-obesity effect of rimonabant is associated with an improved serum lipid profile. *Diabetes Obes Metab.* 2005;7: 65–72. doi:10.1111/j.1463-1326.2004.00374.x
102. Tam J, Cinar R, Liu J, Godlewski G, Wesley D, Jourdan T, et al. Peripheral Cannabinoid-1 Receptor Inverse Agonism Reduces Obesity by Reversing Leptin Resistance. *Cell Metabolism.* 2012;16: 167–179. doi:10.1016/j.cmet.2012.07.002
103. Bermudez-Silva FJ, Cardinal P, Cota D. The role of the endocannabinoid system in the neuroendocrine regulation of energy balance. *Journal of Psychopharmacology.* 2012;26: 114–124. doi:10.1177/0269881111408458
104. Matias I, Gonthier M-P, Petrosino S, Docimo L, Capasso R, Hoareau L, et al. Role and regulation of acylethanolamides in energy balance: focus on adipocytes and beta-cells. *Br J Pharmacol.* 2007;152: 676–690. doi:10.1038/sj.bjp.0707424
105. Gonthier M-P, Hoareau L, Festy F, Matias I, Valenti M, Bès-Houtmann S, et al. Identification of endocannabinoids and related compounds in human fat cells. *Obesity (Silver Spring).* 2007;15: 837–845. doi:10.1038/oby.2007.581
106. Mallipedhi A, Prior SL, Dunseath G, Bracken RM, Barry J, Caplin S, et al. Research Article. *Journal of Diabetes Research.* Hindawi Publishing Corporation; 2015;: 1–8.

doi:10.1155/2015/680867

107. Alvheim AR, Malde MK, Osei-Hyiaman D, Hong Lin Y, Pawlosky RJ, Madsen L, et al. Dietary linoleic acid elevates endogenous 2-AG and anandamide and induces obesity. *Obesity*. 2012;20: 1984–1994. doi:10.1038/oby.2012.38
108. Alvheim AR, Torstensen BE, Lin YH, Lillefosse HH, Lock E-J, Madsen L, et al. Dietary linoleic acid elevates endogenous 2-arachidonoylglycerol and anandamide in Atlantic salmon (*Salmo salar* L.) and mice, and induces weight gain and inflammation in mice. *The British journal of nutrition*. 2013;109: 1508–1517.
109. Shepherd GM. Smell images and the flavour system in the human brain. *Nature*. 2006;444: 316–321. doi:10.1038/nature05405
110. Stevenson RJ. An initial evaluation of the functions of human olfaction. *Chemical Senses*. 2010;35: 3–20. doi:10.1093/chemse/bjp083
111. Aschenbrenner K, Hummel C, Teszmer K, Krone F, Ishimaru T, Seo H-S, et al. The Influence of Olfactory Loss on Dietary Behaviors. *Laryngoscope*. 2008;118: 135–144. doi:10.1097/MLG.0b013e318155a4b9
112. Aschenbrenner K, Scholze N, Joraschky P, Hummel T. Gustatory and olfactory sensitivity in patients with anorexia and bulimia in the course of treatment. *Journal of Psychiatric Research*. Elsevier Ltd; 2008;43: 129–137. doi:10.1016/j.jpsychires.2008.03.003
113. Dazzi F, Nitto SD, Zambetti G, Loredi C, Ciofalo A. Alterations of the olfactory-gustatory functions in patients with eating disorders. *Eur Eat Disord Rev*. 2013;21: 382–385. doi:10.1002/erv.2238
114. Schreder T, Albrecht J, Kleemann AM, Schöpf V, Kopietz R, Anzinger A, et al. Olfactory performance of patients with anorexia nervosa and healthy subjects in hunger and satiety. *Rhinology*. 2008;46: 175–183.
115. Rapps N, Giel KE, Söhngen E, Salini A, Enck P, Bischoff SC, et al. Olfactory deficits in patients with anorexia nervosa. *Eur Eat Disord Rev*. 2010;18: 385–389. doi:10.1002/erv.1010

116. Richardson BE, Vander Woude EA, Sudan R, Thompson JS, Leopold DA. Altered Olfactory Acuity in the Morbidly Obese. 2014;: 1–3.
117. Kringelbach ML. The human orbitofrontal cortex: linking reward to hedonic experience. *Nature Publishing Group*. 2005;6: 691–702. doi:10.1038/nrn1747
118. Yeomans MR. Olfactory influences on appetite and satiety in humans. *Physiology & Behavior*. 2006;87: 800–804. doi:10.1016/j.physbeh.2006.01.029
119. Jansen A, Theunissen N, Slechten K, Nederkoorn C, Boon B, Mulkens S, et al. Overweight children overeat after exposure to food cues. *Eating Behaviors*. 2003;4: 197–209. doi:10.1016/S1471-0153(03)00011-4
120. Bragulat V, Dzemidzic M, Bruno C, Cox CA, Talavage T, Considine RV, et al. Food-Related Odor Probes of Brain Reward Circuits During Hunger: A Pilot fMRI study. *Obesity*. *Nature Publishing Group*; 2009;18: 1566–1571. doi:10.1038/oby.2010.57
121. Palouzier-Paulignan B, Lacroix MC, Aimé P, Baly C, Caillol M, Congar P, et al. Olfaction Under Metabolic Influences. *Chemical Senses*. 2012;37: 769–797. doi:10.1093/chemse/bjs059
122. Soria-Gomez E, Bellocchio L, Reguero L, Lepousez G, Martin C, Bendahmane M, et al. The endocannabinoid system controls food intake via olfactory processes. *Nat Neurosci*. 2014;17: 407–415. doi:10.1038/nn.3647
123. Brisbois TD, de Kock IH, Watanabe SM, Mirhosseini M, Lamoureux DC, Chasen M, et al. Delta-9-tetrahydrocannabinol may palliate altered chemosensory perception in cancer patients: results of a randomized, double-blind, placebo-controlled pilot trial. *Annals of Oncology*. 2011;22: 2086–2093. doi:10.1093/annonc/mdq727
124. Tong J, Mannea E, Aimé P, Pfluger PT, Yi C-X, Castaneda TR, et al. Ghrelin enhances olfactory sensitivity and exploratory sniffing in rodents and humans. *Journal of Neuroscience*. 2011;31: 5841–5846. doi:10.1523/JNEUROSCI.5680-10.2011
125. Thanos PK, Robison LS, Robinson JK, Michaelides M, Wang G-

- J, Volkow ND. Obese rats with deficient leptin signaling exhibit heightened sensitivity to olfactory food cues. *Synapse*. 2012;67: 171–178. doi:10.1002/syn.21627
126. Ketterer C, Heni M, Thamer C, Herzberg-Schäfer SA, Häring H-U, Fritsche A. Acute, short-term hyperinsulinemia increases olfactory threshold in healthy subjects. *Int J Obes Relat Metab Disord*. 2010;35: 1135–1138. doi:10.1038/ijo.2010.251
127. Shepherd GM. Perspectives on Olfactory Processing, Conscious Perception, and Orbitofrontal Cortex. *Annals of the New York Academy of Sciences*. 2007;1121: 87–101. doi:10.1196/annals.1401.032
128. Gottfried JA. Central mechanisms of odour object perception. *Nature Publishing Group*. 2010;11: 628–641. doi:10.1038/nrn2883
129. Hoover KC. Smell with inspiration: The evolutionary significance of olfaction. *Am J Phys Anthropol*. 2010;143: 63–74. doi:10.1002/ajpa.21441
130. Kadohisa M. Effects of odor on emotion, with implications. *Front Syst Neurosci*. 2013;7: 66. doi:10.3389/fnsys.2013.00066
131. Doty RL, Shaman P, Applebaum SL, Giberson R, Siksorski L, Rosenberg L. Smell identification ability: changes with age. *Science*. 1984;226: 1441–1443.
132. Hummel T, Kobal G, Gudziol H, Mackay-Sim A. Normative data for the “Sniffin’ Sticks” including tests of odor identification, odor discrimination, and olfactory thresholds: an upgrade based on a group of more than 3,000 subjects. *Eur Arch Otorhinolaryngol*. 2006;264: 237–243. doi:10.1007/s00405-006-0173-0
133. Barresi M, Ciurleo R, Giacoppo S, Foti Cuzzola V, Celi D, Bramanti P, et al. Evaluation of olfactory dysfunction in neurodegenerative diseases. *J Neurol Sci*. 2012;323: 16–24. doi:10.1016/j.jns.2012.08.028
134. Hedner M, Larsson M, Arnold N, Zucco GM, Hummel T. Cognitive factors in odor detection, odor discrimination, and odor identification tasks. *J Clin Exp Neuropsychol*. 2010;32: 1062–1067. doi:10.1080/13803391003683070

135. Li W, Howard JD, Gottfried JA. Disruption of odour quality coding in piriform cortex mediates olfactory deficits in Alzheimer's disease. *Brain*. 2010;133: 2714–2726. doi:10.1093/brain/awq209
136. Djordjevic J, Jones-Gotman M, De Sousa K, Chertkow H. Olfaction in patients with mild cognitive impairment and Alzheimer's disease. *Neurobiology of Aging*. 2008;29: 693–706. doi:10.1016/j.neurobiolaging.2006.11.014
137. Hummel T, Sekinger B, Wolf SR, Pauli E, Kobal G. 'Sniffin' sticks': olfactory performance assessed by the combined testing of odor identification, odor discrimination and olfactory threshold. *Chemical Senses*. 1997;22: 39–52.
138. Fanelli F, Di Lallo VD, Belluomo I, De Iasio R. Estimation of reference intervals of five endocannabinoids and endocannabinoid related compounds in human plasma by two dimensional-LC/MS/MS. *Journal of lipid ...* 2012.
139. Zoerner AA, Gutzki F-M, Batkai S, May M, Rakers C, Engeli S, et al. Quantification of endocannabinoids in biological systems by chromatography and mass spectrometry: a comprehensive review from an analytical and biological perspective. *Biochim Biophys Acta*. 2011;1811: 706–723. doi:10.1016/j.bbalip.2011.08.004
140. Zoerner AA, Batkai S, Suchy MT, Gutzki FM. ... UPLC–MS/MS quantification of the endocannabinoids 2-arachidonoyl glycerol (2AG), 1-arachidonoyl glycerol (1AG), and anandamide in human plasma: minimization of matrix-effects, 2AG/1AG isomerization and degradation by toluene solvent extraction. *J Chromatography B Analyt Technol Biomed Life Sci*. 2012;883-884:161-171
141. Buczynski MW, Parsons LH. Quantification of brain endocannabinoid levels: methods, interpretations and pitfalls. *Br J Pharmacol*. 2010;160: 423–442. doi:10.1111/j.1476-5381.2010.00787.x
142. Rouzer CA, Ghebreselasie K, Marnett LJ. Chemical stability of 2-arachidonoylglycerol under biological conditions. *Chem Phys Lipids*. 2002;119: 69–82.
143. Jian W, Edom R, Weng N, Zannikos P, Zhang Z, Wang H.

- Validation and application of an LC-MS/MS method for quantitation of three fatty acid ethanolamides as biomarkers for fatty acid hydrolase inhibition in human plasma. *J Chromatogr B Analyt Technol Biomed Life Sci.* 2010;878: 1687–1699. doi:10.1016/j.jchromb.2010.04.024
144. Iannotti FA, Piscitelli F, Martella A, Mazzarella E, Allarà M, Palmieri V, et al. Analysis of the “endocannabinoidome” in peripheral tissues of obese Zucker rats. *Prostaglandins Leukot Essent Fatty Acids.* Elsevier; 2013;89: 127–135. doi:10.1016/j.plefa.2013.06.002
145. Zoerner AA, Gutzki FM, Suchy MT, Beckmann B, Engeli S, Jordan J, et al. Targeted stable-isotope dilution GC-MS/MS analysis of the endocannabinoid anandamide and other fatty acid ethanol amides in human plasma. *J Chromatogr B Analyt Technol Biomed Life Sci.* 2009;877: 2909–2923. doi:10.1016/j.jchromb.2009.04.016
146. Skonberg C, Artmann A, Cornett C, Hansen SH, Hansen HS. Pitfalls in the sample preparation and analysis of N-acylethanolamines. *J Lipid Res.* 2010;51: 3062–3073. doi:10.1194/jlr.D004606
147. Sugiura T, Kishimoto S, Oka S, Gokoh M. Biochemistry, pharmacology and physiology of 2-arachidonoylglycerol, an endogenous cannabinoid receptor ligand. *Progress in Lipid Research.* 2006;45: 405–446. doi:10.1016/j.plipres.2006.03.003
148. Bisogno T, Howell F, Williams G, Minassi A, Cascio MG, Ligresti A, et al. Cloning of the first sn1-DAG lipases points to the spatial and temporal regulation of endocannabinoid signaling in the brain. *J Cell Biol.* 2003;163: 463–468. doi:10.1083/jcb.200305129
149. Mattson FH, Volpenhein RA. The digestion and absorption of triglycerides. *J Biol Chem.* 1964.
150. Kindel T, Lee DM, Tso P. The mechanism of the formation and secretion of chylomicrons. *Atherosclerosis Supplements.* 2010.
151. Hoover HS, Blankman JL, Niessen S, Cravatt BF. Selectivity of inhibitors of endocannabinoid biosynthesis evaluated by activity-based protein profiling. *Bioorg Med Chem Lett.* 2008;18: 5838–5841. doi:10.1016/j.bmcl.2008.06.091

152. Sternby B, Hartmann D, Borgström B, Nilsson A. Degree of in vivo inhibition of human gastric and pancreatic lipases by Orlistat (Tetrahydrolipstatin, THL) in the stomach and small intestine. *Clin Nutr.* 2002;21: 395–402.
153. Karpe F, Olivecrona T, Walldius G, Hamsten A. Lipoprotein lipase in plasma after an oral fat load: relation to free fatty acids. *J Lipid Res.* 1992;33: 975–984.
154. Goodman KB, Bury MJ, Cheung M, Cichy-Knight MA, Dowdell SE, Dunn AK, et al. Discovery of potent, selective sulfonylurea endothelial lipase inhibitors. *Bioorg Med Chem Lett.* 2009;19: 27–30. doi:10.1016/j.bmcl.2008.11.033
155. HOFMANN AF, BORGSTROM B. Hydrolysis of long-chain monoglycerides in micellar solution by pancreatic lipase. *Biochim Biophys Acta.* 1963;70: 317–331.
156. Cameron JD, Goldfield GS, Doucet É. Fasting for 24h improves nasal chemosensory performance and food palatability in a related manner. *Appetite.* 2012;58: 978–981. doi:10.1016/j.appet.2012.02.050
157. Stafford LD, Welbeck K. High Hunger State Increases Olfactory Sensitivity to Neutral but Not Food Odors. *Chemical Senses.* 2011;36: 189–198. doi:10.1093/chemse/bjq114
158. Albrecht J, Schreder T, Kleemann AM, Schöpf V, Kopietz R, Anzinger A, et al. Olfactory detection thresholds and pleasantness of a food-related and a non-food odour in hunger and satiety. *Rhinology.* 2009;47: 160–165.
159. Stafford LD, Whittle A. Obese Individuals Have Higher Preference and Sensitivity to Odor of Chocolate. *Chemical Senses.* 2015;40: 279–284. doi:10.1093/chemse/bjv007
160. Trellakis S, Tagay S, Fischer C, Rydleuskaya A, Scherag A, Bruderek K, et al. Regulatory Peptides. *Regulatory Peptides.* Elsevier B.V; 2011;167: 112–117. doi:10.1016/j.regpep.2010.12.005
161. Thiebaud N, Johnson MC, Butler JL, Bell GA, Ferguson KL, Fadool AR, et al. Hyperlipidemic Diet Causes Loss of Olfactory Sensory Neurons, Reduces Olfactory Discrimination, and Disrupts Odor-Reversal Learning. *Journal of Neuroscience.*

- 2014;34: 6970–6984. doi:10.1523/JNEUROSCI.3366-13.2014
162. Massa F, Mancini G, Schmidt H, Steindel F, Mackie K, Angioni C, et al. Alterations in the Hippocampal Endocannabinoid System in Diet-Induced Obese Mice. *Journal of Neuroscience*. 2010;30: 6273–6281. doi:10.1523/JNEUROSCI.2648-09.2010
163. Rivera P, Luque-Rojas MJ, Pastor A, Blanco E, Pavon FJ, Serrano A, et al. Diet-dependent modulation of hippocampal expression of endocannabinoid signaling-related proteins in cannabinoid antagonist-treated obese rats. *Eur J Neurosci*. 2013;37: 105–117. doi:10.1111/ejn.12012
164. Kanoski SE, Davidson TL. Western diet consumption and cognitive impairment: Links to hippocampal dysfunction and obesity. *Physiology & Behavior*. 2011;103: 59–68. doi:10.1016/j.physbeh.2010.12.003
165. Fagundo AB, la Torre de R, Jimenez-Murcia S, Aguera Z, Pastor A, Casanueva FF, et al. Modulation of the Endocannabinoids N-Arachidonylethanolamine (AEA) and 2-Arachidonoylglycerol (2-AG) on Executive Functions in Humans. *PloS one*. 2013;8: e66387.
166. Harrold JA, Elliott JC, King PJ, Widdowson PS. Down-regulation of cannabinoid-1 (CB-1) receptors in specific extrahypothalamic regions of rats with dietary obesity: a role for endogenous cannabinoids in driving appetite for palatable food?. *Brain research*. 2002;952: 232–238.
167. Rolls ET, Rolls JH. Olfactory sensory-specific satiety in humans. *Physiology & Behavior*. 1997;61: 461–473.
168. Monteleone P, Piscitelli F, Scognamiglio P, Monteleone AM, Canestrelli B, Di Marzo V, et al. Hedonic eating is associated with increased peripheral levels of ghrelin and the endocannabinoid 2-arachidonoyl-glycerol in healthy humans: a pilot study. *J Clin Endocrinol Metab*. 2012;97: E917–24. doi:10.1210/jc.2011-3018
169. Monteleone P, Matias I, Martiadis V, De Petrocellis L, Maj M, Di Marzo V. Blood Levels of the Endocannabinoid Anandamide are Increased in Anorexia Nervosa and in Binge-Eating Disorder, but not in Bulimia Nervosa. *Neuropsychopharmacology*. 2005;30: 1216–1221. doi:10.1038/sj.npp.1300695

170. Engeli S, Lehmann A-C, Kaminski J, Haas V, Janke J, Zoerner AA, et al. Influence of dietary fat intake on the endocannabinoid system in lean and obese subjects. *Obesity*. 2014;22: E70–E76. doi:10.1002/oby.20728
171. Touriño C, Oveisi F, Lockney J, Piomelli D, Maldonado R. FAAH deficiency promotes energy storage and enhances the motivation for food. *Int J Obes Relat Metab Disord*. 2010;34: 557–568. doi:10.1038/ijo.2009.262

ANNEX

Analysis of ECs and related compounds in plasma: artifactual isomerization and ex vivo enzymatic generation of 2-MGs[§]

Antoni Pastor,^{*,†} Magí Farré,^{*,†} Montserrat Fitó,^{§,***} Fernando Fernandez-Aranda,^{§,††} and Rafael de la Torre^{1,*;§,§§}

Human Pharmacology and Clinical Neurosciences Research Group, Neuroscience Research Program,^{*} and Cardiovascular Risk and Nutrition Research Group, Inflammatory and Cardiovascular Disorders Research Program,^{**} IMIM (Hospital del Mar Medical Research Institute), Barcelona, Spain; Department of Pharmacology,[†] School of Medicine, Universitat Autònoma de Barcelona, Barcelona, Spain; CIBER Fisiopatología Obesidad y Nutrición (CIBEROBn),[§] Instituto Salud Carlos III, Santiago de Compostela, Spain; Department of Psychiatry,^{††} University Hospital of Bellvitge-IDIBELL, Hospitalet del Llobregat, Spain; and Department of Experimental and Health Sciences,^{§§} Pompeu Fabra University, Barcelona, Spain

Abstract The analysis of peripheral endocannabinoids (ECs) is a good biomarker of the EC system. Their concentrations, from clinical studies, strongly depend on sample collection and time processing conditions taking place in clinical and laboratory settings. The analysis of 2-monoacylglycerols (MGs) (i.e., 2-arachidonoylglycerol or 2-oleoylglycerol) is a particularly challenging issue because of their ex vivo formation and chemical isomerization that occur after blood sample collection. We provide evidence that their ex vivo formation can be minimized by adding Orlistat, an enzymatic lipase inhibitor, to plasma. Taking into consideration the low cost of Orlistat, we recommend its addition to plasma collecting tubes while maintaining sample cold chain until storage. We have validated a method for the determination of the EC profile of a range of MGs and N-acylethanolamides in plasma that preserves the original isomer ratio of MGs. Nevertheless, the chemical isomerization of 2-MGs can only be avoided by an immediate processing and analysis of samples due to their instability during conservation. We believe that this new methodology can aid in the harmonization of the measurement of ECs and related compounds in clinical samples.—Pastor, A., M. Farré, M. Fitó, F. Fernandez-Aranda, and R. de la Torre. Analysis of ECs and related compounds in plasma: artifactual isomerization and ex vivo enzymatic generation of 2-MGs. *J. Lipid Res.* 2014. 55: 966–977.

Supplementary key words 2-arachidonoylglycerol • 2-oleoylglycerol • validation • Orlistat • human • endocannabinoids • 2-monoacylglycerol

This work was supported by DICE (Department of Innovation, Universities and Enterprise) de la Generalitat de Catalunya 2009 (grant SGR 718) and CIBEROBn (Spanish Biomedical Research Centre in Physiopathology of Obesity and Nutrition, CB06/03, CIBEROBn is an initiative of ISCIII).

Manuscript received 2 October 2013 and in revised form 21 February 2014.

Published, JLR Papers in Press, March 4, 2014
DOI 10.1194/jlr.D043794

The neuromodulatory activities of the endocannabinoid (EC) system are involved in many human physiological and pathological functions (1–5). It comprises: *i*) two G-protein-coupled receptors, known as cannabinoid (CB)1 and CB2; *ii*) endogenous ligands for these two receptors, known as ECs, N-arachidonoyl ethanolamine [AEA (anandamide)] and 2-arachidonoylglycerol (AG) being the most studied; and *iii*) proteins that regulate EC tissue concentration (anabolic and catabolic enzymes), cellular distribution (EC-binding proteins and transporters), and CB receptor activity (CB receptor-interacting proteins) (1).

In addition to AEA and 2-AG, there are a number of structurally related compounds, also known as EC-related compounds (ERCs), derived from less unsaturated fatty acids: N-acylethanolamides (NAEs) such as N-linoleoyl ethanolamide (LEA), N-oleoyl ethanolamide (OEA), N-palmitoyl ethanolamide (PEA), N-palmitoleoyl ethanolamide

Abbreviations: AEA, N-arachidonoyl ethanolamide; AG, arachidonoylglycerol; Am. Ac., ammonium acetate; CB, cannabinoid; CV, coefficient of variation; DAG, diacylglycerol; DAGL, *sn*-1-diacylglycerol lipase; DEA, N-docosatetraenoyl ethanolamide; DGLA, N-dihomo- γ -linolenoyl ethanolamide; DHEA, N-docosahexaenoyl ethanolamide; EC, endocannabinoid; EPEA, N-icosapentaenoyl ethanolamide; ERC, endocannabinoid-related compound; ISTD, internal standard; LEA, N-linoleoyl ethanolamide; α -LEA, N- α -linolenoyl ethanolamide; LG, linoleoylglycerol; LLOQ, lower limit of quantification; LOD, limit of detection; MG, monoacylglycerol; MRM, multiple reaction monitoring; NAE, N-acylethanolamide; OEA, N-oleoyl ethanolamide; OG, oleoylglycerol; PEA, N-palmitoyl ethanolamide; POEA, N-palmitoleoyl ethanolamide; QC, quality control; QC-H, quality control-high; QC-L, quality control-low; QC-M, quality control-mid; RF, response factor; SA, surrogated analyte; SEA, N-stearoyl ethanolamide; TBME, tert-butylmethyl-ether.

¹To whom correspondence should be addressed.

e-mail: rtorre@imim.es

[§]The online version of this article (available at <http://www.jlr.org>) contains supplemental data in the form of one table.

Copyright © 2014 by the American Society for Biochemistry and Molecular Biology, Inc.

This article is available online at <http://www.jlr.org>

(POEA), and N-stearoyl ethanolamide (SEA), among others. Analogously, for the 2-monoacylglycerol (MG) series, there are also homologs such as 2-oleoylglycerol (OG) and 2-linoleoylglycerol (LG). Most of these molecules do not directly bind to CB receptors but may enhance/modify the actions of ECs (entourage effect) (6) or display biological activities related to their interactions with other receptors such as GPR119 (OEA, POEA, LEA, 2-OG) (7, 8), transient receptor potential vanilloid type 1 (TRPV1) (OEA), GPR55 (PEA), or PPAR- α (OEA) (9). Finally, two putative ECs, N-eicosapentaenoyl ethanolamide (EPEA) and N-docosahexaenoyl ethanolamide (DHEA), derived from the n-3 polyunsaturated fatty acids, are able to bind with low affinity to the CB1 and CB2 receptors and may have biological significance in the brain (10, 11).

A number of publications have been devoted to the analysis of ECs in plasma, and an effort has recently been made to establish reference intervals for five ECs in human plasma (12). As the chemistry and biology of ECs are better understood, so is the need to improve measurements in human plasma through greater control of factors that introduce variability. At present, such factors still limit the interchangeability of EC plasma concentrations from clinical studies. It has already been established that the chemical properties of ECs, with respect to their stability during analytical procedures (extraction solvents, pH conditions, and evaporation of organic solvents) and their absorption by glassware and plastic materials, are very relevant factors to take into consideration. A comprehensive review has provided a full discussion on these issues (13) and several analytical methods have already taken these factors into account (12, 14). Discrepancies among laboratories probably originate from preanalytical sample procurement protocols and compound-specific factors.

Concerning biological matrices, ECs are unstable in those where enzymes are involved in their synthesis and clearance: the fatty acid amide hydrolase hydrolyzes AEA to arachidonic acid and ethanolamine, and the MG lipase is responsible for the hydrolysis of 2-AG to arachidonic acid and glycerol. Nevertheless, accumulated experience suggests that the incorporation of unspecific enzyme inhibitors of amidases, esterases, and proteases, such as PMSF, to sample collection tubes is not justified. However, blood-containing tubes not centrifuged immediately in cold conditions after withdrawal may cause artifactual exaggerated NAE concentrations due to ex vivo release of from erythrocytes or leukocytes (12). Additionally, it has been reported that ex vivo synthesis of 2-AG for plasma preserved at room temperature and abundant 2-AG/1-AG isomerization is due to sample analysis conditions (12, 14). The two main ECs, AEA and 2-AG, are produced from different biosynthetic pathways. AEA is generated from N-arachidonoyl phosphatidylethanolamines by several possible biosynthetic routes with multiple enzymes implicated: the N-acyl phosphatidylethanolamine-specific phospholipase D, the α,β -hydrolase-4 (ABHD4), the glycerophosphodiesterase-1 (GDE1), a soluble phospholipase A2, an unidentified phospholipase C, and phosphatases (15). In contrast, the biosynthetic precursors for 2-AG, the *sn*-1-acyl-2-AGs, are mostly produced by phospholipase C β acting

on membrane phosphatidylinositols, and then being converted to 2-AG by the action of either of two isoforms of the same enzyme, the *sn*-1-diacylglycerol lipases α and β (DAGL α and DAGL β) (15, 16).

In clinical studies, the determination of ECs and ERCs is limited by methodological issues which particularly concern 2-MGs. Both their chemical isomerization and ex vivo generation are major issues that limit their inclusion as disease/physiological biomarkers. The aim of the present work is to improve current available methodological approaches for a better understanding of the biological significance of ECs.

MATERIALS AND METHODS

Chemicals and laboratory material

Ammonium acetate (Am. Ac.), acetic acid, tert-butyl-methyl-ether (TBME), acetonitrile, and formic acid were from Merck (Darmstadt, Germany). 1-AG, 1-AG-d5, 2-AG, 2-AG-d5, 2-AG-d8, 2-LG, 1-LG, AEA, AEA-d4, AEA-d8, N-docosatetraenoyl ethanolamide (DEA), N-dihomo- γ -linolenoyl ethanolamide (DGLEA), DHEA, DHEA-d4, LEA, LEA-d4, PEA, PEA-d4, POEA, POEA-d4, OEA, OEA-d4, and SEA were from Cayman Chemical (Ann Harbor, MI). 1-OG and 2-OG were from Sigma-Aldrich (St. Louis, MO). 1-OG-d5 and 2-OG-d5 were from Toronto Research Chemicals (North York, ON, Canada). FIFI hydrochloride (CAS 939055-18-2), D609 (CAS 83373-60-8), edelfosine (CAS 77286-66-9), and GSK 264220A (CAS 685506-42-7) were from Tocris Bioscience (Bristol, UK). Orlistat (tetrahydrolipstatin) was from Cayman Chemical. KT172, KT109, and RHC 80267 (CAS 83654-05-1) were from Sigma-Aldrich. KIMAX 16 \times 125 mm screw cap glass borosilicate tubes were from Kimble Chase (Mexico). Nunc 1.8 ml cryotube vials were from Thermo Fisher Scientific (Roskilde, Denmark). Ultrapure deionized water was produced by a Milli-Q Advantage A10 system from Millipore (Madrid, Spain).

Standard solutions

The purity of the NAE standards AEA, DEA, DGLEA, DHEA, DHEA, LEA, PEA, PEA, POEA, POEA, OEA, and SEA was >98% as provided by the manufacturer. Purity of the MG standards was >95% for 2-AG, 1-AG, and 2-LG; >94% for 2-OG; >99% for 1-OG; and >90% for 1-LG. The 2-MG standards were a combination of 90% isomer 2 and 10% isomer 1. The isomeric purity of the MG standards and their deuterated analogs was verified by injecting the individual standard solutions into the LC/MS-MS system with the following results: 91.2%, 2-AG; 91.5%, 2-AG-d5; 100%, 1-AG; 100%, 1-AG-d5; 97.3%, 2-OG; 94.3%, 2-OG-d5; 100%, 1-OG; 88.0%, 1-OG-d5; 98.7%, 2-LG; and 100%, 1-LG. The isotopic purity of the deuterated analogs of NAEs and MGs was >99% for all compounds. Stock and working standard solutions were prepared in acetonitrile and stored at -20°C . While working standard solutions of up to 10 $\mu\text{g}/\text{ml}$ were stable for protracted periods of time, a limited solubility was observed at a higher concentration (1 mg/ml) of stock solutions of saturated and monounsaturated NAEs and MGs after conservation at -20°C . Two mixtures of internal standards (ISTDs) were used: ISTD mix 1 prepared at 0.01 $\mu\text{g}/\text{ml}$ AEA-d4, 0.01 $\mu\text{g}/\text{ml}$ DHEA-d4, 0.02 $\mu\text{g}/\text{ml}$ LEA-d4, 0.04 $\mu\text{g}/\text{ml}$ PEA-d4, 0.04 $\mu\text{g}/\text{ml}$ OEA-d4, 0.2 $\mu\text{g}/\text{ml}$ 2-AG-d5, and 1 $\mu\text{g}/\text{ml}$ 2-OG-d5; and ISTD mix 2 prepared at 5.0 $\mu\text{g}/\text{ml}$ 2-AG-d8 and 0.25 $\mu\text{g}/\text{ml}$ AEA-d8. The two mixes of ISTD were spiked into the plasma samples at a fixed volume of 25 μl . The structures of the EC analytes and deuterated analogs are represented in **Figs. 1** and **2**.

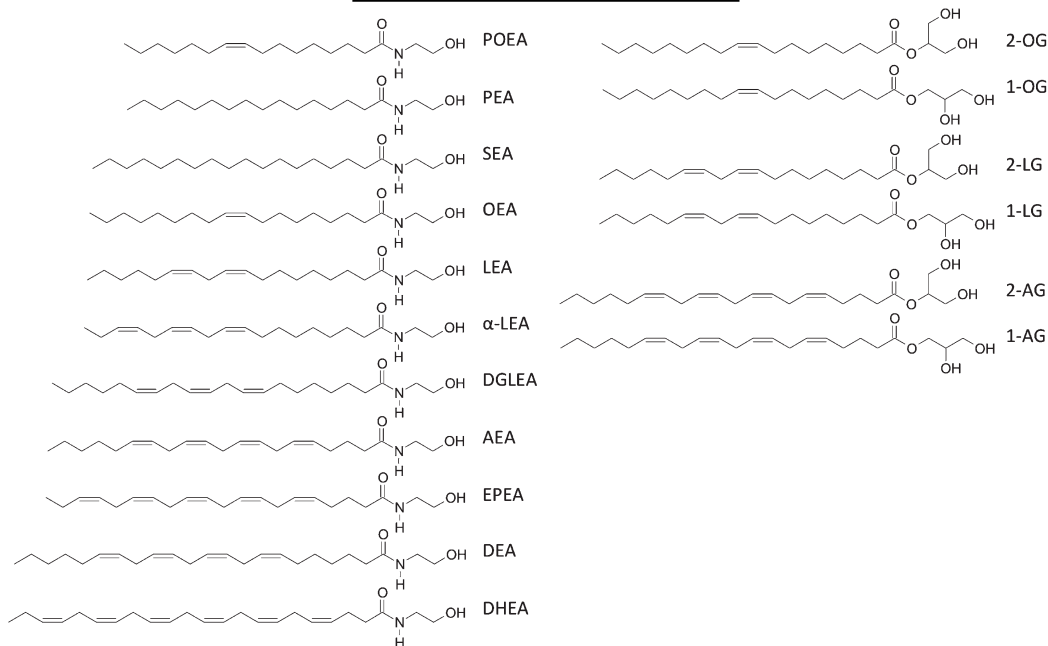


Fig. 1. Structures of the ECs and ERCs.

Human volunteers

Three human male volunteers were recruited for the procurement of blood samples following protocol MUESBIOL/1 (protocol for the collection of biological samples for biomedical research studies). Twenty-five female healthy control volunteers with a BMI of $<25 \text{ kg/m}^2$ were recruited for the procurement of blood samples following the TANOBE protocol. Both protocols were approved by the Ethical Committee of Parc de Salut Mar Barcelona (CEIC-PSMAR) and comply with the Declaration of Helsinki. An informed consent was obtained from the human subjects.

Sample preparation

Freshly extracted blood from human volunteers was collected in 10 ml K2E 18.0 mg (EDTA) BD Vacutainer tubes and centrifuged immediately for 15 min at 2,800 *g* in a refrigerated centrifuge (4°C). Plasma was then immediately separated from the blood and distributed in aliquots for further processing or stored at -80°C . Discarded human plasma batches from the Blood Bank of Hospital del Mar of Barcelona were used for the validation experiments.

Plasma samples were thawed in less than 30 min at room temperature and processed on ice. Aliquots of 0.5 ml were transferred into glass borosilicate tubes, spiked with 25 μl of ISTD mix

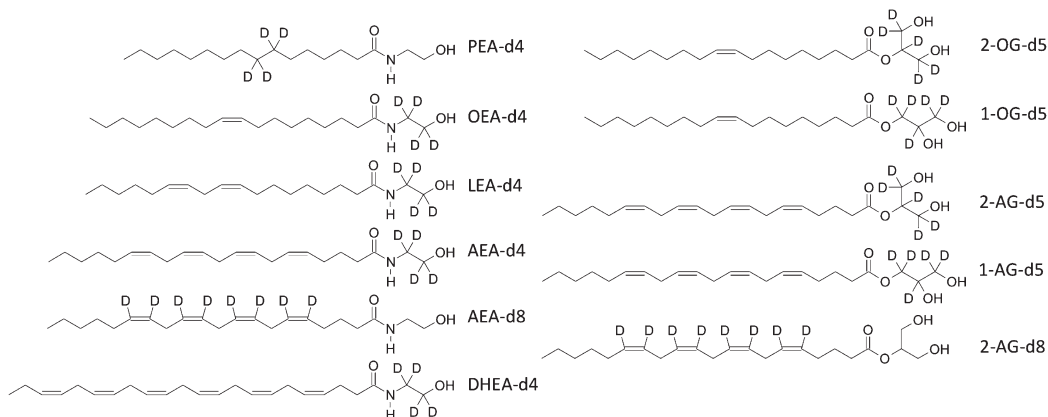


Fig. 2. Structures of the deuterated analogs of ECs and ERCs.

TABLE 1. Experimental LC/MS-MS parameters for the analyte detection

Analyte	MW	T (min)	CV (%)	P (<i>m/z</i>)	Q (<i>m/z</i>)	I (<i>m/z</i>)	F (V)	CE (eV)	ISTD	RF ^a
2-AG	378.6	7.65	0.08	379.2	287	269, 203	135	12	2-AG-d5	1.00
1-AG	378.6	7.77	0.30	379.2	287	269, 203	135	12	2-AG-d5	1.00
2-LG	354.5	7.76	0.06	355.2	263	245, 337	135	12	2-OG-d5	0.79
1-LG	354.5	7.94	0.08	355.2	263	245, 337	135	12	2-OG-d5	0.79
2-OG	356.5	8.61	0.41	357.3	265	247, 339	135	12	2-OG-d5	1.00
1-OG	356.5	8.82	0.08	357.3	265	247, 339	135	12	2-OG-d5	1.00
AEA	347.5	7.22	0.07	348.3	62	44, 287	135	12	AEA-d4	1.00
DEA	375.6	7.99	0.08	376.3	62	44	135	12	AEA-d4	1.26
DGLEA	349.6	7.61	0.08	350.2	62	44	135	12	AEA-d4	1.68
DHEA	371.6	7.11	0.07	372.6	62	44	135	12	DHEA-d4	1.00
EPEA	345.5	6.66	0.13	346.2	62	44	135	12	AEA-d4	1.00
LEA	323.5	7.26	0.07	324.5	62	44	135	12	LEA-d4	1.00
α-LEA	321.5	6.66	0.11	322.2	62	44	135	12	LEA-d4	1.00
OEA	325.5	8.05	0.06	326.1	62	44, 309	135	12	OEA-d4	1.00
PEA	299.5	7.81	0.07	300.1	62	44, 283	135	12	PEA-d4	1.00
POEA	297.5	6.94	0.08	298.2	62	44	135	12	PEA-d4	1.00
SEA	327.5	9.11	0.07	328.1	62	44, 311	135	12	OEA-d4	1.00

MW, molecular weight; T, retention time; P, precursor ion; Q, quantifier product ion; I, identifier(s) product ion(s); F, fragmenter; CE, collision energy.

^aResponse factor of the analyte versus the internal standard.

1 or mix 2, diluted up to 1 ml with 0.1 M Am. Ac. buffer (pH 4.0), extracted with 6 ml of TBME, and centrifuged (3,500 rpm, 5 min) at room temperature. The organic phase was transferred to clean tubes, evaporated (40°C, 20 min) under a stream of nitrogen, and extracts were reconstituted in 100 μl of a mixture of water:acetonitrile (10:90, v/v) with 0.1% formic acid (v/v) and transferred to HPLC vials. Twenty microliters were injected into the LC/MS-MS system.

LC/MS-MS analysis

An Agilent 6410 triple quadrupole mass spectrometer (Agilent Technologies, Wilmington, DE) equipped with a 1200 series binary pump, a column oven, and a cooled autosampler (4°C) was used. Chromatographic separation was carried out with a Waters C18-CSH column (3.1 × 100 mm, 1.8 μm particle size) maintained at 40°C with a mobile phase flow rate of 0.4 ml/min. The composition of mobile phase A was 0.1% (v/v) formic acid in water and mobile phase B was 0.1% (v/v) formic acid in acetonitrile. The initial conditions were 40% B. The gradient was first increased linearly to 90% B over 4 min, then increased linearly to 100% B over 5 min and maintained at 100% B for 3 min, to return to initial conditions for a further 4 min with a total run time of 16 min. The ion source was operated in the positive electrospray mode. A desolvation gas temperature of 350°C and a gas flow rate of 10 l/min were used. The pressure of the nebulizer was set at 40 psi and the capillary voltage at 4,000 V. The multiple reaction monitoring

(MRM) mode was employed for quantification. The experimental MS conditions for each compound are listed in **Tables 1 and 2**.

Linearity

The linearity of the method was assessed for seven surrogated analytes (SAs) by construction of calibration curves using plasma samples spiked with deuterated analogs of NAEs and MGs. Analysis was performed in quadruplicate for the following SAs: AEA-d4, LEA-d4, PEA-d4, OEA-d4, DHEA-d4, 2-AG-d5, and 2-OG-d5. The ISTDs were 2-AG-d8 and AEA-d8 (ISTD mix 2), which have additional deuterium atoms in their structure. 2-AG-d8 was used as ISTD of 2-MGs, and AEA-d8 as ISTD of NAEs. The regression analyses of the calibration curves were calculated with SPSS 12.0 with a 1/x weighting factor.

Quantification

Experimental LC/MS-MS parameters for the detection of analytes and the deuterated analogs are presented in **Tables 1 and 2**. The quantification of the SAs was calculated by interpolation of the response ratios on the calibration curves. The quantification of the authentic analytes was carried out by isotope dilution with the following formula: [EC]ng/ml = (ng ISTD × analyte response)/(ISTD response × RF × ml aliquot volume). The response factor (RF) was calculated as the ratio of the response area of the analyte divided by the response area of its ISTD for a standard solution mix directly injected without extraction into the LC/MS-MS system and in which equal amounts of the analyte

TABLE 2. Experimental LC/MS-MS parameters for the deuterated analogs detection

Deuterated Analog	MW	T (min)	Q1 (<i>m/z</i>)	Q3 (<i>m/z</i>)	F (V)	CE (eV)
2-AG-d5	383.6	7.63	384.3	287	135	12
1-AG-d5	383.6	7.77	384.3	287	135	12
2-AG-d8	386.6	7.59	387.5	295	135	12
2-OG-d5	361.6	8.59	362.2	265	135	12
1-OG-d5	361.6	8.79	362.2	265	135	12
AEA-d4	351.6	7.21	352.2	66	135	12
AEA-d8	355.6	7.19	356.2	62	135	12
DHEA-d4	375.6	7.09	376.3	66	135	12
LEA-d4	327.5	7.24	328.5	66	135	12
OEA-d4	329.6	8.04	330.4	66	135	12
PEA-d4	303.5	7.79	304.4	66	135	12

MW, molecular weight; T, retention time; Q1, precursor ion; Q3, product ion; F, fragmenter; CE, collision energy.

and ISTD were present. A deuterated form was not commercially available for some analytes, so a deuterated analog of another NAE or MG with a similar structure was used as ISTD. ISTD mix 1 was used for the quantification of authentic analytes. This fit-for-purpose approach could be employed due to the fact that the basic structure of the NAEs and the MGs is the same, the only difference being the length of the hydrocarbon chain and the number and position of double bonds. For some analytes the RF was considered 1.0 because the differences in the absolute response were less than 10% (Table 1). We found that the responses of 2-AG-d8 and AEA-d8 were considerably lower than their non-deuterated forms (approximately 10-fold), although, as they were not used in the isotope dilution quantification method, calculations were not affected. The decreased response was probably due to the different position of the deuterium atoms in the structure of the d8 analog (and next to the double bonds) compared with the d4 and d5 analogs (Fig. 2). In our LC/MS-MS conditions, responses of the 1-MG and 2-MG isomers were the same.

Limits of detection and quantification

The mathematical estimates of the limits of detection (LODs) and lower limits of quantification (LLOQs) of the SAs were inferred from the equations of the curves by the following formulas: LOD ng/ml = (SD of the replicates of the lowest concentration on calibrator/slope) × 3 and LLOQ ng/ml = (SD of the replicates of the lowest concentration on calibrator/slope) × 10. Additionally, the LLOQs of the SAs were verified experimentally by a six replicate analyses of plasma spiked with d4 or d5 deuterated forms of NAEs and 2-MGs at the following concentrations: PEA-d4, 0.1 ng/ml; OEA-d4, 0.1 ng/ml; LEA-d4, 0.1 ng/ml; AEA-d4, 0.02 ng/ml; DHEA-d4, 0.02 ng/ml; 2-AG-d5, 0.75 ng/ml; and 2-OG-d5, 2.5 ng/ml. The samples were further spiked with ISTD mix 2, which contained 2-AG-d8 and AEA-d8, and were analyzed by LC/MS-MS. The ratio of the SAs and their ISTDs was calculated. A coefficient of variation (CV) of the ratios of less than 20% and a signal to noise ratio greater than three were considered acceptable.

A dilution integrity experiment was carried out for lower sample volumes down to 50 µl, with no significant differences in concentration. However, the standard volume of the method was set at 0.5 ml in order to be able to quantify the ECs and ERCs with lower endogenous concentrations.

Accuracy and imprecision

The within-day and between-day accuracy and imprecision of the method were evaluated by the quadruplicate analysis of quality control (QC) samples at three concentration levels [QC-low (L), QC-mid (M), and QC-high (H)] over a 3 day validation protocol. The QC samples were prepared by spiking a batch of plasma on top of its basal EC and ERC concentrations. QC-L was spiked at 0.05 ng/ml POEA, DGLEA, EPEA, ALA, LEA, AEA, DEA, and DHEA; 1 ng/ml 2-AG, PEA, OEA, and SEA; and 5 ng/ml 2-OG and 2-LG. QC-M was spiked at 0.5 ng/ml POEA, DGLEA, EPEA, LEA, N-α-linolenoyl ethanolamide (α-LEA), AEA, DEA, and DHEA; 5 ng/ml 2-AG, PEA, OEA, and SEA; and 50 ng/ml of 2-OG and 2-LG. QC-H was spiked at 2.5 ng/ml POEA, DGLEA, EPEA, LEA, α-LEA, AEA, DEA, and DHEA; 25 ng/ml 2-AG, PEA, OEA, and SEA; and 250 ng/ml 2-OG and 2-LG. Aliquots of each QC were distributed into cryotubes and stored at -80°C until analysis. The samples were randomly analyzed in order to assess carry over.

Aliquots of 0.5 ml of the QC samples were spiked with ISTD mix 1 at the following amounts of deuterated analogs: 0.25 ng AEA-d4, 0.25 ng DHEA-d4, 0.50 ng LEA-d4, 1 ng PEA-d4, 1 ng OEA-d4, 5 ng 2-AG-d5, and 25 ng 2-OG-d5; and analyzed by LC/MS-MS. The quantification was done by isotope dilution.

TABLE 3. Stability of the isomerization upon extraction from the biological matrix

Extraction Solvent	Ratio	
	2-AG-d5 (ISO1/ISO2)	2-OG-d5 (ISO1/ISO2)
Spiked plasma		
TBME:water (6:1, v/v) ^a	0.59	0.32
TBME:water (6:1, v/v) ^b	0.53	0.20
TBME:Am. Ac. 0.1 M, pH 4.0 (6:1, v/v) ^a	0.10	0.09
Toluene:water (6:1, v/v) ^a	1.40	0.47
Standard solution	0.06	0.05

The stability of the isomerization of isomer 2 to isomer 1 during extraction and evaporation steps was assessed by analyzing the ratio (ISO1/ISO2) of plasma spiked with standard solutions of 2-AG-d5 and 2-OG-d5 subjected to liquid-liquid extraction compared with standard solutions dissolved in mobile phase injected directly into the LC/MS-MS system. ISO1, isomer 1; ISO2, isomer 2.

^a Reused clean tubes.

^b New silanized tubes.

Accuracy was calculated as the percentage of difference between the observed concentration and the nominal concentration. The nominal concentration was calculated as the expected concentration on day 1 of the QC sample after the spiking process, taking into account the basal EC and ERC concentrations. A percentage of difference less than 15% for QC-M and QC-H, and less than 20% for QC-L was considered acceptable.

Imprecision was calculated as the standard error deviation of the QC sample replicates. A standard error deviation less than 15% for QC-M and QC-H, and less than 20% for QC-L was considered acceptable.

Recovery and matrix effect

Recovery and matrix effect were evaluated in plasma from six different sources with deuterated analogs as SAs analyzed in triplicate. First, each batch of plasma was divided into two pools; one pool was spiked with ISTD mix 1 and mix 2 and extracted, while the other pool was spiked with ISTD mix 1 and mix 2 after extraction. Second, ISTD mix 1 and mix 2 were also spiked into clean glass tubes, evaporated, and reconstituted. Finally, extracted samples and pure standards were analyzed by LC/MS-MS. Recovery was calculated as the response of the SAs of samples spiked before extraction versus samples spiked after extraction. The matrix effect was calculated as the response of the SAs of samples spiked after extraction versus the pure standards. Additionally, the CV of the ratio of the SAs with the ISTD of the six plasma sources was calculated.

Stability of the analytes on reinjection

The stability of the reconstituted extract solutions on HPLC vials was tested with the reinjection of a batch in which the vials were kept at 4°C for 24 h and another batch with the vials kept at -20°C for 10 days.

Stability of the isomers 1 and 2 of MGs in the biological matrix

The stability of the isomers 1 and 2 of MGs to isomerization (or acyl migration) in the biological matrix was assessed by measuring the ratio between the isomers after preservation of the plasma at different times and temperatures. For that, one batch of human plasma from the blood bank was spiked with 2-OG-d5 and 2-AG-d5 and another batch was spiked with 1-OG-d5 and 1-AG-d5. Samples were analyzed by LC/MS-MS and the ratios of the 1 and 2 isomers of both batches were calculated. The spiked standards, dissolved in mobile phase, were also injected directly into the LC/MS-MS system and the

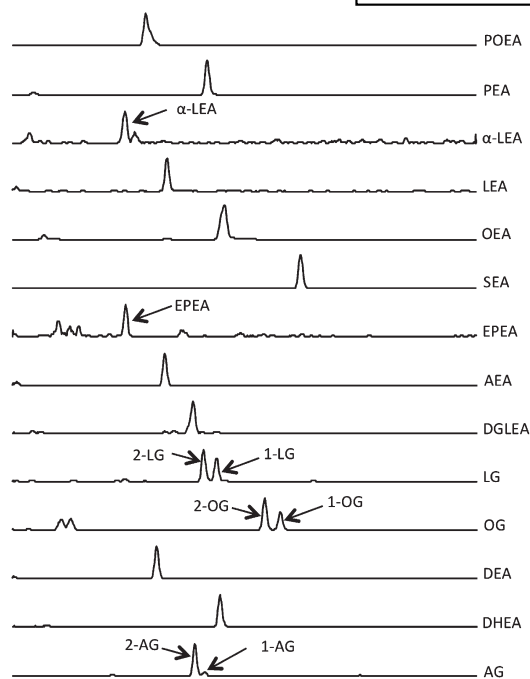


Fig. 3. LC/MS-MS chromatogram of EC and ERC profile of a human plasma sample.

isomer ratio was calculated. Additionally, in another experiment, the isomerization of endogenous MGs (2/1-AG, 2/1-LG, and 2/1-OG) was assessed in freshly obtained plasma samples from human volunteers preserved 2 h at 4°C or room temperature.

Inhibition experiments of the ex vivo generation of MGs from plasma

Blood was obtained from human volunteers and processed immediately. The rate of production of MGs from the separated plasma was assessed by EC analysis after incubation for 2 h at RT under agitation. Basal EC levels (time 0) were estimated by immediate EC analysis. A set of potential inhibitors of MG production were tested by spiking the plasma before incubation for 2 h at RT at different concentrations of inhibitors. In several experiments, the following phospholipase and lipase inhibitors were tested: edelfosine, D609, FIPI, Orlistat, RHC 80267, KT172,

KT109, and GSK 264220A. Stock inhibitor solutions were prepared in ethanol, except D609 that was prepared in water. The volume of spiking solution added was less than 2% with respect to the plasma aliquot volume. Plasma was distributed into cryotubes for the incubation experiments. Edelfosine is a phosphatidylinositol phospholipase C inhibitor ($IC_{50} = 9.6 \mu\text{M}$). D609 is a phosphatidylcholine-specific phospholipase C inhibitor ($K_i = 6.4 \mu\text{M}$). FIPI is a phospholipase D₂ and D₁ inhibitor ($IC_{50} = 20$ and 25 nM , respectively). Orlistat is a gastric and pancreatic lipase inhibitor and a nonselective DAGL α and DAGL β inhibitor ($IC_{50} = 60$ and 100 nM , respectively). RHC 80267 is a nonselective DAGL inhibitor ($IC_{50} = 4 \mu\text{M}$). KT172 and KT109 are selective DAGL β inhibitors ($IC_{50} = 60$ and 42 nM , respectively) and also DAGL α inhibitors ($IC_{50} = 0.14$ and $2.3 \mu\text{M}$, respectively). GSK 264220A is an endothelial lipase and a lipoprotein lipase inhibitor ($IC_{50} = 0.13$ and $0.10 \mu\text{M}$, respectively). The effect of the blood collection tube on the MG production was assessed on EDTA (K2E, 18 mg) or Lithium heparin (LH, 170 IU) in 10 ml BD Vacutainer tubes with or without the presence of the inhibitor. All the inhibitors were tested with EDTA-plasma while Orlistat and GSK 264220A were additionally tested on heparin-plasma. The estimation of the IC_{50} of Orlistat for the generation of 2-AG, 2-LG, and 2-OG was done in EDTA-plasma samples from three human volunteers with the following added concentrations of Orlistat: 0, 50, 150, 450, 900, 1,500, and 2,500 nM. Control plasma samples were kept at 4°C for 2 h until analysis. The percentage of inhibition was calculated with respect to the levels at concentration of inhibitor 0 of each plasma source. The data were modeled by the software GraphPad Prism 5 with the inhibition model: \log [inhibitor] versus percent inhibition and the IC_{50} s for 2-AG, 2-LG, and OG were calculated.

Stabilization of MG measures in plasma with Orlistat

Blood extracted from 25 human female volunteers was collected in 10 ml K2E 18.0 mg (EDTA) BD Vacutainer tubes and centrifuged immediately at 2,800 g in a refrigerated centrifuge (4°C). Plasma of each volunteer was separated immediately from the blood and two equal 0.6 ml aliquots were obtained. One aliquot was spiked at 3.35 μM with 5 μl of Orlistat solution (200 $\mu\text{g}/\text{ml}$, ethanol). Both aliquots were stored at -80°C until EC analysis with our standard procedure.

RESULTS AND DISCUSSION

Method development

While some solid phase extraction methods were tried, recovery was difficult to optimize due to the varying structures of the analyzed compounds (NAEs and MGs). The

TABLE 4. Recovery and matrix interference of the SAs in plasma

Surrogate Analyte	ISTD	Recovery (%)	Matrix Effect (%)	CV (%)
PEA-d4	OEA-d4	96 ± 11	-26 ± 4.7	3.0
LEA-d4	OEA-d4	96 ± 7.1	-19 ± 4.8	3.0
OEA-d4	PEA-d4	95 ± 8.4	-19 ± 5.8	3.4
AEA-d4	AEA-d8	95 ± 7.9	-15 ± 4.9	3.5
DHEA-d4	AEA-d4	89 ± 7.6	-11 ± 6.0	2.9
AEA-d8	AEA-d4	84 ± 8.7	-8.0 ± 5.0	4.2
2-OG-d5	2-AG-d5	84 ± 8.0	-40 ± 5.8	7.9
2-AG-d5	2-AG-d8	85 ± 7.8	-27 ± 4.0	3.9
2-AG-d8	2-AG-d5	81 ± 6.8	-16 ± 4.3	4.9

Mean ± SD of the recovery and matrix effect of the surrogate analytes in plasma of six different sources and analyzed in triplicate; CV of the ratio of the SAs with the ISTDs of the six plasma sources.

TABLE 5. Imprecision and accuracy

Analyte	Within Run						Between Run					
	Imprecision (%)			Accuracy (%)			Imprecision (%)			Accuracy (%)		
	QC-L	QC-M	QC-H	QC-L	QC-M	QC-H	QC-L	QC-M	QC-H	QC-L	QC-M	QC-H
2-AG	8.7	9.0	7.2	88.7	91.0	75.6	11.0	18.4	14.8	88.4	71.7	83.3
2/1-AG	6.7	5.7	5.7	96.9	96.4	93.5	7.4	14.3	8.2	88.7	93.2	102.8
2-LG	11.0	12.8	5.9	95.8	91.3	77.2	16.2	18.2	19.5	80.2	76.3	83.2
2/1-LG	5.4	8.5	5.7	94.9	100.6	104.7	11.2	4.8	9.6	91.4	101.2	109.6
2-OG	10.6	7.6	8.6	86.9	92.9	83.2	10.6	18.3	8.2	88.4	77.5	89.5
2/1-OG	9.7	8.7	6.9	95.3	89.9	97.0	12.1	11.2	5.6	90.8	85.1	104.4
AEA	4.6	6.1	4.3	92.9	88.7	89.6	9.8	10.2	4.8	92.1	92.9	89.4
DEA	4.5	6.1	5.2	91.6	91.4	93.0	11.9	6.9	5.3	95.0	94.1	95.2
DGLEA	7.7	6.1	4.1	97.0	97.6	95.0	10.4	9.0	5.4	101.2	97.5	98.3
DHEA	4.7	8.8	3.0	94.6	92.1	90.6	10.2	9.3	4.6	90.9	94.5	93.7
EPEA	7.2	5.3	4.3	95.3	89.9	88.0	9.8	10.0	6.1	90.6	89.1	89.7
LEA	3.2	7.4	5.4	97.8	97.9	97.5	10.0	10.2	5.5	94.8	99.9	101.1
α -LEA	5.6	9.0	5.7	93.9	88.5	87.0	11.5	12.5	8.1	86.7	88.5	88.1
OEA	2.9	7.5	3.8	97.5	98.4	96.4	9.3	9.7	4.6	94.9	97.2	101.6
PEA	2.9	6.6	3.0	95.4	97.6	96.7	9.4	9.5	3.9	94.5	96.5	100.2
POEA	7.0	11.3	6.2	96.5	93.8	86.3	14.1	12.4	9.8	92.9	89.7	89.8
SEA	4.9	9.4	3.8	93.3	98.3	99.0	10.8	10.5	8.8	100.8	97.2	104

Data represent the mean values of QC sample replicates.

liquid-liquid extraction methods provided the best overall recoveries for ECs and ERCs. In order to assess a method to stabilize the original isomeric ratio after the extraction and evaporation steps, 0.5 ml plasma samples were spiked with the deuterated analog isomers 2-AG-d5 and 2-OG-d5, extracted, and analyzed by LC/MS-MS to evaluate the generation of 1-AG-d5 and 1-OG-d5 by chemical isomerization or acyl migration (Table 3). Several liquid-liquid extraction methods were tested: TBME or toluene as extraction solvents, Am. Ac. buffer 0.1 M at pH 4.0, or water as aqueous solvents, and new silanized borosilicate glass tubes (or clean reused tubes) to test for the activity of catalytic silanols. Aqueous solvents were used to reduce viscosity and control plasma pH. Elevated temperatures, presence of serum albumin in the sample, and high pH values have been reported to accelerate 2-AG/1-AG acyl migration (13, 14, 17). It is worth noting that commercially available solutions of 2-AG and other 2-MG usually contain 5–10% 1-MG. Therefore, it seems impossible to completely avoid 2-MG/1-MG isomerization. The solvent that best preserved the original deuterated MG isomeric ratio of the sample after extraction was the mixture 6:1 TBME: 0.1 M Am. Ac. buffer (pH 4.0). In our experimental conditions, we observed that TBME preserved the 2-MG/1-MG ratio better than toluene, which was the solvent of choice for other

authors (12, 14). However, this is most likely due to the longer evaporation time of toluene compared with TBME, which in our experiment was relevant due to the amount of solvent used (6 ml) in the liquid-liquid extraction. The standard solutions were prepared in acetonitrile because methanol and other protic solvents promote the isomerization of isomer 2 into isomer 1 of MG (13). No differences were observed between extraction tubes that were clean, reused ones, or new silanized tubes.

We found optimal recoveries and peak shapes with the reconstitution of the extract in a mixture of water: acetonitrile (10:90) with 0.1% formic acid. The EC and ERC profiles were separated by reverse phase gradient chromatography in a C18 column (Fig. 3), because with a C8 column complete separation of the MG isomers was not possible. Acetonitrile was used as the organic mobile phase, as we observed that methanol also promoted 2-MG/1-MG isomerization if present in the mobile phase. Formic acid at 0.1% v/v was employed as an additive of the mobile phase to promote the positive ionization of NAEs and MGs. The parent ion adducts selected for fragmentation in the mass spectrometer were in the form of $[M+H]^+$. The product ion m/z 62, which corresponds to ethanolamine, is characteristically generated by fragmentation of NAEs; while a neutral loss of 92 Da, which corresponds

TABLE 6. Stability of MG concentrations on different collection conditions

Blood Tube	Inhibitor in Plasma	2/1-AG		2/1-LG		2/1-OG	
		Time 0	Time, 2 h at room temperature	Time 0	Time, 2 h at room temperature	Time 0	Time, 2 h at room temperature
EDTA	–	0.75 ± 0.21	8.51 ± 4.57	8.57 ± 2.23	102 ± 86.5	9.68 ± 2.28	115 ± 85.9
EDTA	+		1.13 ± 1.03		11.8 ± 5.1		15.6 ± 2.30
Heparin	–	2.82 ± 0.67	30.6 ± 23.0	83.7 ± 12.8	876 ± 729	72.3 ± 0.93	619 ± 475
Heparin	+		2.99 ± 0.05		65.3 ± 3.77		48.0 ± 1.20

Blood was collected in EDTA or heparin tubes. The separated plasma was analyzed immediately (time 0) or after incubation for 2 h at room temperature with or without addition of Orlistat to the plasma collection tube. Orlistat was added at 3.5 μ M to EDTA-plasma and at 15 μ M to heparin-plasma. Data are presented as mean \pm SD of 2/1-MG concentrations (ng/mL) of plasma from one volunteer in an experiment performed in duplicate.

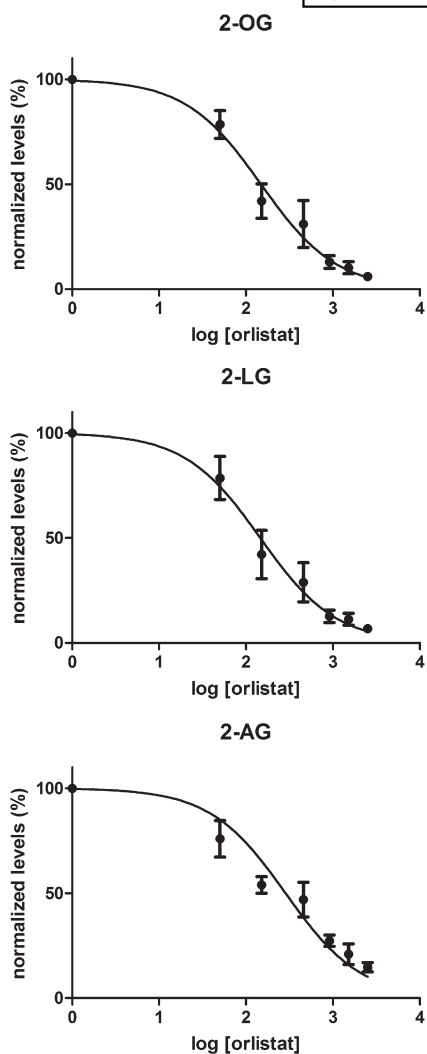


Fig. 4. Inhibition model of ex vivo production of 2-MG in plasma with Orlistat. Plasma from freshly extracted blood was spiked with a range of concentrations of Orlistat, incubated at room temperature for 2 h, and analyzed by LC/MS-MS to detect the levels of 2-AG, 2-OG, and 2-LG. Values represent the normalized 2-MG levels of three different volunteers analyzed in triplicate.

to glycerol, is common to the fragmentation of MGs. The specific MRM transitions are listed in Tables 1 and 2. The method is selective and specific for each analyte with no cross contamination between MRM channels and, in most cases, a single chromatographic peak corresponding to the endogenous analyte was found throughout the acquisition time. The variation in retention time of the individual analytes in a typical batch analysis was less than 0.5%. The retention time and product ion spectra of the endogenous analytes in the matrix matched the ones of the authentic standards.

The quantification of ECs, as for all endogenous analytes, is challenging due to the absence of a blank matrix. Some authors have developed strategies of depletion of the analytes by processing the plasma using five cycles of activated charcoal (12). Other authors have used a surrogated analysis approach (18) or carried out quantification by isotope dilution (19, 20). It is to be noted that EC-depleted plasma still contains MGs, probably due to its high concentrations (12). In this work, we have assessed the linearity, LOD, LLOQ, recovery, matrix effect, and MG acyl migration stability of the method using deuterated analog forms as SAs and ISTDs. Our approach is valid because the original unaltered matrix can be used and, theoretically, the deuterated forms have the same properties as the authentic analytes. However, there are a limited number of deuterated analogs of ECs and ERCs, and in order to use this approach different deuterated analog versions for each analyte are necessary. For this reason, in the analysis of samples of clinical studies (inhibition experiments), and in determining the accuracy and imprecision of the method, quantification was carried out with isotope dilution as described in the Materials and Methods.

Method validation

The method was linear for the ECs and ERCs whose quantification was standardized. Results, which include the mathematically derived LODs and LLOQs, are shown in supplementary Table I. The experimentally verified LLOQs of the method are the following: 0.02 ng/ml for AEA, DEA, DGLEA, EPEA, α -LEA, DHEA and POEA; 0.1 ng/ml for LEA; 0.5 ng/ml for OEA and SEA; 0.75 ng/ml for 2-AG; 1 ng/ml for PEA; and 2.5 ng/ml for 2-OG and 2-LG. The LLOQs of PEA, OEA, and SEA were set at a higher concentration than their mathematical LLOQs due to small basal contaminant concentrations found in the solvents and glassware as reported by other authors (12, 21). No significant carry over was detected. No differences in the concentration values were found after reinjecting vials kept at 4°C for 24 h. Vials kept at -20°C were stable for all analytes except SEA. Recoveries were high (>80%) for all the analytes and matrix effect was substantial (40%) in some analytes such as 2-OG-d5. Minimal differences in the matrix effect of the six plasma sources were, however, observed due to being compensated by the use of deuterated analogs with similar ISTD structure (Table 4). Within-run and between-run accuracy and imprecision values of NAEs and MGs are presented in Table 5 and fit current standard requirements for analytical method validation. With respect to the MGs, we found decreases in the concentration of the separate 2-MG isomers from day 2 of the validation protocol due to acyl migration during conservation of the plasma. This is explained in the section on stability of the isomeric ratio of MGs. The method is deemed fit for the determination of the EC and ERC profile in human plasma samples.

Inhibition experiments of the ex vivo generation of MGs from plasma

Fanelli et al. (12) reported the generation of 2-AG in plasma in the absence of blood cells, with increases in 2/1-AG for plasma preserved for 4 h at 4°C or room temperature. In the course of our MG stability experiments, we observed

TABLE 7. Effect of Orlistat addition to plasma on EC measures

EC/ERC	n	Measured Concentration (ng/ml)		Change (%)	P
		Without Added Orlistat	With Added Orlistat		
2/1-AG	25	2.42 ± 1.10	0.89 ± 0.50	-59.0 ± 23.9	<0.001
2/1-LG	25	15.2 ± 8.48	7.76 ± 3.54	-47.2 ± 17.5	<0.001
2/1-OG	25	16.1 ± 10.4	8.93 ± 4.90	-35.9 ± 25.0	<0.001
AEA	25	0.40 ± 0.19	0.39 ± 0.19	-2.09 ± 9.58	0.225
DEA	25	0.12 ± 0.04	0.11 ± 0.04	0.45 ± 11.8	0.671
DGLEA	25	0.11 ± 0.03	0.12 ± 0.03	-0.33 ± 12.3	0.324
DHEA	25	0.45 ± 0.19	0.44 ± 0.21	-0.74 ± 10.9	0.801
EPEA	14	0.03 ± 0.01	0.03 ± 0.01	-8.67 ± 9.02	0.104
LEA	25	1.30 ± 0.38	1.23 ± 0.38	-4.05 ± 11.7	0.091
α-LEA	25	0.04 ± 0.01	0.04 ± 0.01	-4.39 ± 13.4	0.142
OEA	25	3.16 ± 1.26	3.10 ± 1.22	-1.72 ± 5.46	0.057
PEA	25	2.07 ± 0.67	2.06 ± 0.60	0.75 ± 9.20	0.774
POEA	25	0.18 ± 0.11	0.17 ± 0.10	-2.90 ± 12.0	0.491
SEA	25	1.18 ± 0.33	1.15 ± 0.32	-2.15 ± 8.81	0.214

Plasma of 25 female human volunteers was collected with or without addition of Orlistat (3.4 μM) and stored at -80°C until EC analysis. Data are presented as mean ± SD. EPEA concentration was below the LLOQs for some of the samples. The effect of Orlistat addition to plasma on EC measures was assessed by a paired-samples *t*-test.

approximately 5-fold increases in 2/1-LG and 2/1-OG concentrations in plasma preserved for just 2 h at room temperature compared with plasma preserved at 4°C. In regard to 2/1-AG, we observed differences in concentration when plasma was analyzed immediately after blood extraction versus some time afterwards (2 h), or after a freezing/thawing step even though cold chain (4°C) was maintained. We therefore investigated, in controlled experiments, several phospholipase and lipase inhibitors for their capacity to inhibit ex vivo MG production in plasma. We found no inhibition activity for the phospholipase inhibitors D609, FIPI, and edelfosine (IC₅₀ >30 μM, IC₅₀ >125 nM, and IC₅₀ >50 μM, respectively). On the other hand, we observed inhibition of the ex vivo generation of 2-AG, 2-LG, and 2-OG in plasma spiked with Orlistat, a gastric and pancreatic lipase inhibitor (22) and a potent nonspecific inhibitor of DAGLα and DAGLβ (23). It is to be noted that the artifactual generation of MGs persisted even after immediate sample centrifugation that essentially eliminates all blood cells, which means that this MG buildup should be related to an enzymatic plasma activity. Because Orlistat is a general lipase inhibitor, we also tested the inhibition activity of RHC 80267, another nonspecific inhibitor of DAGLα (23), KT172, and KT109, potent selective DAGLβ inhibitors (24). None of these compounds showed inhibition activity (IC₅₀ >30 μM, IC₅₀ >15 μM, and IC₅₀ >15 μM, respectively), which means that the ex vivo MG production in plasma is a mechanism independent

of DAGL. 2-OG and 2-LG originate from fat digestion in the intestinal lumen, where dietary triacylglycerol is hydrolyzed in the *sn*-1 and *sn*-3 position by pancreatic lipase through a series of directed stepwise reactions to diacylglycerol (DAG), 2-MG, fatty acids, and glycerol. 2-MGs are readily adsorbed and resynthesized to triacylglycerols through the MG pathway (7, 25–27). Therefore, in terms of preventing 2-MG ex vivo formation, results obtained from plasma samples spiked with Orlistat are in agreement with this inhibitory enzymatic activity. The biosynthetic origin of 2-AG, however, is presumably not related to fat digestion but to phospholipids. Arachidonate DAGs, the precursors of 2-AG, are originated by the hydrolysis of membrane phosphoinositides and they are converted to 2-AG by the action of two *sn*-1 selective DAGLs, DAGLα and DAGLβ (16). Further, a direct dietary origin of 2-AG seems unlikely because arachidonic acid, an essential fatty acid and backbone of 2-AG structure, is present at low amounts in the diet, and is mainly obtained through metabolism of triacylglycerols that contain acyl-linoleoyl in their structure. The linoleic acid released is then elongated and unsaturated to form arachidonic acid through the omega-6 pathway. Additionally, we investigated the effect of the blood collection tube on MG generation. We found that MG concentrations were higher in heparin-plasma than in EDTA-plasma. The differences were maintained either for samples analyzed immediately or after incubation at room

TABLE 8. Stability of the isomerization of spiked 2/1-AG-d5 and 2/1-OG-d5 in stored plasma

Spiked analyte	Ratio	Time			
		Time 0	Time, 30 min at room temperature	Time, 20 days at -20°C	Time, 20 days at -80°C
2-AG-d5	ISO1/ISO2	0.08 ± 0.001	0.46 ± 0.06	0.84 ± 0.05	0.41 ± 0.01
1-AG-d5	ISO2/ISO1	0.01 ± 0.01	0.04 ± 0.005	0.07 ± 0.003	0.03 ± 0.002
2-OG-d5	ISO1/ISO2	0.08 ± 0.01	0.36 ± 0.06	0.58 ± 0.03	0.36 ± 0.06
1-OG-d5	ISO2/ISO1	0.13 ± 0.03	0.13 ± 0.03	0.12 ± 0.04	0.13 ± 0.03

A pool of plasma was spiked separately with the deuterated analogs of the isomer 1 (ISO1) and isomer 2 (ISO2) of AG and OG. Aliquots were distributed in cryotubes and chemical stability of the isomer ratio (ISO1/ISO2 and ISO2/ISO1) was assessed upon conservation at time 0, 30 min at room temperature, 20 days at -20°C, or 20 days at -80°C. Data are presented as mean ± SD of replicate analysis.

TABLE 9. Stability of the isomerization of endogenous 2/1-AG, 2/1-LG, and 2/1-OG in stored plasma

Endogenous analyte	Ratio ISO1 / ISO2	
	Time 2 h at 4°C	Time 2 h at room temperature
2/1-AG	0.09 ± 0.10	0.32 ± 0.24
2/1-LG	0.43 ± 0.13	0.76 ± 0.10
2/1-OG	0.28 ± 0.08	0.57 ± 0.06

The stability of the isomer 1/isomer 2 (ISO1/ISO2) ratio of endogenous 2/1-AG, 2/1-LG, and 2/1-OG was assessed in plasma of three different volunteers which was kept 2 h at 4°C or room temperature after extraction from the volunteer. Data are presented as mean ± SD of triplicate analyses.

temperature. Orlistat was able to inhibit MG production in plasma originated from both kind of tubes, but due to the higher MG buildup in heparin-plasma, a higher concentration of Orlistat was needed to achieve full inhibition (Table 6). Further, because heparin-plasma is commonly used for the assay of lipoprotein lipase due to its affinity for heparin (28), we also tested the inhibition activity of GSK 264220A, an endothelial lipase and a lipoprotein lipase inhibitor (29), but we found no inhibition ($IC_{50} > 15 \mu\text{M}$) on EDTA-plasma or heparin-plasma. The reason for the lower MG concentrations on EDTA-plasma is probably due to the chelate effect of EDTA on the cofactors needed for MG biosynthesis. We recommend, therefore, the use of EDTA blood tubes for collection in addition to Orlistat. In a second set of experiments, EDTA-plasma of three human volunteers was used for the calculation of the IC_{50} of Orlistat for the ex vivo generation of 2-AG, 2-LG, and 2-OG. An inhibition model was obtained and the data is graphically presented in Fig. 4. The IC_{50} of Orlistat with the mean, its 95% confidence interval, and the coefficient of determination (R^2) of the inhibition model are as follows: 285.6 nM [212.4, 384.0] for 2-AG ($R^2 = 0.8809$), 146.1 nM [104.9, 203.4] for 2-LG ($R^2 = 0.9087$), and 148.7 nM [110.6, 200.0] for 2-OG ($R^2 = 0.9254$).

Stabilization of MG measures in plasma spiked with Orlistat

The ex vivo generation of MG in plasma can be prevented by Orlistat. Because our MG assay was done at room temperature, we tested, in controlled conditions, whether Orlistat addition to the plasma storage tube had any effect on MG measures when a typical clinical sample collection protocol was followed. For that, 25 female blood samples were collected and processed in a matter of weeks, maintaining the cold chain until they were finally stored at -80°C . EC analysis took place several weeks after all samples had been collected and was done with our standard sample preparation procedure. The results are presented in Table 7 and they show that Orlistat addition during the sample collection protocol leads to a significant reduction of all MG measures (36–59%, $P < 0.001$). The NAEs, which are the other measures of our EC and ERC analysis, were not affected by the addition of Orlistat. We think that differences may have arisen due to the enzymatic activity that took in the freezing/thawing and processing steps. All the NAEs and MGs described in the method could be quantified in

the 25 human female samples (Table 7), with the exception of EPEA that, due to its low levels, could only be quantified in 14 samples. In summary, data show that Orlistat addition as part of the sample collection protocol can be a tool to stabilize MG concentrations in plasma, and this can aid in the harmonization of EC and ERC measurements in clinical samples.

Stability of the isomeric ratio of MGs

The results of the stability experiment of MGs in plasma show that the chemical isomerization of isomer 2 to isomer 1 decreases with decreases in the preservation temperature of the plasma before analysis. However, isomerization is still observed, even if samples are stored at -80°C (Table 8). Furthermore, it has been reported that isomerization is also dependent on the amount of serum albumin present in the sample (17). It is, therefore, possible that even when samples are subjected to the same storage conditions, they could still have different chemical isomerization rates. Additionally, chemical isomerization takes place in plasma preserved for a very short time at room temperature.


We also investigated the endogenous origin of MG isomers in fresh plasma samples (Table 9). As has been previously suggested (14), our data support the hypothesis that 1-AG does not have an endogenous origin and is the result of chemical isomerization during sample storage and processing, because in fresh plasma samples we found that 1-AG was present at the same isomeric ratio as the pure standard mixture. On the other hand, we observed that 1-LG and 1-OG were present at substantial concentrations. 1-MG originates from the in vivo isomerization of 2-MG during digestion and absorption. It has been estimated that approximately 25% of 2-MG is isomerized to the 1-MG form. However, 2-MG is the predominant form in which MGs are absorbed and resynthesized to triacylglycerols, while 1-MGs are eventually hydrolyzed by pancreatic lipase to free fatty acids and glycerol (25–27, 30).

In summary, only EC analysis performed with fresh samples is able to quantify the original isomeric ratio of the sample. Studies that report MG concentrations should specify whether the concentration data are from the separate or combined 1 and 2 isomers. Due to the instability of isomerization during conservation, and the fact that the 1-MG isomer originates either in vivo or ex vivo from the 2-MG isomer, studies that report the concentration of the two isomers together may still provide meaningful data for the interpretation of its biological significance in a fit-for-purpose approach. Alternatively, clinical samples may be spiked with deuterated analogs of known isomer ratios before conservation in order to correct the concentration data.

CONCLUSIONS

MG analysis is a challenging issue; to our knowledge, this is the first time that an enzymatic activity inhibited by the lipase inhibitor Orlistat and able to generate MGs in plasma in the absence of cells has been reported. Our findings suggest that, as happens with EC brain concentrations (31),

peripheral EC concentrations from clinical studies or animal models greatly depend on sample collection and sample time processing conditions that take place in the clinical and laboratory settings due to the natural presence of enzymatic activity in plasma. Because of the instability of EC concentrations in blood, EC studies need to follow strict harmonized sample collection and processing protocols in order to avoid artificial differences between samples. Finally, the collection of plasma samples with Orlistat may be a useful tool in the determination of real endogenous 2-MG concentrations. In addition to immediate centrifugation in refrigerated conditions and separation of plasma from blood to avoid the release of NAE from blood cells, we also recommend the addition of Orlistat to plasma collecting tubes and maintaining the cold chain until storage and processing. Orlistat is inexpensive, and thus may be a cost effective measure to aid in the harmonization of EC and ERC measurements in clinical research. Data suggest that the *ex vivo* generation of MG in plasma is a mechanism independent of DAGL, because besides the general lipase inhibitor Orlistat, other specific or unspecific DAGL inhibitors do not inhibit MG generation, and neither is the result of endothelial lipase or lipoprotein lipase activity. The full characterization of this enzymatic activity goes beyond the scope of this work, but due to the importance of the EC 2-AG as a biomarker, the understanding of this apparent alternative biosynthetic pathway of 2-AG, probably linked to lipid metabolism, would contribute to a better comprehension of the significance of its blood concentrations.

We have validated a method for the determination of a range of MGs and NAEs in plasma. The developed method is able to preserve the original isomeric ratio of MGs. We have found that the chemical isomerization of MGs can only be avoided by immediate processing (at cold temperature and acid pH) and analysis of samples. The report of MGs as the sum of both isomers may be considered. Alternatively, appropriate isomerization controls can be used during sample collection and conservation in order to correct concentrations. Data suggest that isomer 1 of AG is not an endogenous compound, and most probably is the result of chemical isomerization during storage and sample processing. On the other hand, isomer 1 of OG and isomer 1 of LG are likely to be endogenous compounds that result from *in vivo* isomerization that takes places during digestion, and their concentrations can be detected in plasma. 

REFERENCES

- Montecucco, F., and V. Di Marzo. 2012. At the heart of the matter: the endocannabinoid system in cardiovascular function and dysfunction. *Trends Pharmacol. Sci.* **33**: 331–340.
- Bilkei-Gorzó, A. 2012. The endocannabinoid system in normal and pathological brain ageing. *Philos. Trans. R. Soc. Lond. B Biol. Sci.* **367**: 3326–3341.
- Giuffrida, A., and A. Seillier. 2012. New insights on endocannabinoid transmission in psychomotor disorders. *Prog. Neuropsychopharmacol. Biol. Psychiatry.* **38**: 51–58.
- Ashton, C. H., and P. B. Moore. 2011. Endocannabinoid system dysfunction in mood and related disorders. *Acta Psychiatr. Scand.* **124**: 250–261.
- Monteleone, P. 2011. New frontiers in endocrinology of eating disorders. *Curr. Top. Behav. Neurosci.* **6**: 189–208.
- Ben-Shabat, S., E. Frider, T. Sheskin, T. Tamiri, M. H. Rhee, Z. Vogel, T. Bisogno, L. De Petrocellis, V. Di Marzo, and R. Mechoulam. 1998. An entourage effect: inactive endogenous fatty acid glycerol esters enhance 2-arachidonoyl-glycerol cannabinoid activity. *Eur. J. Pharmacol.* **353**: 23–31.
- Hansen, K. B., M. M. Rosenkilde, F. K. Knop, N. Wellner, T. A. Diep, J. F. Rehfeld, U. B. Andersen, J. J. Holst, and H. S. Hansen. 2011. 2-Oleoyl glycerol is a GPR119 agonist and signals GLP-1 release in humans. *J. Clin. Endocrinol. Metab.* **96**: E1409–E1417.
- Syed, S. K., H. H. Bui, L. S. Beavers, T. B. Farb, J. Ficorilli, A. K. Chesterfield, M-S. Kuo, K. Bokvist, D. G. Barrett, and A. M. Efanov. 2012. Regulation of GPR119 receptor activity with endocannabinoid-like lipids. *Am. J. Physiol. Endocrinol. Metab.* **303**: E1469–E1478.
- Borrelli, F., and A. Izzo. 2009. Role of acylethanolamides in the gastrointestinal tract with special reference to food intake and energy balance. *Best Pract. Res. Clin. Endocrinol. Metab.* **23**: 33–49.
- Brown, I., M. G. Cascio, K. W. J. Wahle, R. Smoum, R. Mechoulam, R. A. Ross, R. G. Pertwee, and S. D. Heys. 2010. Cannabinoid receptor-dependent and -independent anti-proliferative effects of omega-3 ethanolamides in androgen receptor-positive and -negative prostate cancer cell lines. *Carcinogenesis.* **31**: 1584–1591.
- Yang, R., G. Fredman, S. Krishnamoorthy, N. Agrawal, D. Irimia, D. Piomelli, and C. N. Serhan. 2011. Decoding functional metabolomics with docosahexaenoyl ethanolamide (DHEA) identifies novel bioactive signals. *J. Biol. Chem.* **286**: 31532–31541.
- Fanelli, F., V. D. Di Lallo, I. Belluomo, and R. De Iasio. 2012. Estimation of reference intervals of five endocannabinoids and endocannabinoid related compounds in human plasma by two dimensional-LC/MS/MS. *J. Lipid Res.* **53**: 481–493.
- Zoerner, A. A., F. M. Gutzki, S. Batkai, M. May, C. Rakers, S. Engeli, J. Jordan, and D. Tsikas. 2011. Quantification of endocannabinoids in biological systems by chromatography and mass spectrometry: a comprehensive review from an analytical and biological perspective. *Biochim. Biophys. Acta.* **1811**: 706–723.
- Zoerner, A. A., S. Batkai, M. T. Suchy, F. M. Gutzki, S. Engeli, J. Jordan, and D. Tsikas. 2012. Simultaneous UPLC-MS/MS quantification of the endocannabinoids 2-arachidonoyl glycerol (2AG), 1-arachidonoyl glycerol (1AG), and anandamide in human plasma: Minimization of matrix-effects, 2AG/1AG isomerization and degradation by toluene solvent extraction. *J. Chromatogr. B Analyt. Technol. Biomed. Life Sci.* **883-884**: 161–171.
- Di Marzo, V. 2011. Endocannabinoid signaling in the brain: biosynthetic mechanisms in the limelight. *Nat. Neurosci.* **14**: 9–15.
- Bisogno, T., F. Howell, G. Williams, A. Minassi, M. G. Cascio, A. Ligresti, I. Matias, A. Schiano-Moriello, P. Paul, E. J. Williams, et al. 2003. Cloning of the first sn1-DAG lipases points to the spatial and temporal regulation of endocannabinoid signaling in the brain. *J. Cell Biol.* **163**: 463–468.
- Rouzer, C. A., K. Ghebreselassie, and L. J. Marnett. 2002. Chemical stability of 2-arachidonoylglycerol under biological conditions. *Chem. Phys. Lipids.* **119**: 69–82.
- Jian, W., R. Edom, N. Weng, P. Zannikos, Z. Zhang, and H. Wang. 2010. Validation and application of an LC-MS/MS method for quantitation of three fatty acid ethanolamides as biomarkers for fatty acid hydrolase inhibition in human plasma. *J. Chromatogr. B Analyt. Technol. Biomed. Life Sci.* **878**: 1687–1699.
- Iannotti, F. A., F. Piscitelli, A. Martella, E. Mazzarella, M. Allarà, V. Palmieri, C. Parrella, R. Capasso, and V. Di Marzo. 2013. Analysis of the “endocannabinoidome” in peripheral tissues of obese Zucker rats. *Prostaglandins Leukot. Essent. Fatty Acids.* **89**: 127–135.
- Zoerner, A. A., F. M. Gutzki, M. T. Suchy, B. Beckmann, S. Engeli, J. Jordan, and D. Tsikas. 2009. Targeted stable-isotope dilution GC-MS/MS analysis of the endocannabinoid anandamide and other fatty acid ethanol amides in human plasma. *J. Chromatogr. B Analyt. Technol. Biomed. Life Sci.* **877**: 2909–2923.
- Skonberg, C., A. Artmann, C. Cornett, S. H. Hansen, and H. S. Hansen. 2010. Pitfalls in the sample preparation and analysis of N-acylethanolamines. *J. Lipid Res.* **51**: 3062–3073.
- Sternby, B., D. Hartmann, B. Borgström, and A. Nilsson. 2002. Degree of *in vivo* inhibition of human gastric and pancreatic lipases by Orlistat (tetrahydrolipstatin, THL) in the stomach and small intestine. *Clin. Nutr.* **21**: 395–402.
- Hoover, H. S., J. L. Blankman, S. Niessen, and B. F. Cravatt. 2008. Selectivity of inhibitors of endocannabinoid biosynthesis evaluated by activity-based protein profiling. *Bioorg. Med. Chem. Lett.* **18**: 5838–5841.
- Hsu, K. L., K. Tsuboi, A. Adibekian, H. Pugh, K. Masuda, and B. F. Cravatt. 2012. DAGLβ inhibition perturbs a lipid network

Supplemental Material can be found at:
<http://www.jlr.org/content/suppl/2014/03/07/jlr.D043794.DC1.html>

- involved in macrophage inflammatory responses. *Nat. Chem. Biol.* **8**: 999–1007.
25. Mattson, F. H., and R. A. Volpenhein. 1964. The digestion and absorption of triglycerides. *J. Biol. Chem.* **239**: 2772–2777.
26. Mu, H., and C. E. Høy. 2004. The digestion of dietary triacylglycerols. *Prog. Lipid Res.* **43**: 105–133.
27. Kindel, T., D. M. Lee, and P. Tso. 2010. The mechanism of the formation and secretion of chylomicrons. *Atheroscler. Suppl.* **11**: 11–16.
28. Karpe, F., T. Olivecrona, G. Walldius, and A. Hamsten. 1992. Lipoprotein lipase in plasma after an oral fat load: relation to free fatty acids. *J. Lipid Res.* **33**: 975–984.
29. Goodman, K. B., M. J. Bury, M. Cheung, M. A. Cichy-Knight, S. E. Dowdell, A. K. Dunn, D. Lee, J. A. Lieby, M. L. Moore, D. A. Scherzer, et al. 2009. Discovery of potent, selective sulfonylfuran urea endothelial lipase inhibitors. *Bioorg. Med. Chem. Lett.* **19**: 27–30.
30. Hofmann, A. F., and B. Borgstrom. 1963. Hydrolysis of long-chain monoglycerides in micellar solution by pancreatic lipase. *Biochim. Biophys. Acta.* **70**: 317–331.
31. Buczynski, M. W., and L. H. Parsons. 2010. Quantification of brain endocannabinoid levels: methods, interpretations and pitfalls. *Br. J. Pharmacol.* **160**: 423–442.

